

AD A093043

✓ DNA 5188F

COLLATERAL DAMAGE PROBABILITY MODELS

LEVEL II

12

Science Applications, Inc.
8400 Westpark Drive
McLean, Virginia 22102

22 January 1980

Final Report for Period 7 May 1979—22 January 1980

CONTRACT No. DNA 001-79-C-0303

APPROVED FOR PUBLIC RELEASE;
DISTRIBUTION UNLIMITED.

DTIC
ELECTRONIC
S DEC 11 1980 D
E

THIS WORK SPONSORED BY THE DEFENSE NUCLEAR AGENCY
UNDER RDT&E RMSS CODE B344079464 Y99QAXSC30106 H2590D.

DDC FILE COPY

Prepared for
Director
DEFENSE NUCLEAR AGENCY
Washington, D. C. 20305

80 12 10 056

Destroy this report when it is no longer
needed. Do not return to sender.

PLEASE NOTIFY THE DEFENSE NUCLEAR AGENCY,
ATTN: STTI, WASHINGTON, D.C. 20305, IF
YOUR ADDRESS IS INCORRECT, IF YOU WISH TO
BE DELETED FROM THE DISTRIBUTION LIST, OR
IF THE ADDRESSEE IS NO LONGER EMPLOYED BY
YOUR ORGANIZATION.



UNCLASSIFIED

SECURITY CLASSIFICATION OF THIS PAGE (When Data Entered)

19 REPORT DOCUMENTATION PAGE		READ INSTRUCTIONS BEFORE COMPLETING FORM
1. REPORT NUMBER 18 DNA 5188F	2. GOVT ACCESSION NO. AD-A093 043	3. RECIPIENT'S CATALOG NUMBER
4. TITLE (and Subtitle) 6 COLLATERAL DAMAGE PROBABILITY MODELS.		5. TYPE OF REPORT & PERIOD COVERED 9 Final Report, for Period 7 May 79-22 Jan 80
7. AUTHOR(s) 10 Gilbert C./Binninger		6. PERFORMING ORG. REPORT NUMBER 14 SAI-80-136-WA ✓
9. PERFORMING ORGANIZATION NAME AND ADDRESS Science Applications, Inc. 8400 Westpark Drive McLean, Virginia 22102		8. CONTRACT OR GRANT NUMBER(s) 15 DNA 001-79-C-0303 new
11. CONTROLLING OFFICE NAME AND ADDRESS Director Defense Nuclear Agency Washington, D.C. 20305 17 C301 / 11		10. PROGRAM ELEMENT, PROJECT, TASK AREA & WORK UNIT NUMBERS 16 Subtask Y99QAXSC301-06
14. MONITORING AGENCY NAME & ADDRESS (if different from Controlling Office) 6270-11		12. REPORT DATE 22 Jan 1980
		13. NUMBER OF PAGES 12 178
		15. SECURITY CLASS (of this report) UNCLASSIFIED
		15a. DECLASSIFICATION/DOWNGRADING SCHEDULE
16. DISTRIBUTION STATEMENT (of this Report) Approved for public release; distribution unlimited.		
17. DISTRIBUTION STATEMENT (of the abstract entered in Block 20, if different from Report)		
18. SUPPLEMENTARY NOTES This work sponsored by the Defense Nuclear Agency under RDT&E RMSS Code B344079464 Y99QAXSC30106 H2590D.		
19. KEY WORDS (Continue on reverse side if necessary and identify by block number) Collateral Damage Area Target Random Error Shoot-Look-Shoot Probability		
20. ABSTRACT (Continue on reverse side if necessary and identify by block number) This report includes an analysis of the Japanese structures damage data and application of this information in a targeting context for problems related to collateral damage. The Japanese data analysis focused on problems currently being investigated in DNA-sponsored collateral damage programs. This data analysis was performed to support DNA efforts directed toward assessing the significance of blast wave shielding, building orientation and building characteristics with regard to the vulnerability of residential structures. →		

408404

JAB

UNCLASSIFIED

SECURITY CLASSIFICATION OF THIS PAGE(When Data Entered)

20. ABSTRACT (Continued)

A targeting analysis to assess the impact of these vulnerability parameters to collateral damage is included in this report. The targeting analysis is performed and evaluated relative to an example small town typical of those located in Western Europe. Also included in this analysis is an assessment of the distance damage function "tail" relative to collateral damage, and demonstration of a shoot-look-shoot targeting strategy to minimize collateral damage.

This report also contains a prototype targeting algorithm developed for predicting collateral damage to urban area structures. The mathematics underlying this algorithm and demonstration of its utility are extensively documented in this report. The size and complexity of this algorithm, designed primarily for area targets, has been deliberately suppressed for ease in operation on a programmable hand-held calculator.

A

UNCLASSIFIED

SECURITY CLASSIFICATION OF THIS PAGE(When Data Entered)

PREFACE

This report represents the final report, under Contract DNA 001-79-C-0303 sponsored by the Defense Nuclear Agency. The work sponsored under this contract includes an investigation of the Japanese structures damage data for trends relevant to collateral damage issues currently being addressed under DNA-sponsored programs. Also included in this report is a demonstration and evaluation of vulnerability factors relevant to predicting the extent of collateral damage that could be incurred by residential structures in a tactical nuclear operation. The third and final subject addressed in this report pertains to the improvement of damage prediction techniques for use in field operations. Included in this report is a detailed description of a prototype algorithm, suitable for hand-held calculators, developed for predicting collateral damage to small urban towns.

This study was sponsored by the Strategic Structures Division of DNA with Dr. Kent Goering and Capt. Mike Moore, USA, serving as technical monitors; their support and comments are gratefully acknowledged.

A special appreciation is extended to members of the SAI staff who provided support toward this effort. In particular, the work of Roger Craver, Bob Doenges, and Charles Thomas helped make this effort possible.

Accession For	
NTIS GRA&I	<input checked="" type="checkbox"/>
DDC TAB	<input type="checkbox"/>
Unannounced	<input type="checkbox"/>
Justification	<input type="checkbox"/>
By _____	
Distribution/ _____	
And Other Codes	
Dist	Avail and/or special
A	

TABLE OF CONTENTS

<u>Section</u>	<u>Page</u>
PREFACE.....	1
TABLE OF CONTENTS.....	2
LIST OF ILLUSTRATIONS.....	4
LIST OF TABLES.....	8
1 ANALYSIS OF JAPANESE STRUCTURES DATA.....	11
1.1 BACKGROUND.....	11
1.2 PURPOSE AND SCOPE OF ANALYSIS.....	12
1.3 EXPLORATORY STATISTICAL ANALYSIS FOR BLAST WAVE SHIELDING.....	13
1.3.1 Data Included in Shielding Analysis.....	13
1.3.2 Exploratory Statistical Data Analysis.....	25
1.4 CORRELATION OF BUILDING ORIENTATION WITH REPORTED DAMAGE.....	29
1.4.1 Analysis of Multi-Story Load-Bearing-Wall Buildings.....	30
1.4.2 Analysis of Single-Story Load-Bearing-Wall Structures at Hiroshima.....	32
1.4.3 Analysis of Single-Story Load-Bearing-Wall Structures at Nagasaki.....	32
1.4.4 Summary.....	35
1.5 VULNERABILITY EVALUATIONS FOR LOAD-BEARING-WALL BUILDINGS.....	35
1.5.1 Wall Damage to Load-Bearing-Wall Structures at Japan.....	36
1.5.2 Roof Damage to Load-Bearing-Wall Structures.....	39
1.5.3 Superficial Damage to Load-Bearing-Wall Structures.....	40
1.5.4 Damage Analysis Summary.....	40

2	COLLATERAL DAMAGE SENSITIVITY ANALYSES.....	42
	2.1 OBJECTIVE AND SCOPE OF ANALYSIS.....	42
	2.2 CITY DAMAGE ANALYSIS.....	43
	2.3 DAMAGE PREDICTION METHODOLOGY.....	46
	2.4 SENSITIVITY ANALYSIS OF VULNERABILITY UNCERTAINTY ON COLLATERAL DAMAGE.....	47
	2.4.1 Objective and Scope of Analysis.....	47
	2.4.2 Vulnerability Uncertainty and Targeting Analysis.....	48
	2.4.3 City Core Damage Predictions.....	58
	2.5 IMPACT OF DAMAGE CRITERIA ON COLLATERAL DAMAGE....	63
	2.6 SIGNIFICANCE OF DISTANCE DAMAGE SIGMA VALUES IN COLLATERAL DAMAGE PREDICTIONS.....	69
	2.7 IMPACT OF SHIELDING ON PREDICTING COLLATERAL DAMAGE.....	76
	2.8 RANDOM UNCERTAINTY INHERENT TO DAMAGE PREDICTIONS.	79
3	SHOOT-LOOK-SHOOT.....	94
	3.1 OBJECTIVE AND SCOPE.....	94
	3.2 PROBABILISTIC MODELS FOR BASIC TARGETING PROB- LEMS.....	94
	3.3 COMPARISON OF COLLATERAL DAMAGE PREDICTIONS FOR A SHOOT-LOOK-SHOOT STRATEGY VS. THE "BLIND" METHOD.....	99
4	A PROTOTYPE ALGORITHM FOR PREDICTING COLLATERAL DAMAGE.	103
	4.1 BACKGROUND.....	103
	4.2 COLLATERAL DAMAGE ALGORITHM REQUIREMENTS.....	105
	4.3 ALGORITHM ASSUMPTIONS.....	106
	4.4 MATHEMATICS OF COLLATERAL DAMAGE PREDICTION ALGORITHM.....	111
	4.5 APPLICATION OF ALGORITHM TO AREA TARGETS.....	124
	4.5.1 Application of Algorithm to Circular Area Targets.....	124
	4.5.2 Application of Algorithm to an Actual Town.	130
	4.6 SUMMARY OBSERVATIONS.....	136
5	SUMMARY REMARKS.....	138
6	REFERENCES.....	141
	APPENDIX A.....	143
	APPENDIX B.....	161

LIST OF ILLUSTRATIONS

<u>Figure</u>		<u>Page</u>
1.1	Building Cluster, GROUP 17, Nagasaki.	14
1.2	Building Cluster, GROUP 15, Nagasaki.	16
1.3	Building Cluster, GROUP 20 and GROUP 40, Nagasaki . . .	17
1.4	Building Cluster Within GROUP 36, Nagasaki.	20
1.5	Building Cluster, GROUP 33, Nagasaki.	22
1.6	Building Clusters Within GROUP 40, Nagasaki	23
1.7a	Distance Damage Data, Nagasaki.	26
1.7b	Distance Damage Data, Nagasaki.	27
1.8	Building Orientation Groups	30
1.9	Building Orientation and Damage Data, Hiroshima	31
1.10	Building Damage and Orientation Data, Hiroshima	33
1.11	Building Damage and Orientation Data, Nagasaki.	34
1.12	Single-Story Wall Damage.	37
1.13	Multi-Story Buildings, Wall Damage.	38
2.1	Example Town.	44
2.2	Log-Normal Distance Damage Function	46
2.3	Significance of Vulnerability Uncertainty	51
2.4	Significance of Vulnerability Uncertainty	53
2.5	Significance of Vulnerability Uncertainty	54
2.6	Significance of Vulnerability Uncertainty	55
2.7	Significance of Vulnerability Uncertainty	56
2.8	Significance of Vulnerability Uncertainty	57
2.9	Significance of Vulnerability Variation to Structures in Core of City	60
2.10	Significance of Vulnerability Variation to Structures in Core of City	61
2.11	Significance of Vulnerability Variation to Structures in Core of City	62
2.12	Significance of Damage Criteria to Collateral Damage Predictions	65

<u>Figure</u>	<u>Page</u>
2.13 Significance of Damage Criteria to Collateral Damage Predictions.	66
2.14 Significance of Damage Criteria to Collateral Damage Predictions.	67
2.15 Significance of Damage Criteria to Collateral Damage Predictions.	68
2.16 Impact of σ_d on Shape of Distance Damage Function.	70
2.17 Significance of Distance Damage Sigma to Collateral Damage Predictions	72
2.18 Significance of Distance Damage Sigma to Collateral Damage Predictions	73
2.19 Significance of Distance Damage Sigma to Collateral Damage Predictions	74
2.20 Significance of Distance Damage Sigma to Collateral Damage Predictions	75
2.21 Example Town	78
2.22 Impact of Shielding on City Damage Predictions	82
2.23 Impact of Shielding on City Damage Predictions	83
2.24 Impact of Shielding on City Damage Predictions	84
2.25 Impact of Shielding on City Damage Predictions	85
2.26 Impact of Shielding on City Damage Predictions	86
2.27 Impact of Shielding on City Damage Predictions	87
2.28 Impact of Random Error on City Damage Predictions.	91
2.29a Distribution of Outcomes	92
2.29b Cumulative Distribution.	92
3.1 Example Town	98
3.2 Collateral Damage Predictions vs. Weapons Expended	100
3.3 Collateral Damage Predictions vs. Weapons Expended	101
4.1 Probability of Damage to Point Targets	109
4.2 Probability of Damage to Point Targets	110
4.3 Targeting Distance Damage Function	112
4.4 Damage Function Parameters	115

<u>Figure</u>	<u>Page</u>
4.5 Relationship Between Damage Function Parameters, (SIGMA-20)	117
4.6 Relationship Between Damage Function Parameters, (SIGMA-30)	119
4.7 Target Area Representation.	122
4.8 DGZ Locations for Comparing Damage Predictions.	125
4.9 Target Area Representation.	126
4.10a Damage Prediction Comparisons Circular Area Target, Offset/TR = 1	127
4.10b Damage Prediction Comparisons Circular Area Target, Offset/TR = 2	128
4.10c Damage Prediction Comparisons Circular Area Target, Offset/TR = 3	129
4.11 Comparison of Damage Predictions, Total Enumeration Vs. Prototype Algorithm	131
4.12 Example Town.	133
A.1 Example Town.	144
A.2 Significance of Vulnerability Uncertainty	145
A.3 Significance of Vulnerability Uncertainty	146
A.4 Significance of Vulnerability Uncertainty	147
A.5 Significance of Vulnerability Uncertainty	148
A.6 Significance of Vulnerability Uncertainty	149
A.7 Significance of Vulnerability Uncertainty	150
A.8 Significance of Vulnerability Variation to Structures in Core of City	151
A.9 Significance of Vulnerability Variation to Structures in Core of City	152
A.10 Significance of Vulnerability Variation to Structures in Core of City	153
A.11 Impact of Shielding on City Damage Predictions.	154
A.12 Impact of Shielding on City Damage Predictions.	155
A.13 Impact of Shielding on City Damage Predictions.	156
A.14 Impact of Shielding on City Damage Predictions.	157
A.15 Impact of Shielding on City Damage Predictions.	158
A.16 Impact of Shielding on City Damage Predictions.	159

<u>Figure</u>	<u>Page</u>
B.1 Flow Chart for Targeting Algorithm.	163
B.1 Flow Chart for Targeting Algorithm (Continued)	164

LIST OF TABLES

<u>Table</u>	<u>Page</u>
1.1 Damage Survey Data, Building Cluster Within GROUP 17, Nagasaki.	15
1.2 Damage Survey Data, GROUP 15, Nagasaki.	16
1.3 Damage Survey Data, GROUP 20, Nagasaki.	19
1.4 Damage Survey Data, GROUP 36, Nagasaki.	21
1.5 Damage Survey Data, GROUP 33, Nagasaki.	22
1.6 Damage Survey Data, GROUP 40, Nagasaki.	24
1.7 Distribution of Single-Story Buildings, Roof Damage . .	39
1.8 Distribution of Multi-Story Buildings, Roof Damage. . .	40
1.9 Vulnerability Ranges, Load-Bearing-Hall Structures. . .	40
2.1 Residential Statistical Description	45
2.2 Weapon System Parameters.	46
2.3 Targeting Variations to Assess Vulnerability Uncertainty	50
2.4 Targeting Parameter Variations to Assess Impact of Damage Criteria	64
2.5 Targeting Parameters Used to Assess Impact of σ_d Values.	71
2.6a Parameter Variations to Assess Impact of Assumed Shielding Consequences.	80
2.6b Parameter Variations to Assess Impact of Assumed Shielding Consequences.	81
3.1 Weapon Number Requirements, Blind Method vs. Shoot- Look-Shoot.	97
3.2 Targeting Parameters and Strategy, Blind vs. JLS. . . .	99
3.3 Collateral Damage Statistics for 1000 Structures. . . .	102
4.1 Damage Function Parameters, SIGMA-20.	116
4.2 Damage Function Parameters, SIGMA-30.	118
4.3 Targeting Parameters, Damage Prediction Comparisons . .	130

<u>Table</u>	<u>Page</u>
4.4a Data Input and Damage Prediction Results.	134
4.4b Data Input and Damage Prediction Results.	135
B.1 Problem Input Procedures.	163
B.2 Program Listing	167

Section 1

ANALYSIS OF JAPANESE STRUCTURES DATA

1.1 BACKGROUND

The Defense Nuclear Agency is currently sponsoring experimental and analytical research efforts directed towards defining and evaluating collateral damage issues relevant to residential structures. In particular, these research efforts are focusing on building vulnerability issues for structures common to small population centers located in western Europe. The principal structures of interest include single family detached housing units and multi-family dwellings. This latter group includes structures which also contain floor space allocated for commercial purposes.

This research effort is currently investigating building vulnerability primarily attributable to a nuclear weapon produced blast environment. Topics of interest include the importance of architectural design, construction materials and practice, and building geometry to the overall structural response under a blast loading environment. As previously indicated, these particular building characteristics are defined for residential dwelling units common to small urban areas. This general urban description is intended to include towns ranging in population size from about 5,000 to 15,000 people.

The experimental portion of this DNA-sponsored program is investigating the impact of shielding* on building damage created in a built-up urban area. It is anticipated that the evaluation of this empirical data will better define the extent and manner to which a

*Defined as having another structure "between" the blast and the building of interest that absorbs or deflects the blast wave.

free-field blast wave is perturbed when it encounters a built-up area. The information obtained from this data evaluation will be used in a structures vulnerability algorithm to determine the significance of the shielding phenomena relative to building damage and subsequent vulnerability estimates.

1.2 PURPOSE AND SCOPE OF ANALYSIS

The purpose of this analysis is to identify statistical signatures in the Japanese damage data base which may be relevant to the current research effort and collateral damage in general. Building damage as reported in the U.S. Strategic Bombing Survey^{1,2} will be reviewed for indicators which might suggest the significance of building characteristics relative to the reported damage. Additionally, this data will be explored for reported damage anomalies which could be attributable to the shielding concept previously mentioned.

This data analysis will focus exclusively on reported damage to masonry load-bearing-wall structures located at Hiroshima and Nagasaki. Although there were additional structure types reported in the bombing survey this particular category appears to be the most relevant for vulnerability questions about the residential dwellings of interest. In addition to the blast wave shielding issue, the data will be reviewed to detect damage variabilities attributable to building orientation relative to the blast wave and to structural characteristics including reported damage for single-story versus multi-story buildings. Where feasible, varying degrees of damage criteria will be considered for vulnerability comparisons.

The method of this data analysis will be of an exploratory nature accomplished primarily by data plots and graphs. The objective is to isolate trends and anomalies in the damage survey for specific questions of interest. As such, standard statistical methods such as were used in the Lulejian³ analysis will not be employed in this

investigation. While these classical type statistical methods were well suited for the purpose of the referenced analysis, they tend to break down for small data sets and are often insensitive to faint signatures in the data.

1.3 EXPLORATORY STATISTICAL ANALYSIS FOR BLAST WAVE SHIELDING

The objective of this analysis is to identify statistical signatures in the Japanese structures damage data which could be related to the shielding phenomena. This analysis will concentrate exclusively on masonry load-bearing-wall structures and only those structures reported in the Nagasaki damage survey. This type of structure was selected for the statistical signature analysis because its construction materials and behavioral response to airblast loading conditions could appear similar to the structures currently under investigation. The masonry load-bearing-wall buildings reported at Hiroshima were not included in this analysis due to insufficient detail in the damage survey for this city. Unlike the damage survey reported for Nagasaki, the building location information reported in the Hiroshima damage survey is not of sufficient detail to identify building cluster samples suitable for this analysis.

1.3.1 Data Included in Shielding Analysis

Six building cluster samples were selected from the Nagasaki damage survey for this analysis. Two of these clusters have 2 structures while the remaining four clusters have at least five buildings. Each of these six building clusters are described in the following paragraphs.

The first cluster was located about 1400 feet east of ground zero. This cluster, depicted in Figure 1.1, was part of a larger group of buildings denoted as GROUP 17 in the U.S. Strategic Bombing Survey. Building number 16, depicted in this figure, is the only load-bearing-wall structure in the illustrated cluster.

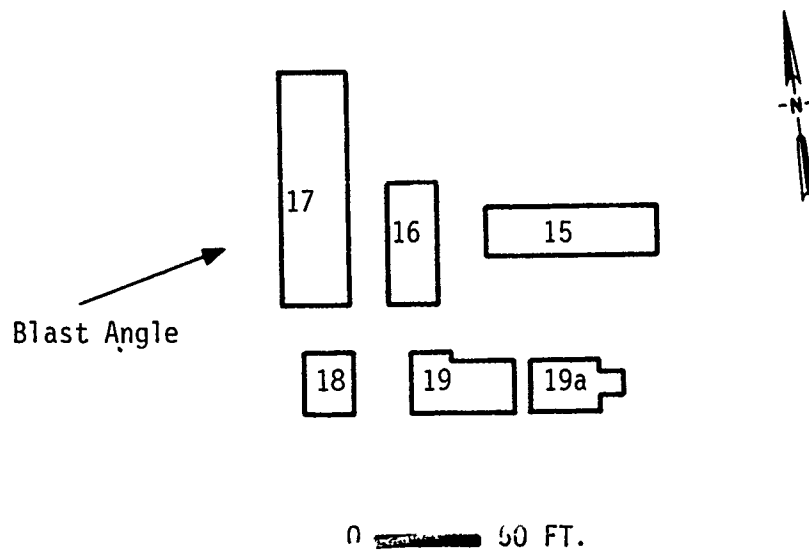


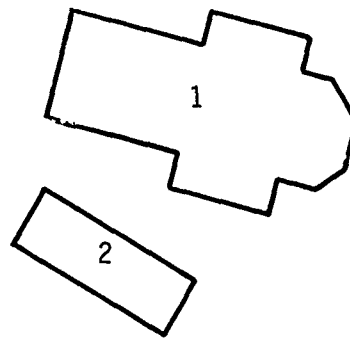
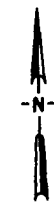
Figure 1.1 Building Cluster, GROUP 17, Nagasaki

Table 1.1 presents characteristics of the buildings in this cluster and includes summary comments as to the reported damage.

The second building cluster contains only two structures as depicted in Figure 1.2. This cluster, referenced as GROUP 15 in the damage survey, was situated about 1800 feet east north-east of ground zero.

Table 1.1 Damage Survey Data, Building Cluster Within GROUP 17, Nagasaki

Building Identification Number	Structure Type	Exterior Walls	Ground Floor Dimensions (Feet)	Eave Height (Feet)	Comments
15	Single-Story Wood Frame	U	U	U	Totally demolished
16	Load-Bearing	13" Brick	20 x 57	U	Wall collapsed by blast
17	Single-Story Wood Frame	U	U	U	Totally demolished
18	d.o.	U	U	U	d.o.
19	d.o.	U	U	U	d.o.
19a	d.o.	U	U	U	d.o.



Blast Angle

0 — 50 FT.

Figure 1.2 Building Cluster, GROUP 15, Nagasaki

Table 1.2 contains a description of these structures and damage comments as reported in the damage survey.

Table 1.2 Damage Survey Data, GROUP 15, Nagasaki

Building Identification Number	Physical Characteristics	Comments
1	Single-story load-bearing 28" brick walls 40' eave height 126' x 215' dimensions	Most walls demolished
2	Wood frame 45' x 125' dimensions U eave height	Completely demolished

The third cluster, a subset of buildings in GROUP 20, was located about 2800 feet south south-east of ground zero. Four buildings are contained in this cluster as depicted in Figure 1.3. Also shown in this figure is a partial description of the buildings in GROUP 40 which were located about 6300 feet south of ground zero.

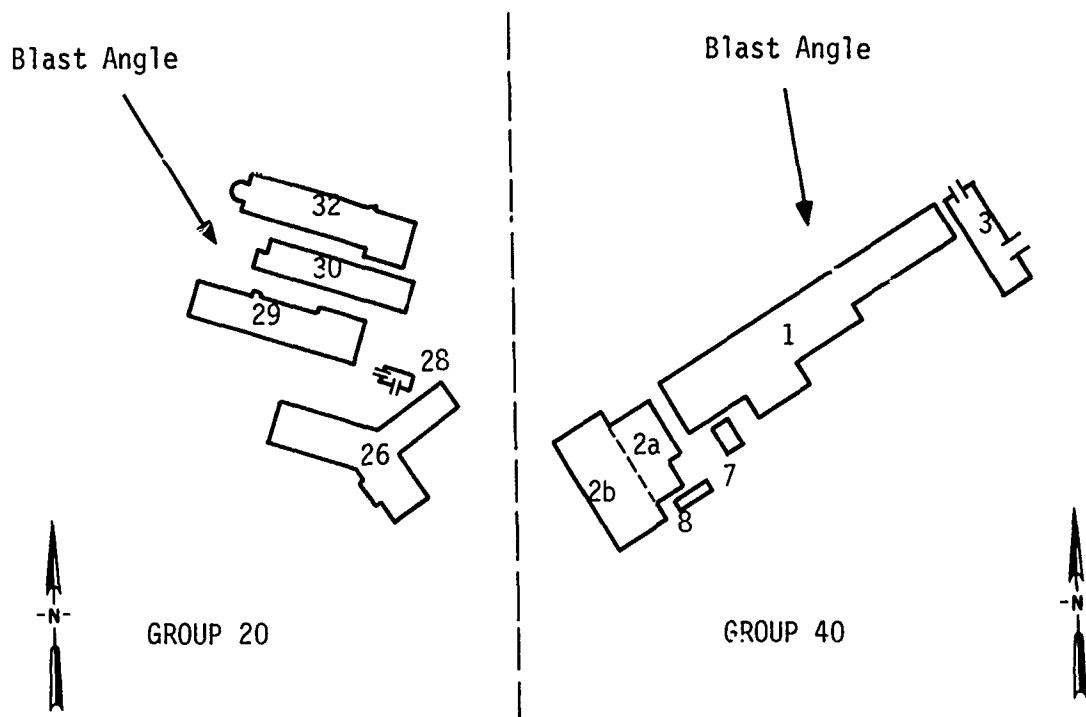


Figure 1.3 Building Cluster, GROUP 20 and GROUP 40
Nagasaki

This partial description of GROUP 40 is presented with the cluster description of GROUP 20 to demonstrate a possible anomaly in the reported damage data. In particular, the damage sustained by Building 28 in GROUP 20, when compared with the damage to Building 3 in GROUP 40, may represent a data signature related to the shielding phenomena. The comparative damage information between these two structures is indicated on the following page.

- Both structures, 20; 28 and 40; 3, sustained a comparable level of damage, i.e., two walls collapsed. Structure 20; 28 may have been exposed to about 25 psi whereas building 40; 3 may have been exposed to only about 4 psi. These structures had comparable brick wall thickness dimensions.
- Both structures were oriented in the same manner relative to the approaching blast wave. The two collapsed walls of building 40; 3 were those directly positioned toward the blast wave. Just the opposite occurred, however, for building 20; 28.
- Building 20; 28 was located within the shadow of building 20; 29, i.e., the separation distance was apparently less than the height of building 20; 29. The three structures immediately "in front" of building 20; 28 were considerably larger than this structure, two of which were known to be at least 3 times greater in height. These two taller structures sustained virtually no structural damage.
- There were no reported structures in the vicinity of building 40; 3 that should have perturbed the blast loading on this structure.

Table 1.3 contains additional information relevant to the structures in this cluster and Building 3 in GROUP 40.

Table 1.3 Damage Survey Data, GROUP 20, Nagasaki

Identification Group; Building	Structure Type	Exterior Wall Thickness (Inches)	Ground Floor Dimensions (Feet)	Eave Height (Feet)	Comments
20; 28	Load-Bearing	13	15 x 33	14	North and East Walls Intact, Remainder of Structure Demolished. Approximately 50 Feet Removed From Building 20; 29.
20; 29	3-Story Reinforced Concrete	--	45 x 200	52	Virtually No Structural Damage
20; 30	1-Story Wood Frame	--	40 x 185	U	Completely Destroyed
20; 31	3-Story Reinforced Concrete	--	45 x 200	54	Virtually No Structural Damage
40; 3	Load-Bearing	12	22 x 95	18	South Wall Cracked and Partly Wrecked; West Wall Almost Intact; Remainder of Structure Demolished

The fourth cluster of interest was identified in GROUP 36 located about 5300 feet south of ground zero. As depicted in Figure 1.4, 7 structures are contained in this cluster.

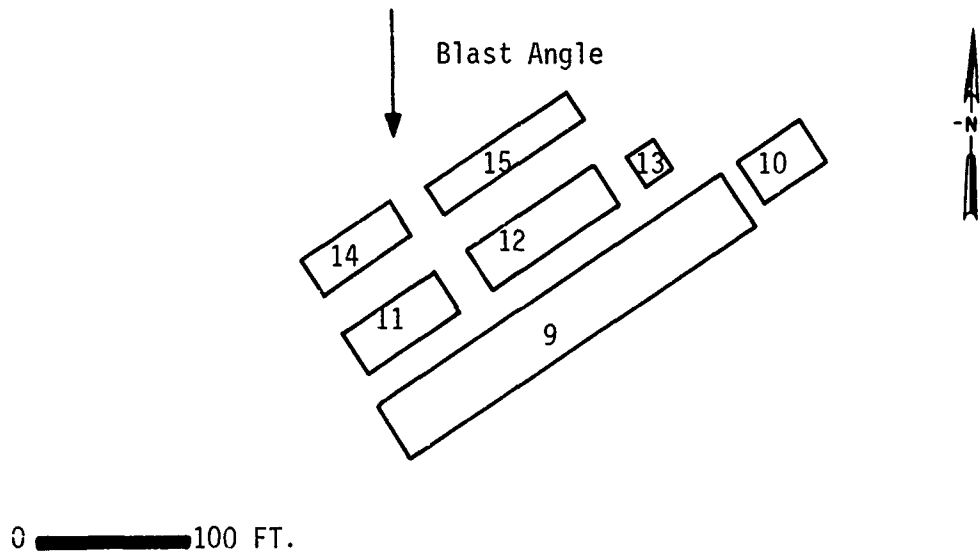


Figure 1.4 Building Cluster Within GROUP 36, Nagasaki

Table 1.4 contains damage survey information relevant to this cluster.

Table 1.4 Damage Survey Data, GROUP 36, Magasaki

Building Identification Number	Physical Characteristics	Comments
9	Single-story load-bearing wall Wall thickness: U Eave height: 14' Dimensions: 42' x 256'	Almost completely demolished
10	Single-story reinforced concrete 10" exterior walls Eave height: 20' Dimensions: 32' x 48'	No structural damage
11, 12, 13, 14	Single-story load-bearing wall Information missing or not well defined	Demolished
15	Single-story wood frame Eave height: 10' Dimensions: 20' x 120'	Demolished

The fifth cluster, denoted as GROUP 33 in the damage survey, consists of two buildings. This cluster, depicted in Figure 1.5, was located about 5400 feet south of ground zero.

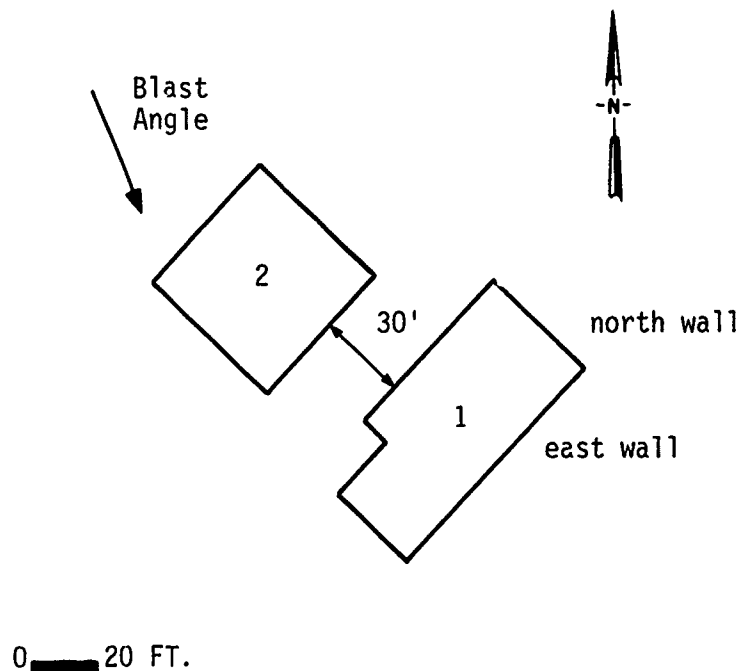


Figure 1.5 Building Cluster, GROUP 33, Nagasaki
 Building characteristics and reported damage are summarized in Table 1.5.

Table 1.5 Damage Survey Data, GROUP 33, Nagasaki

Building Identification Number	Physical Characteristics	Comments
1	Single-story load-bearing-wall 12"-18" brick walls Eave Height: 32' Dimensions: 40' x 83'	East wall blown in; north wall demolished
2	Single-story load-bearing-wall 12" brick walls Eave Height: 20' Dimensions: 50' x 50'	Completely demolished

The sixth cluster included in this analysis is contained in Building GROUP 40. This group was located about 6400 feet south of ground zero. The buildings included in this cluster are depicted in Figure 1.6. The shading in this figure indicates load-bearing-wall structures. Details of the buildings in this cluster are presented in Table 1.6.

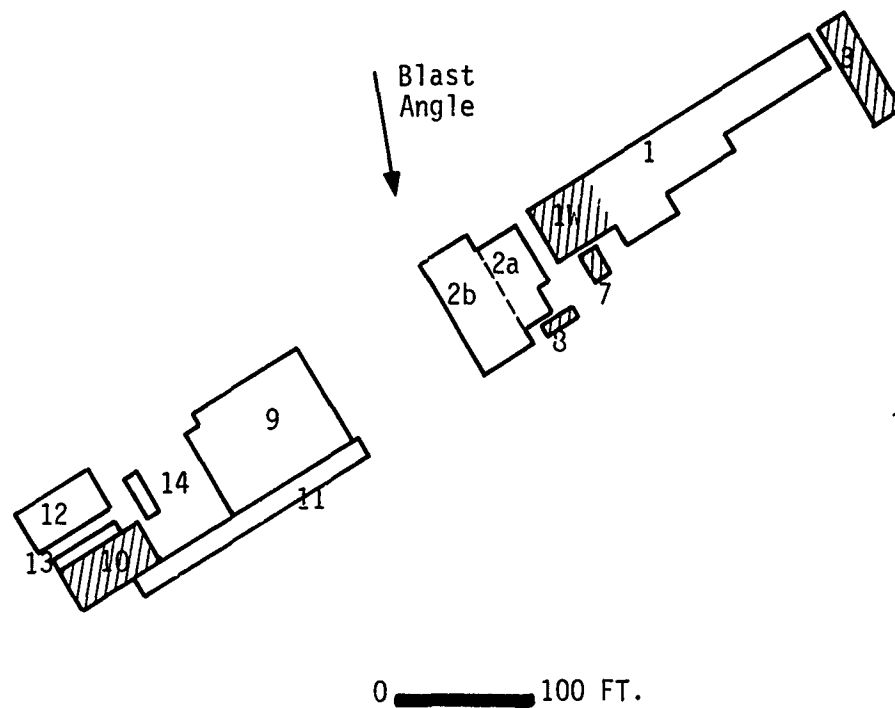


Figure 1.6 Building Clusters Within GROUP 40, Nagasaki

Table 1.6 Damage Survey Data, GROUP 40, Nagasaki

Identification Group; Building	Structure Type	Exterior Wall Thickness (Inches)	Ground Floor Dimensions (Feet)	Eave Height (Feet)	Comments
40; 10	Load-Bearing	12	38 x 74	20	Part of West Wall Still Standing, Otherwise Demolished
40; 13	Single-Story Wood Frame	--	11 x 50	10	Canted Toward Southwest but Still Standing
40; 12	One-Story Shed	--	U	U	Completely Demolished
40; 2A	Single-Story Steel Frame	--	33 x 65	15	Steel Columns Distorted But in Place
40, 2B	Single-Story Wood Frame	--	40 x 90	U	Completely Demolished
40; 1W	Load-Bearing	12	30 x 50	13	Walls Collapsed Southward
40; 7	Load-Bearing	8	12 x 27	9	Roof Collapsed, Minimal Damage to Exterior Walls
40; 8	Load-Bearing	12	19 x 31	13	Roof Collapsed, Minimal Damage to Exterior Walls

1.3.2 Exploratory Statistical Data Analysis

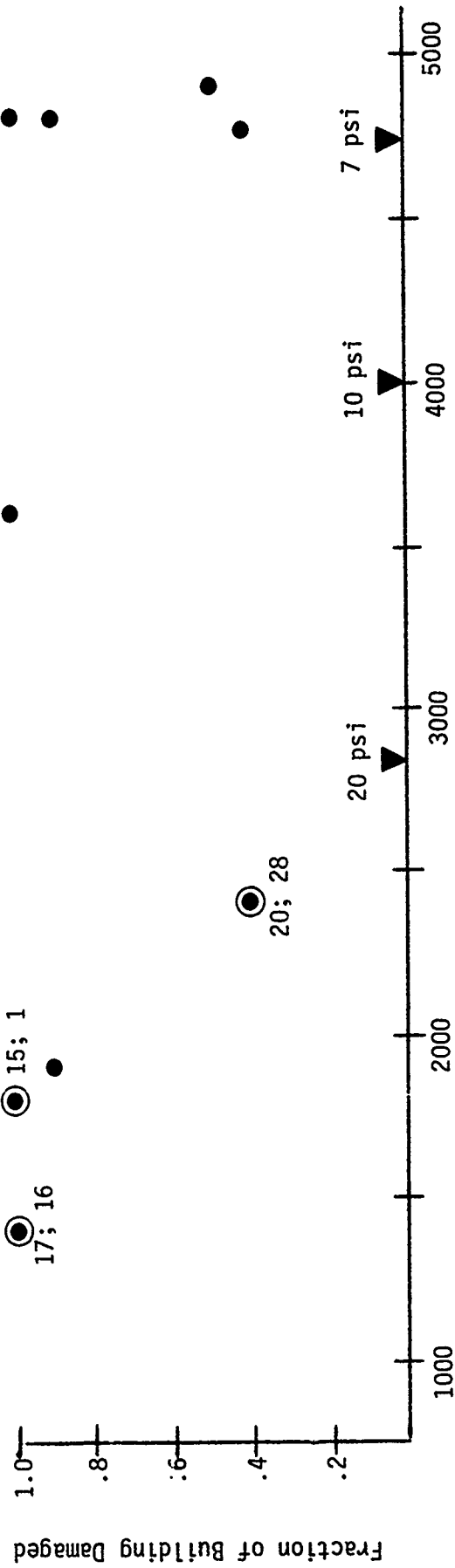
Given the data presented in the previous paragraphs the objective of this analysis is to determine if this damage data appears to be inconsistent with the damage reported for all load-bearing-wall structures. Specifically, this analysis will focus on identifying trends in the reported damage data that would distinguish those structures which may have sustained lesser damage because of their proximity to adjacent structures.

Figures 1.7a and 1.7b depict the distance damage data, as reported in the damage survey, for single-story load-bearing-wall structures at Nagasaki. The circled data points depicted in these figures denote the buildings which may have been shielded from the blast wave due to their position within a building cluster. Damage data reported for structures in excess of 9000 feet from ground zero are not included in these figures since they did not appear to be relevant to this analysis. The peak surface overpressure values included in these figures are based upon an assumed weapon yield of 22 KT and an actual height of burst of 1650 feet.

The statistical exploratory analysis for this data set is as follows.

- Visually observing all data points there is no apparent tendency for the circled observations to appear at a lesser fractional damage value with increasing ground range than does the population as a whole.
- Where data points are clustered within a small range interval there is no apparent signature in the reported fractional damage data to suggest that shielded structures were less vulnerable to damage than were all structures within the range interval. For example, in the 5000-5500 feet range interval all structures were reported at an equivalent level of damage. Likewise, within the range interval of about 6200-6700 feet structures which may have been shielded do not appear to have been less vulnerable than were all the structures overall.

STRUCTURAL WALL DAMAGE
SINGLE STORY LOAD-BEARING-WALL STRUCTURES



Range From Ground Zero - Feet
Figure 1.7a Distance Damage Data, Nagasaki

STRUCTURAL WALL DAMAGE
SINGLE STORY LOAD-BEARING WALL STRUCTURES

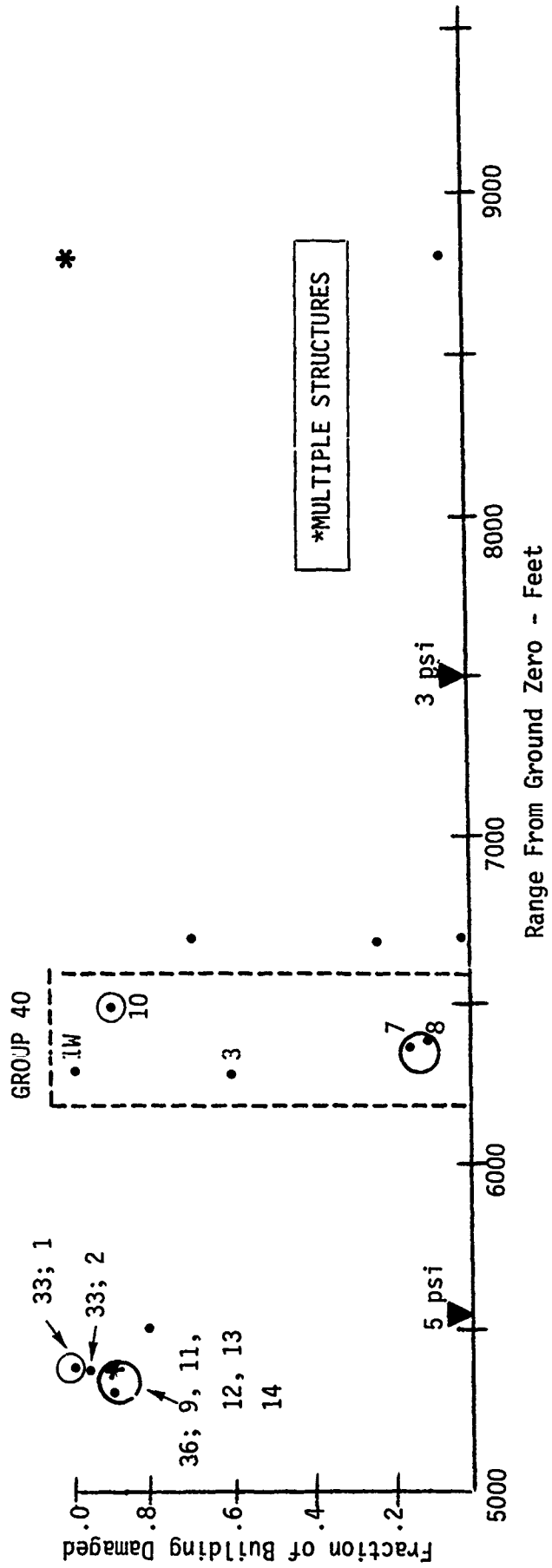


Figure 1.7b Distance Damage Data, Nagasaki

Based upon these observations in context of the total sample population there is no apparent statistical signature to suggest that the shielded structures, as a subgroup, may have been less vulnerable than the entire population overall.

The vulnerability engineer should not necessarily conclude from the absence of a data trend, however, that shielding did not influence the resultant damage. The proper inference to be made from this analysis is that a shielding signature in the damage data does not appear to exist. This statement need not be equivalent to a conclusion that shielding is not a major factor or that a shielding factor was not present at Nagasaki for this type of structure. There are a multitude of possible reasons why a statistical signature for shielding cannot be detected in the data. The first and strongest argument applies to the data itself and the completeness to which it was reported in the damage survey. Although the Nagasaki data may be the largest empirical source of information for questions of shielding the fact still remains that this is happenstance data. As such, it is not necessarily fair to conclude that a similar inference would be drawn from a controlled experiment. In addition, the spatial geometry and building characteristics reported in the survey may not be of sufficient detail to uncouple the shielding signature from the data. For example, the eave height of structures was not always reported. For whatever reason this data was omitted, the absence of this information in several instances precluded knowing the height of a structure on the cluster boundary. Obviously, this kind of information is necessary to properly evaluate the data.

Although a statistical approach cannot resolve the question of shielding at Nagasaki, the cluster data presented in the previous paragraphs may be of use for a comparative engineering analysis approach to evaluating this data for shielding consequences. For example, the brief discussion of comparative damage results presented within the building cluster information for GROUP 20 may be relevant to this shielding issue from an engineering viewpoint.

1.4 CORRELATION OF BUILDING ORIENTATION WITH REPORTED DAMAGE

The objective of this analysis is to identify signatures in the damage data which would suggest that building orientation relative to the approaching blast wave may have influenced the resultant damage. This analysis will focus on damage data trends for single-story load-bearing-wall structures reported at Hiroshima and Nagasaki, and multi-story load-bearing-wall structures at Hiroshima. Damage data from Nagasaki for this latter building-type will not be considered since these buildings were apparently too far removed from ground zero for any damage to occur.

The method to be used in this analysis will be the same as that used in the previous section. The objective is to detect trends in the distance damage data as reported in the damage survey for the respective cities. Specifically, this analysis will focus on identifying damage data anomalies between 3 general groupings of building orientation. These 3 groupings are defined to be normal, parallel, and approximately 45 degrees. This first group, denoted by normal, will consist of those buildings for which the major (long) axis of the structure was approximately perpendicular to the approaching blast wave. The group referred to as parallel consists of buildings for which the major axis of the structure was parallel to the approaching blast wave. The third group consists of those structures for which the diagonal building vector tended to be parallel to the approaching blast wave. Figure 1.8 depicts the geometry of these 3 groups relative to the approaching blast wave.

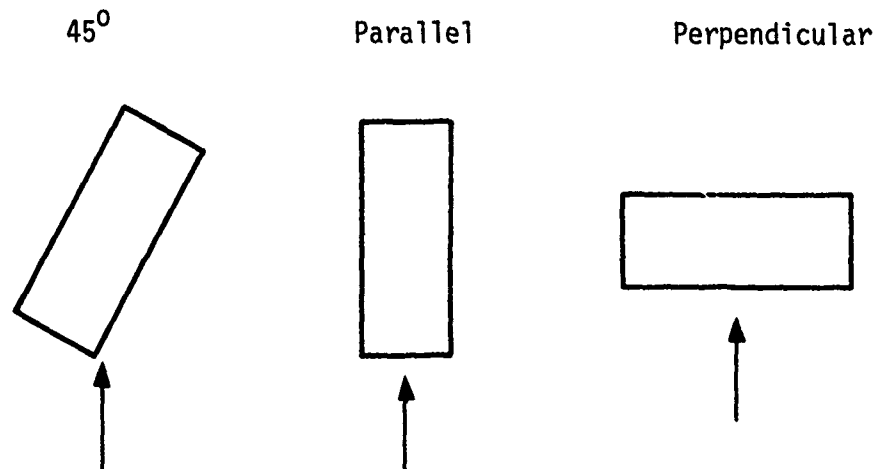


Figure 1.8 Building Orientation Groups

1.4.1 Analysis of Multi-Story Load-Bearing-Hall Buildings

The method used in this analysis to identify a correlation between angle of blast wave attack and reported damage is an application of exploratory statistics using plotted data. Figure 1.9 depicts the reported building damage versus ground range from the burst point at Hiroshima. The peak surface overpressure indicators presented in this figure are based upon a weapon yield of 12 KT and an actual burst height of 1850 feet. The symbol associated with each building data point denotes orientation relative to the approaching blast wave. These symbols are defined by the key in this figure. Although there were buildings beyond the range depicted in this figure they were reported as undamaged. As such, they cannot provide any additional information.

Based upon the information plotted in Figure 1.9 there is no apparent signature in the data to support an argument that orientation was an important factor in the resultant building damage. This statement is simply based upon the absence of between group differences in the reported damage. That is, of the 3 orientation groups no one group stands out as being more vulnerable than the population as a whole.

1.4.2 Analysis of Single-Story Load-Bearing-Wall Structures at Hiroshima

The same method of analysis will be applied to this data set as was demonstrated for the multi-story structures. Figure 1.10 depicts the reported distance damage data and the corresponding building orientation information. Building damage data for structures within 3000 feet and in excess of 8000 feet from ground zero were intentionally omitted to facilitate depicting the data most applicable to this analysis. These structures, omitted from the figure, were either demolished or undamaged, respective to these 2 range intervals.

Based upon the plotted data in Figure 1.10 there is, again, no data trend signature correlating building orientation with the resultant damage. This data set is more informative than the previous set, however, in that there is an overlap of damaged and undamaged data points between 5500 and 8000 feet from ground zero. The numbers directed toward these data points denote the brick wall thickness values for the individual structures as reported in the damage survey. Based upon these wall thickness values it appears that the noise in the damage data over this range interval can be attributed to vulnerability differences between structures with 19" brick walls and those with 9"-13" thick brick walls.

1.4.3 Analysis of Single-Story Load-Bearing-Wall Structures at Nagasaki

The data used for this analysis is depicted in Figure 1.11. The structures beyond 9000 feet from ground zero were intentionally omitted. These structures do not provide any additional insight into the question of orientation. Although there was considerable noise in the damage data between 4000 feet and 7000 feet from ground zero, it is not too difficult to observe a somewhat random scatter for the 3 orientation groupings. The only apparent anomaly in the orientation signature is the data point at about 2400 feet from ground zero reported to be 40 percent damaged. Most likely, the reported damage fraction

STRUCTURAL WALL DAMAGE
SINGLE STORY LOAD-BEARING-WALL STRUCTURES

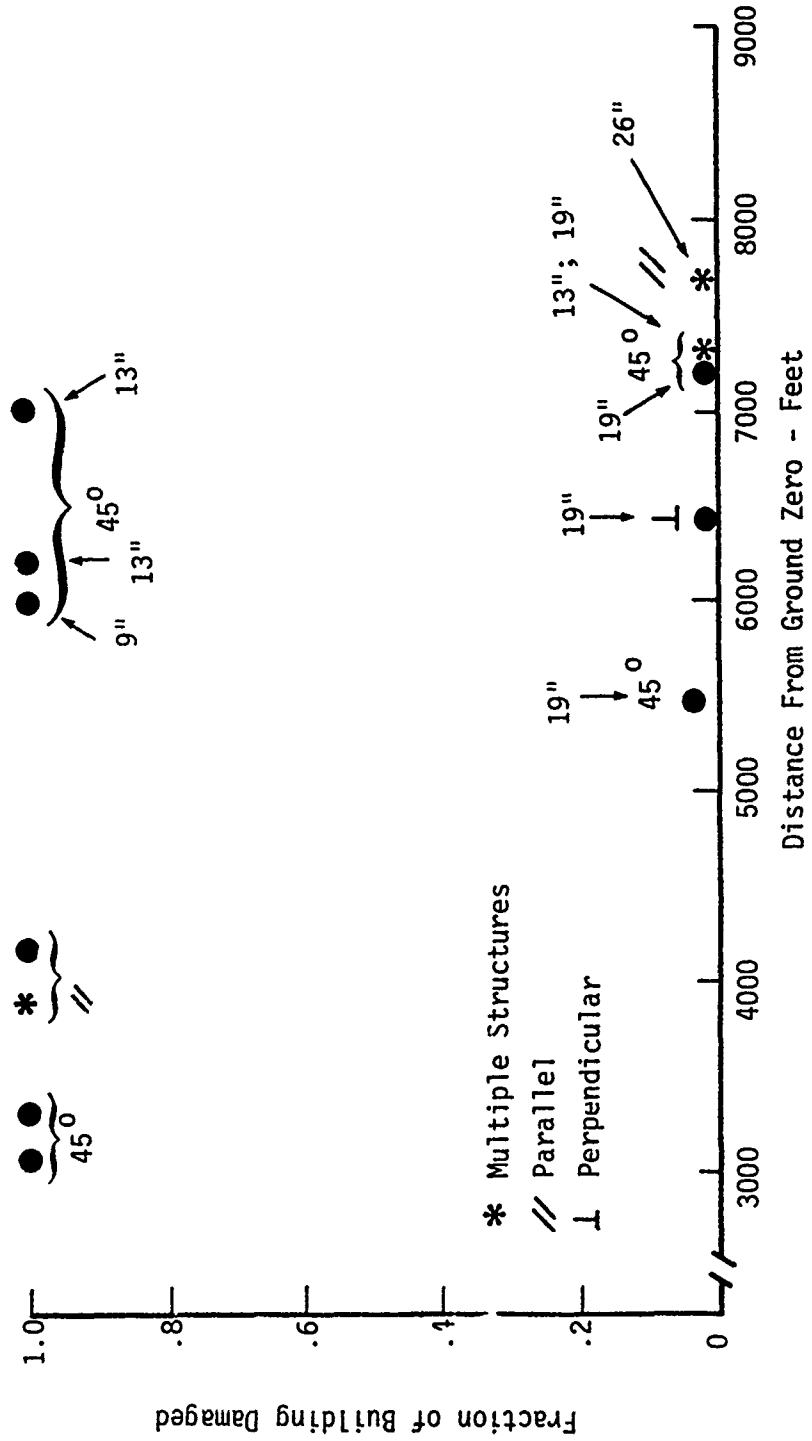


Figure 1.10 Building Damage and Orientation Data, Hiroshima

STRUCTURAL WALL DAMAGE
SINGLE-STORY LOAD-BEARING-WALL STRUCTURES

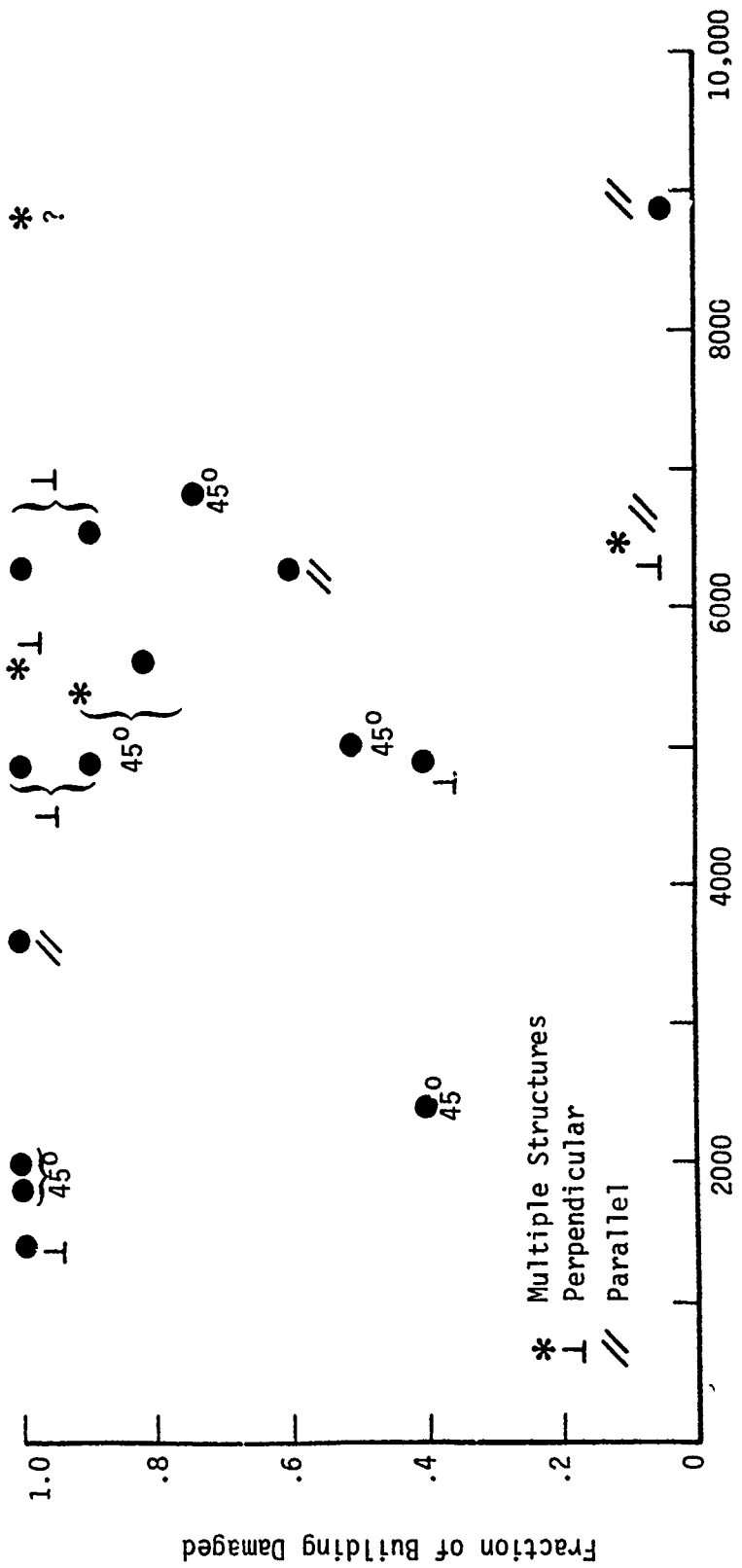


Figure 1.11 Building Damage and Orientation Data, Nagasaki

is incorrect since there were other structures with comparable damage reported to be 100 percent damaged.

1.4.4 Summary

Approximately 70 buildings combined over both cities were included in this analysis. Of this total, approximately 25 may have been subjected to at least 10 psi peak surface overpressure. The remaining 45 buildings were fairly evenly dispersed over a range interval where the predicted peak surface overpressure would fall from about 10 psi to 2 psi. All of the load-bearing-wall structures reported to have sustained at least some degree of structural wall damage are included within this combined range interval, i.e., ground zero out to the ground range at which 2 psi would be predicted. Considering all of this data, there is no apparent signature in the damage that would suggest a correlation between building orientation and the resultant building damage.

1.5 VULNERABILITY EVALUATIONS FOR LOAD-BEARING-WALL BUILDINGS

The purpose of the following analysis is to extract vulnerability information from the Japanese damage data for use in targeting sensitivity analyses presented in a subsequent section of this document. This targeting analysis is intended to demonstrate the impact of damage criteria and vulnerability uncertainties on collateral damage predictions. In particular, the targeting analyses will focus on vulnerability issues for predicting collateral damage to residential structures located in small urban areas typical to western Europe. The vulnerability information to be used in this targeting analysis will be based on an interpretation of damage data for single-story and multi-story load-bearing-wall structures included in the damage surveys reported at Hiroshima and Nagasaki. This vulnerability interpretation to be developed in the following analysis will reflect a range of vulnerability assessments for 3 damage criteria. No effort will be made in this analysis to quantify a best vulnerability value

within the range of determined values. The principal reason for not identifying a best vulnerability value is that any one single value extracted from this data may be highly conditional on the Japanese experience. That is, a most probable vulnerability value derived from this data source may not necessarily be a most probable value for residential structures in western Europe. As such, quantifying a range of vulnerability values from this data source representing near absolute vulnerability bounds for a multitude of varying building shapes and physical properties may better serve the purposes of the targeting analysis.

The damage data analysis presented in the following paragraphs will develop a range of vulnerability values for each of 3 damage criteria. These 3 damage criteria are:

- Wall damage - collapse of at least one load-bearing wall
- Roof Damage - collapse of at least 1/2 of the structural roof support members
- Superficial damage - any physical damage sustained by a structure in excess of window breakage.

The major portion of this analysis consisted of reviewing damage descriptions and supporting photos in the survey literature. The objective was to identify those structures that sustained sufficient damage to satisfy these damage definitions. The following paragraphs present the results of this analysis.

1.5.1 Wall Damage To Load-Bearing-Wall Structures at Japan

To develop a range of vulnerability values for collapse of at least 1 exterior wall the damage data was plotted within overpressure range bins. Figure 1.12 depicts this plotted data for all single-story buildings reported in the damage surveys. The method used for determining which bin a structure would be placed in was based upon

SINGLE-STORY LOAD-BEARING-WALL-STRUCTURES
JAPANESE DATA

Wall Thickness

- A >20"
- B 16-20"
- C 12-16"
- D 8-12"
- U Unknown

35 Structures at ranges
outside 2 psi; no wall damage

■ at least one wall collapsed

* no data

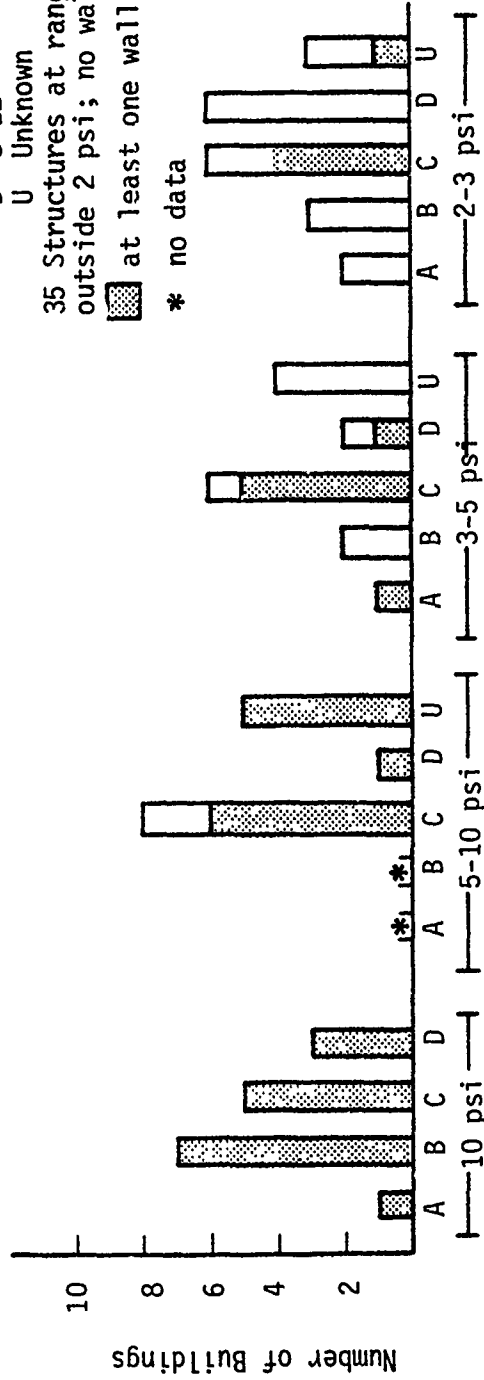


Figure 1.12 Single-Story Wall Damage

MULTI-STORY LOAD-BEARING-WALL STRUCTURES
JAPANESE DATA

Wall Thickness

- A > 20"
- B 16-20"
- C 12-16"
- D 8-12"
- U Unknown

24 Structures at ranges outside
2 psi; no wall damage

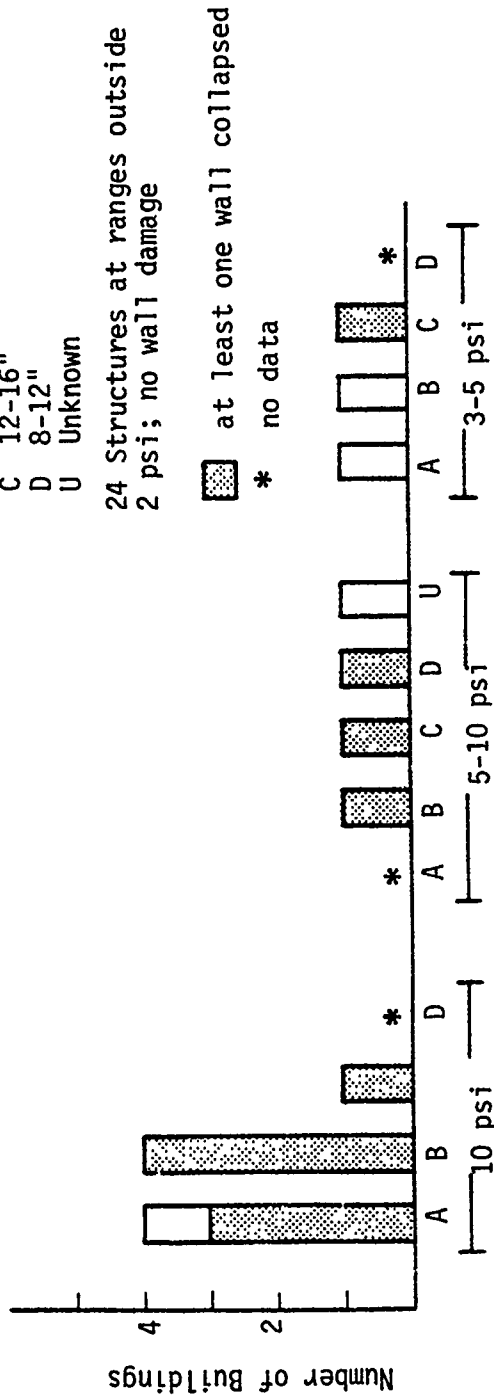


Figure 1.13 Multi-Story Buildings, Wall Damage

the predicted peak surface overpressure value at the building for the weapon yield and height of burst assumptions previously mentioned. As may be observed from this plotted damage data the transition from no wall damage to at least 1 wall collapsed tends to occur in the 3-5 psi bin for most of the structures. Accordingly, this range will be used in the subsequent targeting analysis for wall damage to single-story structures.

Figure 1.13 depicts similar damage information for the multi-story structures surveyed in Japan. It is readily apparent from this plotted data that the transition from survival to failure in terms of wall collapse tends to range between 5 psi and 10 psi for all multi-story structures.

1.5.2 Roof Damage To Load-Bearing-Wall Structures

A comparable data analysis was performed for the roof damage criteria mentioned previously. The distribution of buildings damaged within each bin are depicted in Tables 1.7 and 1.8. Table 1.7 illustrates the distribution of single-story structures sustaining roof damage within each of the 4 bins. Based upon the information in this table a range of 2 psi-4 psi was selected for the subsequent targeting analyses.

Table 1.7 Distribution of Single-Story Buildings, Roof Damage

BIN	NUMBER FAILED	NUMBER SURVIVED	TOTAL
<2 psi	0	35	35
2-3 psi	37	9	46
3-4 psi	2	2	4
>4 psi	13	2	15

Table 1.8 contains similar information for roof damage to multi-story structures. Based on the information in this table a range of 3 psi-5 psi was selected for roof damage to multistory structures.

Table 1.8 Distribution of Multi-Story Buildings, Roof Damage

BIN	NUMBER FAILED	NUMBER SURVIVED	TOTAL
<3 psi	0	24	24
3-5 psi	2	1	3
>5 psi	15	1	16

1.5.3 Superficial Damage to Load-Bearing-Wall Structures

Review of the damage data at Nagasaki and Hiroshima indicated that only 2 of approximately 140 load-bearing-wall structures sustained superficial damage outside the predicted 2 psi peak surface overpressure contours. At predicted overpressure values in excess of 3 psi the majority of structures were experiencing the structural roof damage criteria. This trend in the damage data applies to both the single-story and multi-story structures. Accordingly, a range of 2 psi-3 psi was selected for superficial damage.

1.5.4 Damage Analysis Summary

A summary of the vulnerability ranges extracted from the Japanese data are presented in Table 1.9.

Table 1.9 Vulnerability Ranges, Load-Bearing-Wall Structures

BUILDING	DAMAGE CRITERIA		
	SUPERFICIAL	ROOF	WALL
Single-story	2-3 psi	2-4 psi	3-5 psi
Multi-story	2-3 psi	3-5 psi	5-10 psi

These vulnerability ranges will be used in the subsequent targeting analyses to assess the impact of vulnerability uncertainty in a collateral damage context.

It should be noted that these vulnerability ranges are not intended to convey any statistical statement of confidence. These intervals merely represent the range over which most of the structures were reported to have been damaged according to the criteria previously given. Also, these ranges are being extended to include the vulnerability of residential structures in western Europe primarily on a heuristic argument. The completion of DNA sponsored current research should determine the relevancy of these vulnerability ranges to describing European residential structure vulnerability values.

Section 2

COLLATERAL DAMAGE SENSITIVITY ANALYSES

2.1 OBJECTIVE AND SCOPE OF ANALYSIS

The objective of this analysis is to demonstrate the significance of uncertainty in targeting parameters to damage prediction estimates with respect to collateral damage. This analysis will address both aspects of the general meaning of uncertainty, that is, random as well as non-random error. This random error component often discounted in large scale targeting analyses may be a very important factor when the objective is to minimize or constrain the extent of collateral damage in a localized area.

There are 5 topics which will be addressed in this analysis. These particular topics and a brief discussion of each is presented as follows.

1. Vulnerability Uncertainty. The objective in reviewing this topic is to quantitatively demonstrate the significance of non-random error in a vulnerability estimate with regard to predicting collateral damage. The vulnerability information used in this analysis is an interpretation of the Japanese experience. In particular, the vulnerability information, presented in Section 1.5.4, for load-bearing wall structures will be used exclusively throughout this analysis.

2. Damage Criteria. Again, based upon an interpretation of the Japanese data this analysis will attempt to demonstrate the significance of various damage criteria that could be used to define the physical damage aspect of collateral damage.

3. Distance Damage Sigma. In the mathematics for predicting target damage the distance damage sigma is intended to be a measure of random uncertainty in target resistance and the weapon-produced environment. As will be explained in further paragraphs this measure

is believed to be an important factor toward collateral damage. Accordingly, this analysis attempts to demonstrate the significance of varying this measure.

4. Significance of Shielding to Collateral Damage. Although the data analysis did not identify a data trend signature for shielding it is possible that it did have some role in the resultant damage. The purpose of this analysis is to quantify the significance of shielding under somewhat arbitrary but possibly bounding conditions for this phenomenon.

5. Random Variability. Most nuclear weapon targeting analyses rely exclusively on the expected damage estimate for planning and evaluating targeting scenarios. As such, consideration is not given to the range of possible outcomes that could occur other than the expected or average outcome. By itself, the expected outcome may not be a sufficient measure to ensure collateral damage is held to a minimum. The objective of this analysis is to measure this variability and demonstrate its impact on attempting to restrict collateral damage.

2.2 CITY DAMAGE ANALYSIS

The ultimate objective of this analysis is to demonstrate the significance of these 5 targeting factors in a collateral damage context. As a means toward achieving this objective the subsequent analyses are demonstrated for a small urban population center located in western Europe. This town, depicted in Figure 2.1 has a population of approximately 7000 people and covers an area of roughly 2 square miles.

The residential dwelling units in this town are basically of two general configurations. The core of the town, highlighted in Figure 2.1, tends to consist of multi-story structures that serve both a commercial and residential housing function. The structures removed from the city core are primarily single family two story structures. Based upon the detail shown on this map, the total population size,

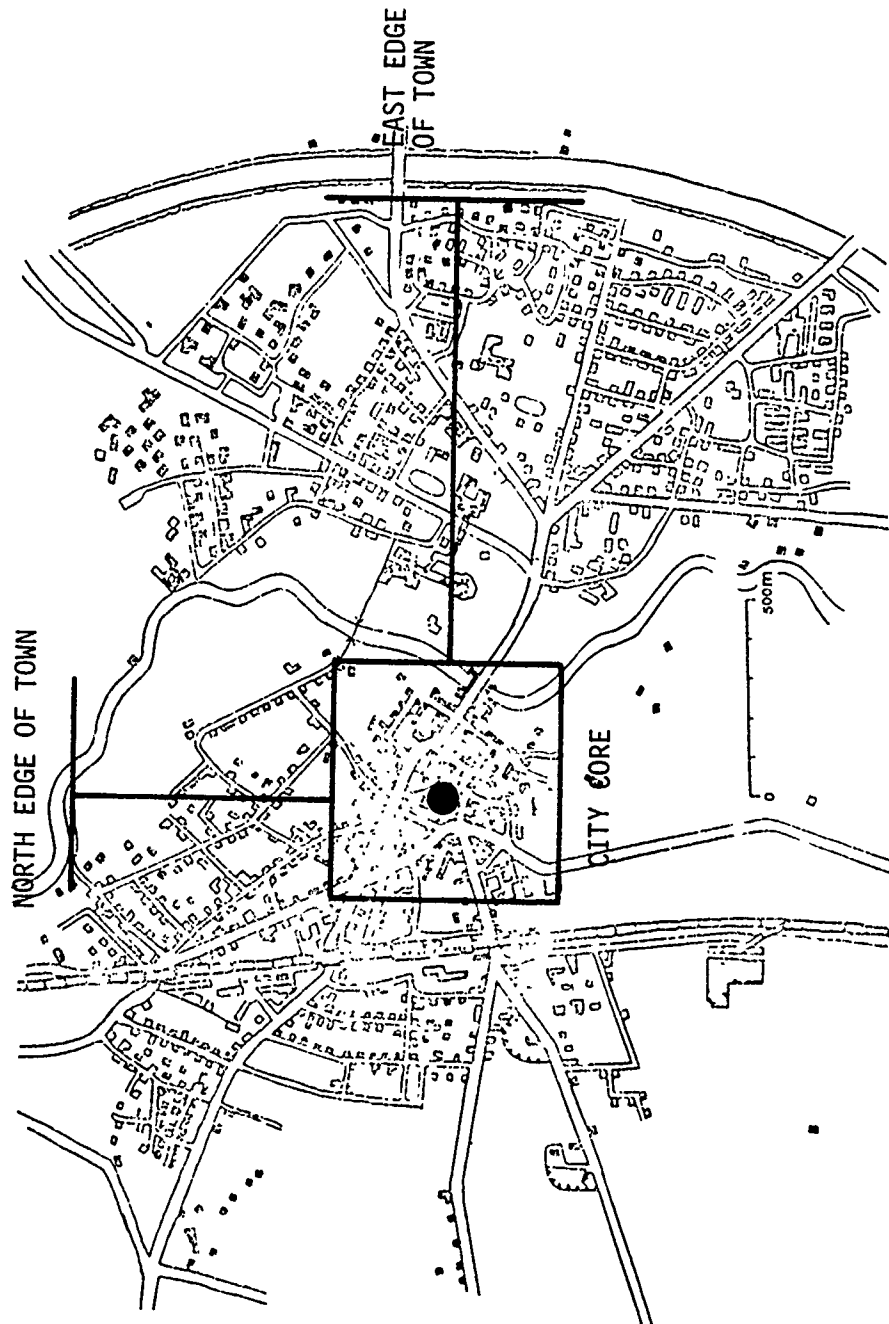


Figure 2.1 Example Town

and auxiliary information, Table 2.1 presents a simple statistical description of this city.

Table 2.1 Residential Statistical Description

LOCATION	ESTIMATED TOTAL RESIDENTIAL STRUCTURES	ESTIMATED AVERAGE NUMBER OF PEOPLE PER STRUCTURE
City Core	200	20
Suburb	800	4

In the subsequent collateral damage analyses the predicted damage is expressed as a percentage of all residential structures. This damage prediction was assessed by evaluating each of the approximately 1000 structures. As such, these analyses are not based upon an area model representation of the city but rather a total enumeration of each identified structure. These city damage predictions are presented in terms of the DGZ location relative to an origin selected near the center of the town. This central reference location is depicted in Figure 2.1. The DGZ locations were selected along a north and east axis originating at this central reference point. The "edge of town" markers depicted in Figure 2.1 are presented in each set of damage prediction curves for additional location reference purposes.

The damage sensitivity analyses are demonstrated for two tactical-type weapon systems, and two azimuthal directions measured from the city core. This city "center" reference point is depicted in Figure 2.1. The two weapon systems will be referred to as the 1 KT system and the 10 KT system. The actual parameter values used for these two systems are given in Table 2.2.

Table 2.2 Weapon System Parameters

PARAMETER	1 KT SYSTEM	10 KT SYSTEM
Yield (KT)	1	10
Scaled Height of Burst (FT/KT ^{1/3})	400	200
CEP (FT)	150	150

2.3 DAMAGE PREDICTION METHODOLOGY

The targeting mathematics used in this analysis were taken directly from the Defense Intelligence Agency publication, DI-550-27-74.⁴ The analytic form of the distance damage function is the compliment of a cumulative log normal distribution. This distribution can be characterized by two parameters, the weapon radius WR, and the distance damage sigma σ_d . The mathematical definition of these two parameters is presented in section 4.3 of this report. Basically, this damage prediction function is defined to be a value of 1 at ground zero and is asymptotic to zero with increasing ground range. Figure 2.2 depicts the general form of this function.

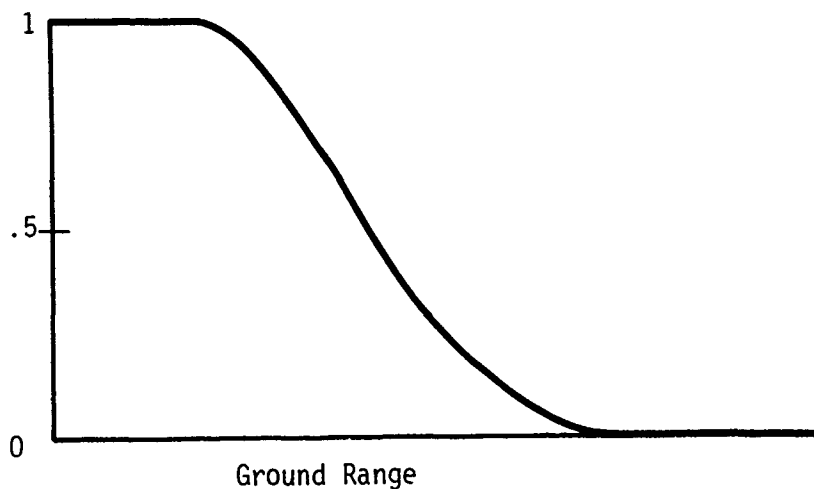


Figure 2.2 Log-Normal Distance Damage Function

The air blast model used for this targeting analysis was taken directly from DASA 2506.⁵ The mathematical expressions presented in this document were used to calculate a weapon radius for a given weapon yield, height of burst, and target hardness expressed in units of psi.

2.4 SENSITIVITY ANALYSIS OF VULNERABILITY UNCERTAINTY ON COLLATERAL DAMAGE

2.4.1 Objective and Scope of Analysis

The basic objectives of this analysis are

1. to demonstrate the implication of vulnerability assessments and the impact of their uncertainty in the context of collateral damage, and to demonstrate to the targeting community the implication of these measures when predicting collateral damage to a moderately small population center using tactical type weapon systems.
2. to provide the vulnerability engineer with a near complete quantitative data base suitable for assessing the operational implication of vulnerability uncertainties. It is anticipated that this information will provide the engineer with valuable insight for deciding the orientation of future research efforts.

With regard to the first objective, this targeting analysis is based upon an application of the Japanese building damage data to a small town typical of those located in western Europe. The purpose for using this data base was that it contains building damage data for a relatively diverse population of structural characteristics and design. As stated previously, only damage information for load-bearing wall structures was extracted from the Japanese data for these targeting sensitivity analyses. The intent of using this data was not to focus on a best vulnerability estimate but rather to use the range of damage information for all structures within this generic building-type

description. Certainly, any single best vulnerability estimate derived from this data need not necessarily be in agreement with the vulnerability of west European structures. This may be particularly true for residential structures since the Japanese building damage data primarily reflects damage sustained by commercial and industrial buildings. Also, the method and materials of construction common to the Japanese structures may not be consistent with European standards. Given the diversity of specific building characteristics and the basic physics of structural response, however, one may argue at least heuristically that the bounding range of vulnerability information extracted from this data base should contain the vulnerability estimates for most common building configurations. Hence, the vulnerability uncertainty addressed in this targeting analysis is not intended to reflect about any particular value but merely that an adequate vulnerability description may be contained in the specified range of values.

Toward the second objective it is anticipated that a sufficient degree of targeting information will be demonstrated in this analysis to aid in defining further vulnerability research efforts. In the near future engineers supporting a DIIA sponsored program will be evaluating research information oriented directly on residential and commercial structures in west Europe. The objective of this program is to clarify and validate building vulnerability information for the purpose of ensuring that collateral damage can be held to a minimum in the event of a nuclear war. As will be presented in the following pages extensive targeting information directly related to this research project has been compiled for aiding the engineering research decision process.

2.4.2 Vulnerability Uncertainty and Targeting Analysis

The targeting information presented in this section is based upon three ranges of vulnerability descriptions as extracted from the Japanese data. The ranges are:

- 2-3 psi
- 3-5 psi
- 5-10 psi

The basis for these numbers was discussed in the first section of this report. For the purposes of this section no specific damage criteria is to be inferred within a range of values. Rather, there is some damage criteria ranging between superficial damage and collapse of at least one exterior wall such that the subsequent building vulnerability assessment would be contained within one of these three intervals. For the purposes of the targeting mathematics and to remain within the familiar VII-T-K format these building hardness values are interpreted in the sense of P_{50} (psi) values.

Table 2.3 summarizes the targeting parameter variations performed to demonstrate the impact of vulnerability assessments on collateral damage and the possible consequences of vulnerability uncertainty. As shown in this table targeting calculations were performed along the east and north axis leading from the town center. The north axis calculations are contained in Appendix A of this document. It may also be noted that each targeting analysis is based upon a common vulnerability assessment for all structures in the town. It is recognized that the multistory buildings that dominate the city core may not be of the same vulnerability as the two story detached dwelling units common to the suburbs. The number of pages in this report would almost double, however, if graphic targeting analyses were included for all possible combinations of multistory and one-two story vulnerability assessments. As an alternative to this dilemma a simple mathematical expression and auxiliary targeting information is presented in the next section. By means of this additional information virtually any combination of building vulnerabilities may be easily assessed in these targeting applications.

Table 2.3 Targeting Variations to Assess Vulnerability Uncertainty

Weapon System (KT)	Range of Building Vulnerability P ₅₀ (psi) - All Structures -	Distance Damage Sigma	Direction/ Figure Number
1	2-3	0.2	East/2.3 North/A.2
1	3-5	0.2	East/2.4 North/A.3
1	5-10	0.2	East/2.5 North/A.4
10	2-3	0.2	East/2.6 North/A.5
10	3-5	0.2	East/2.7 North/A.6
10	5-10	0.2	East/2.8 North/A.7

Figure 2:3 depicts the 1 KT damage predictions for all structures in the city as a function of building hardness and DGZ location. The upper curve is based upon all structures being 2 psi hard for some arbitrary damage criteria. The lower curve is based on all structures being 3 psi hard, and the center curve for all structures at 2.5 psi hard. The 2.5 psi vulnerability may be thought of in terms of a compromise value given that the "true" vulnerability is bounded between 2 psi and 3 psi. The purpose of this compromise value could be to serve as an interim, "balanced error", vulnerability measure until such time as the appropriate measure can be determined from within the range 2-3 psi. Alternatively, this compromise value could be used as a final assessment if the "balanced error" is deemed to be insignificant. The idea of this so-called "balanced error" is that the compromise assessment is recognized to be a potentially biased estimator and the

CITY DAMAGE FUNCTIONS
 1 KT SYSTEM
 - EAST -

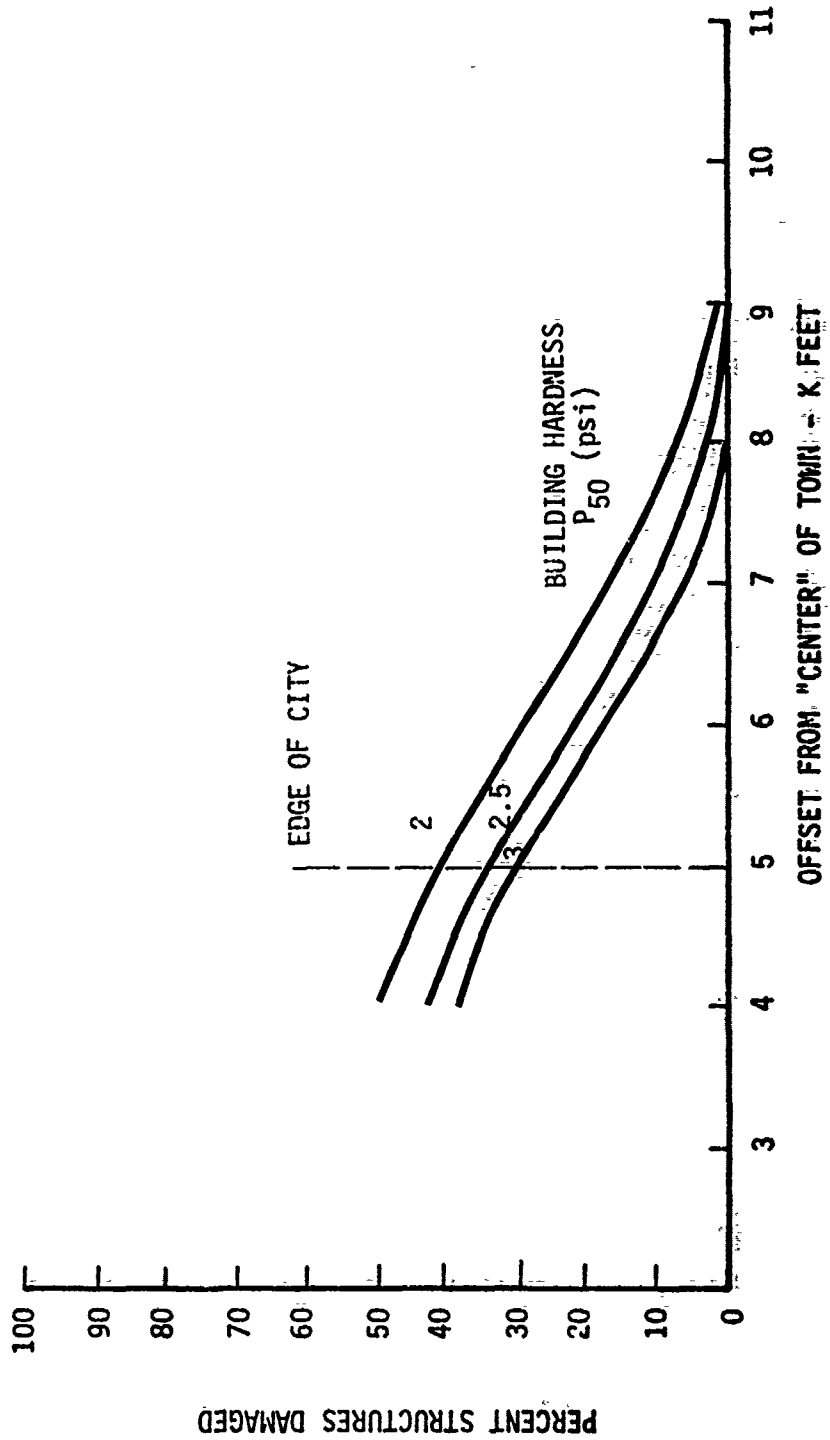


Figure 2.3 Significance of Vulnerability Uncertainty

maximum possible consequence of this error in terms of a damage prediction is equally balanced in terms of the bounding vulnerability values. For example, the damage predictions in Figure 2.3 at 7000 feet are approximately 0.06, 0.11, and 0.18 for the hardness assessments of 3 psi, 2.5 psi, and 2 psi, respectively. If the 2.5 psi assessment is used as a compromise value for predicting damage then the estimate of 0.11 will not be in error by more than about 0.06 absolute damage units.

The reason for including this so-called compromise vulnerability assessment in the targeting analysis is to aid the vulnerability engineer with directing this research program. For example, if it is strongly suspected that the true vulnerability is contained in the interval 2-3 psi then in a targeting context the damage prediction error between the compromise and true vulnerabilities will not exceed the magnitude of the balanced error. Accordingly, once the vulnerability bounds have been defined the utility of further research may be evaluated in terms of this balanced error concept. Of course, there can be additional factors which enter into this decision process. In terms of operational targeting requirements and objectives, however, this measure appears well suited for aiding the research decision process.

In the additional vulnerability ranges of 3-5 psi and 5-10 psi the compromise values are 4 psi and 7 psi, respectively. As depicted in Figures 2.3, 2.4, and 2.5 for the 1 KT weapon system, the potential biased error that could be introduced by using the compromise values does not appear to be very significant in a collateral damage context. For the 10 KT weapon system, however, the uncertainty is greater and could be viewed as unacceptable in terms of predicting collateral damage. The impact of this uncertainty would continue to grow, of course, with increasing yield due to enhanced area coverage.

CITY DAMAGE FUNCTIONS
 1 KT SYSTEM
 - EAST -

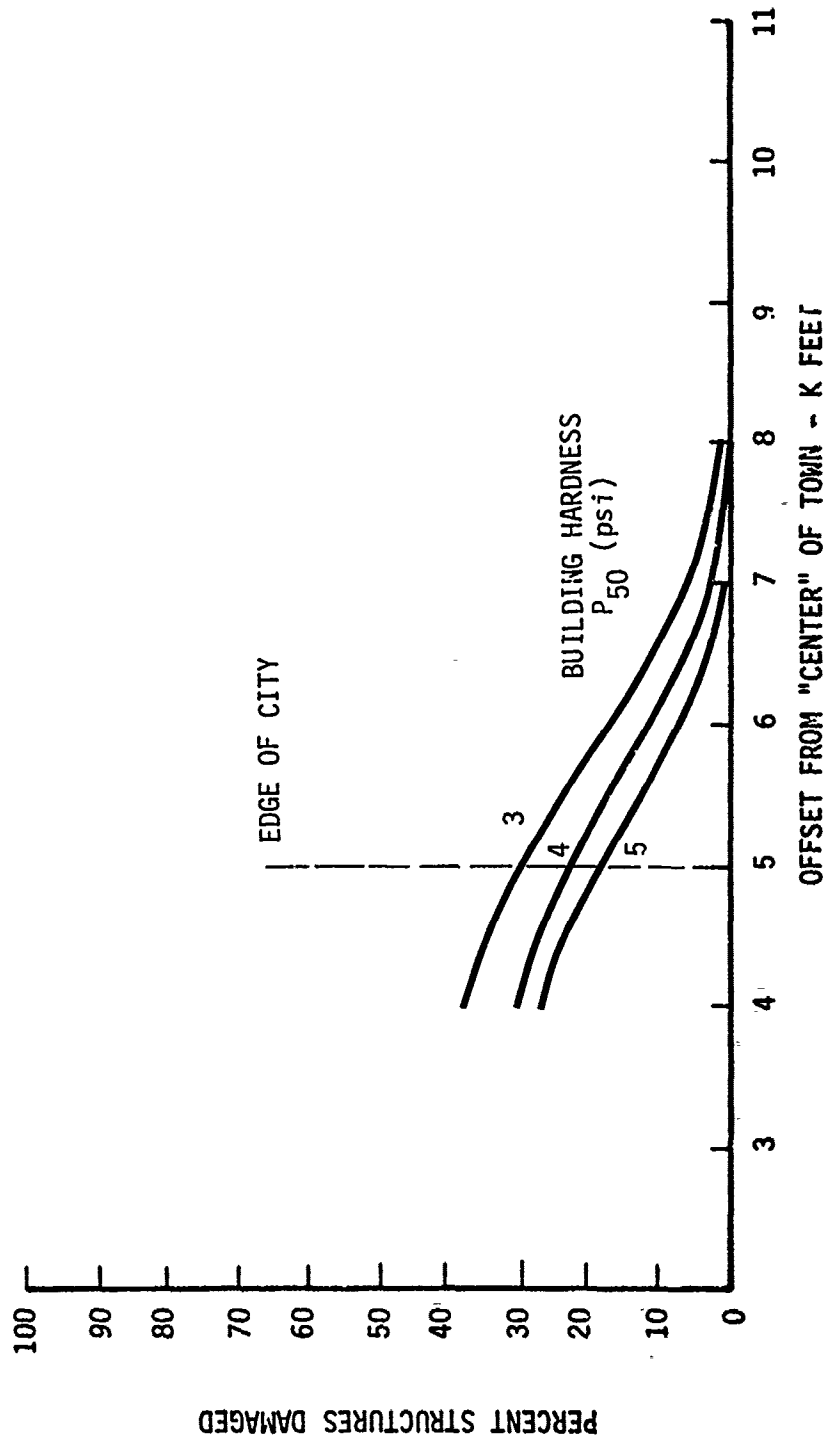


Figure 2.4 Significance of Vulnerability Uncertainty

CITY DAMAGE FUNCTIONS
 1 KT SYSTEM
 - EAST -

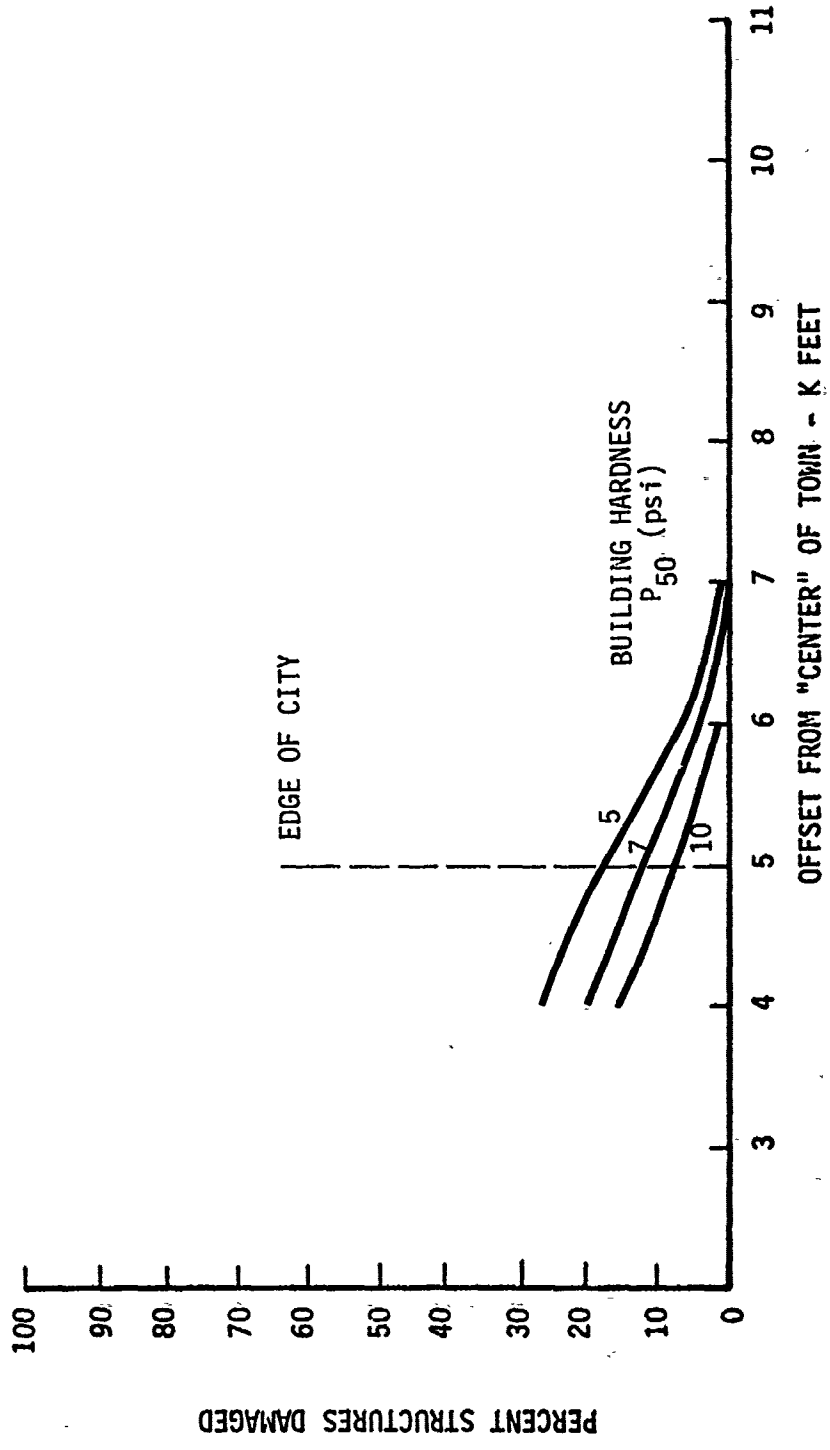


Figure 2.5 Significance of Vulnerability Uncertainty

CITY DAMAGE FUNCTIONS
 10 KT SYSTEM
 - EAST -

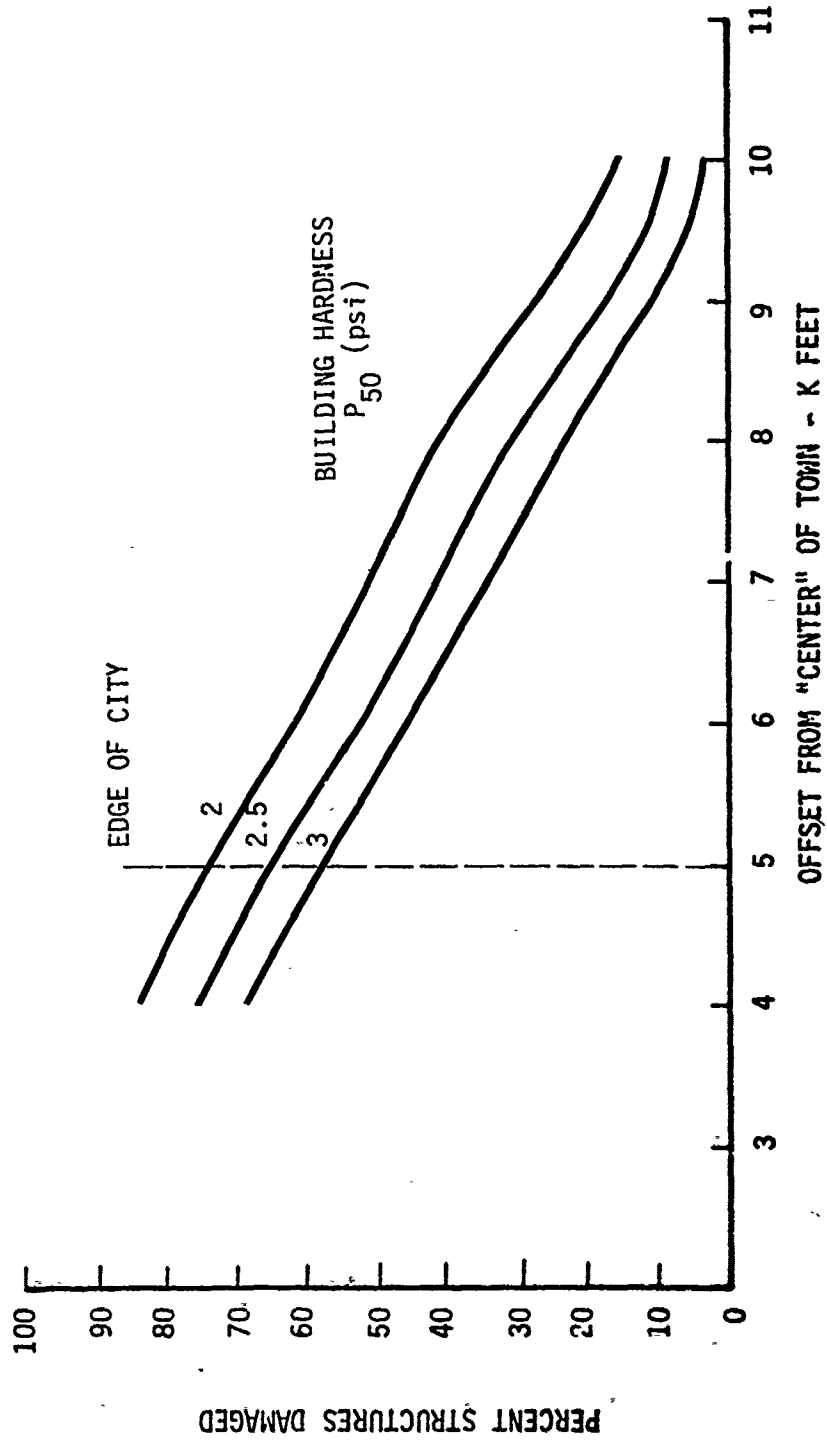


Figure 2.6 Significance of Vulnerability Uncertainty

CITY DAMAGE FUNCTIONS
 10 KT SYSTEMS
 - EAST -

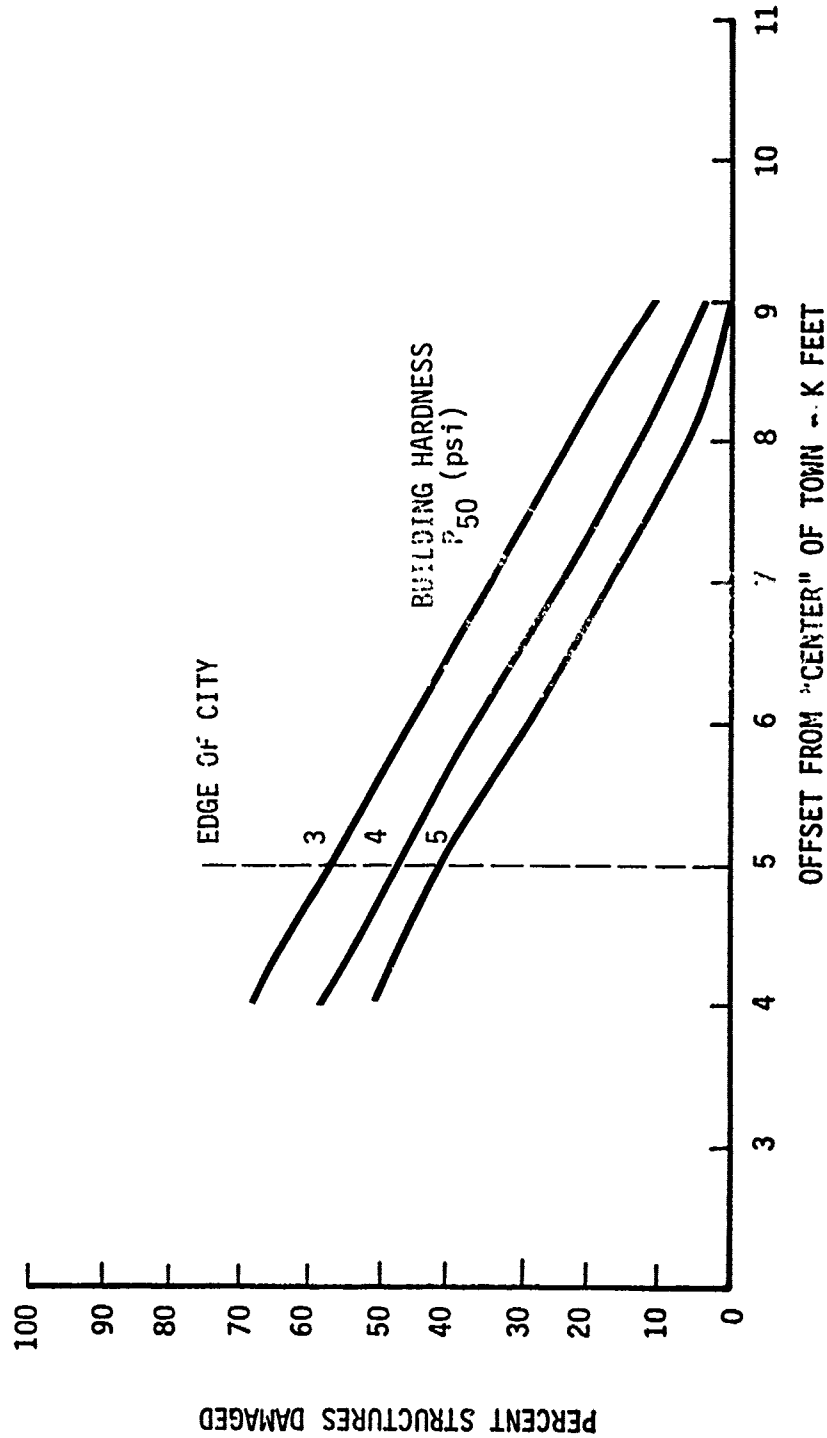


Figure 2.7 Significance of Vulnerability Uncertainty

CITY DAMAGE FUNCTIONS
 10 KT SYSTEM
 - EAST -

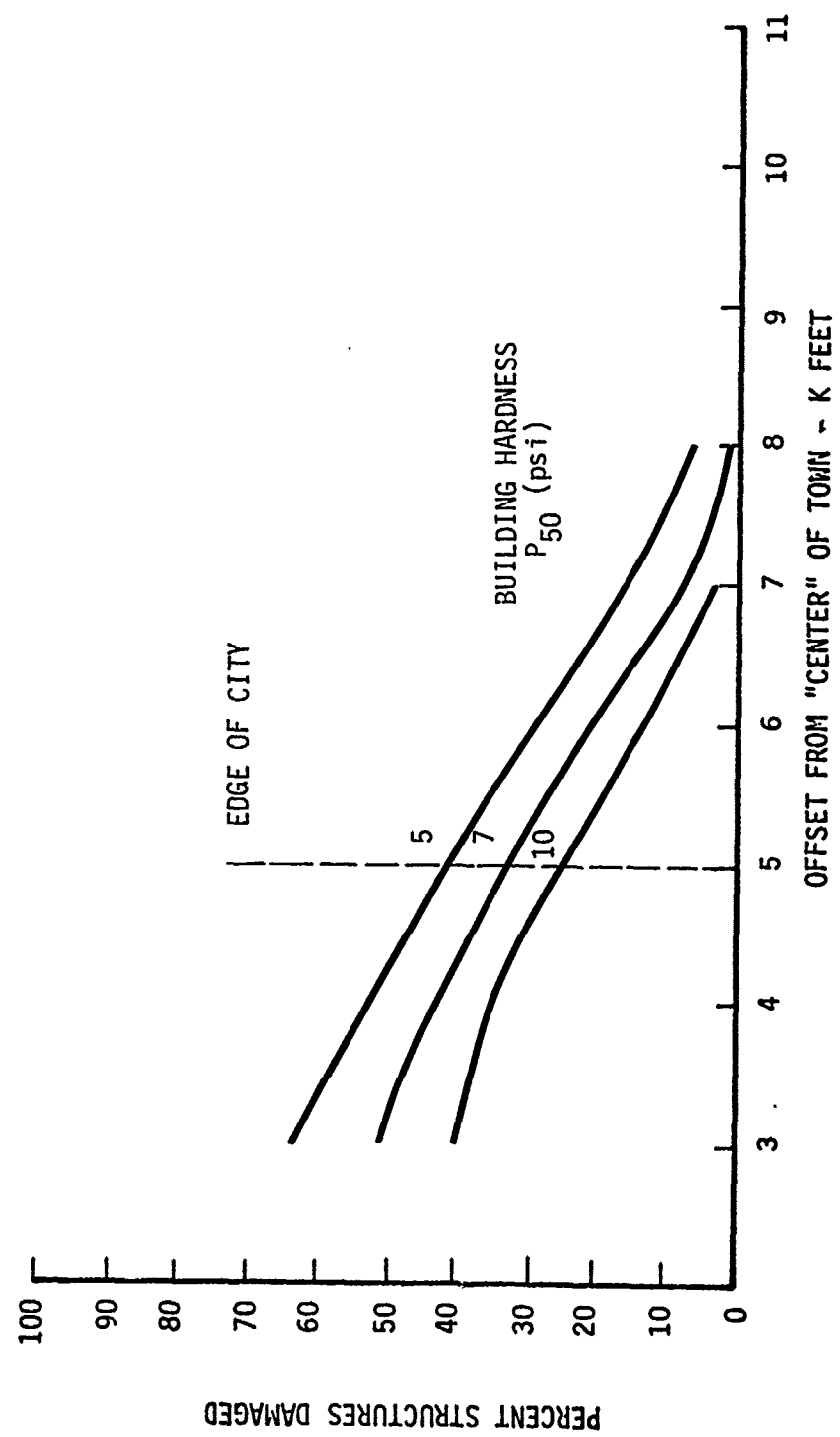


Figure 2.8 Significance of Vulnerability Uncertainty

The impact of the vulnerability uncertainty within these 3 ranges is comparable along the north axis to that observed along the east axis (see Appendix A). Based upon these total city damage functions one might infer that vulnerability uncertainty within these overpressure ranges is not especially critical to collateral damage. Of course, this observation may be conditional upon this example city. Population centers with different geometries, area size, and number of structures could result in a different conclusion when viewed in a targeting context.

2.4.3 City Core Damage Predictions

As stated in a previous paragraph it was not feasible to include targeting analysis results from all possible vulnerability combinations in this document. Recognizing the importance of this information, however, the following damage function curves are included which pertain only to structures in the core of the city. The following three figures, 2.9, 2.10, and 2.11, were derived from DGZ locations along the east axis. Similar curves are provided in Appendix A for aim points on the north axis.

The reason for including these damage prediction curves is to provide the analyst with a means for predicting damage when the core structure vulnerability is different from that of the structures in the suburbs. When the initial vulnerability analyses being sponsored by DNA are evaluated it may very well be that the city core structures are of a different vulnerability than the housing units in the immediate suburbs. Also, a lesser collateral damage criteria may need to be applied to the core structures given the high population densities that tend to reside in these small regions. For example, the city used for this targeting analysis has about 20 percent of the estimated total structures located in the core. As indicated in Table 2.1, however, these structures may be providing housing for over 50 percent of the total population.

Figure 2.9 depicts the percentage of core structures damaged for hardness values ranging from 2 psi to 5 psi. At an offset distance of 3000 feet and greater the damage fractions are negligible for 7 psi and 10 psi assessments. Figures 2.10 and 2.11 depict the city core damage fractions for the 10 KT system.

The method by which this damage prediction information may be used to construct city damage functions in addition to those previously presented is as follows. The only assumption required is that the building vulnerability estimate (P_{50}) is constant for all structures in the core and likewise for all structures removed from the core. The mathematical expression that can be used to assess a city wide damage fraction for different hardness estimates between the core and suburb structures is as follows.

$$T_f = 0.2 C_f + 0.8 S_f$$

where

T_f is the total city damage fraction

C_f is the total core damage fraction

S_f is the total suburb damage fraction

the coefficients 0.2, and 0.8 represent the distribution of structures between the core and suburbs

The following example demonstrates application of this mathematical expression. Assume the analyst is interested in determining the city damage fraction (T_f) for the case when the core structures are 4 psi and the structures outside the core are assessed at 2 psi. This information is desired for the 10 KT system with the DGZ located 5000 feet east of the town center. From Figure 2.6 the T_f value is about 0.75 for all structures evaluated at 2 psi, and the weapon DGZ offset 5000 feet east of the town center. Now,

$$T_f = 0.2 C_f + 0.8 S_f = 0.75 \quad .$$

CITY CORE
 DAMAGE FUNCTIONS
 1 KT SYSTEM
 - EAST -

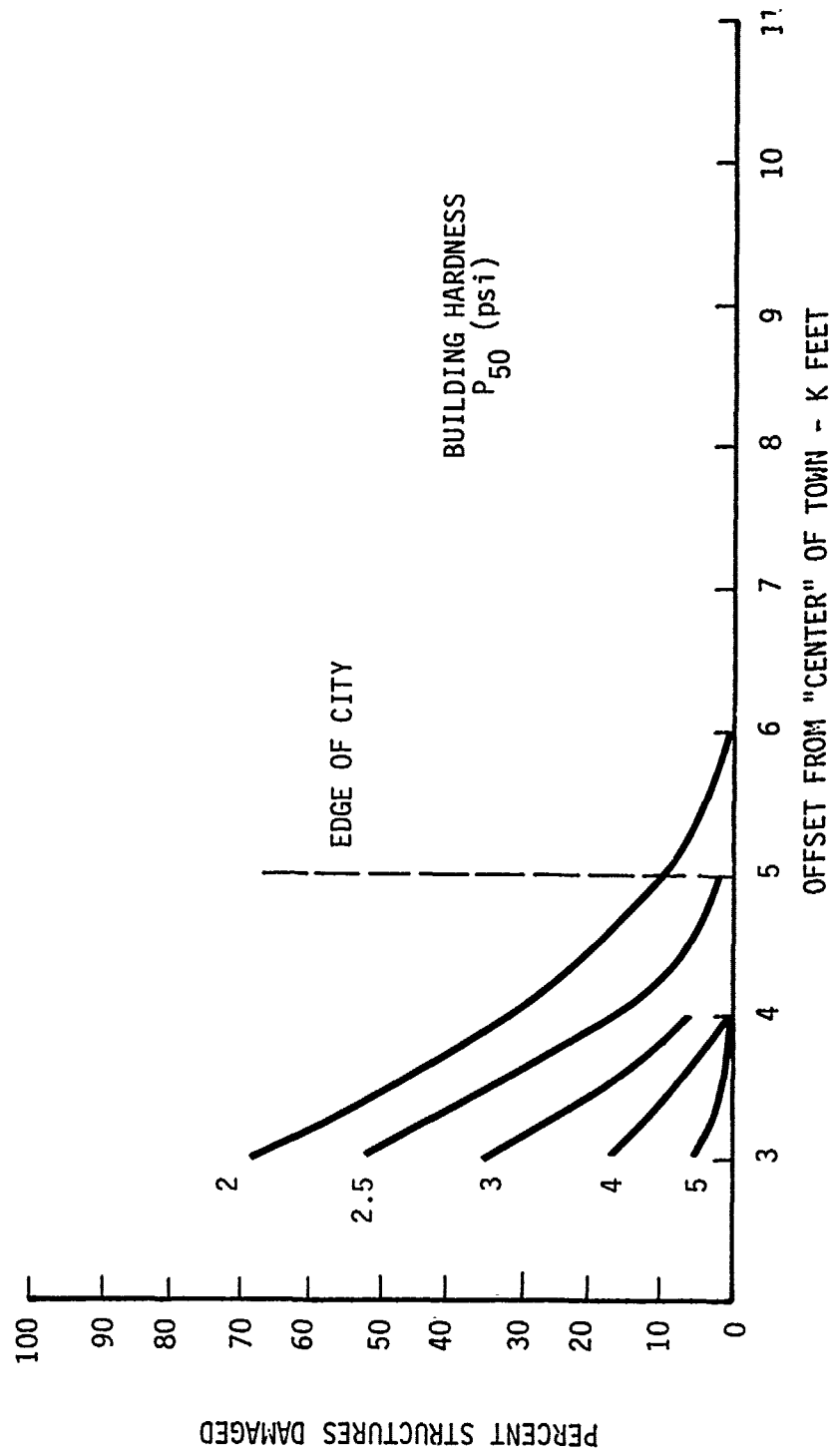


Figure 2.9 Significance of Vulnerability Variation to Structures in Core of City

CITY CORE
DAMAGE FUNCTIONS
10 KT SYSTEM
- EAST -

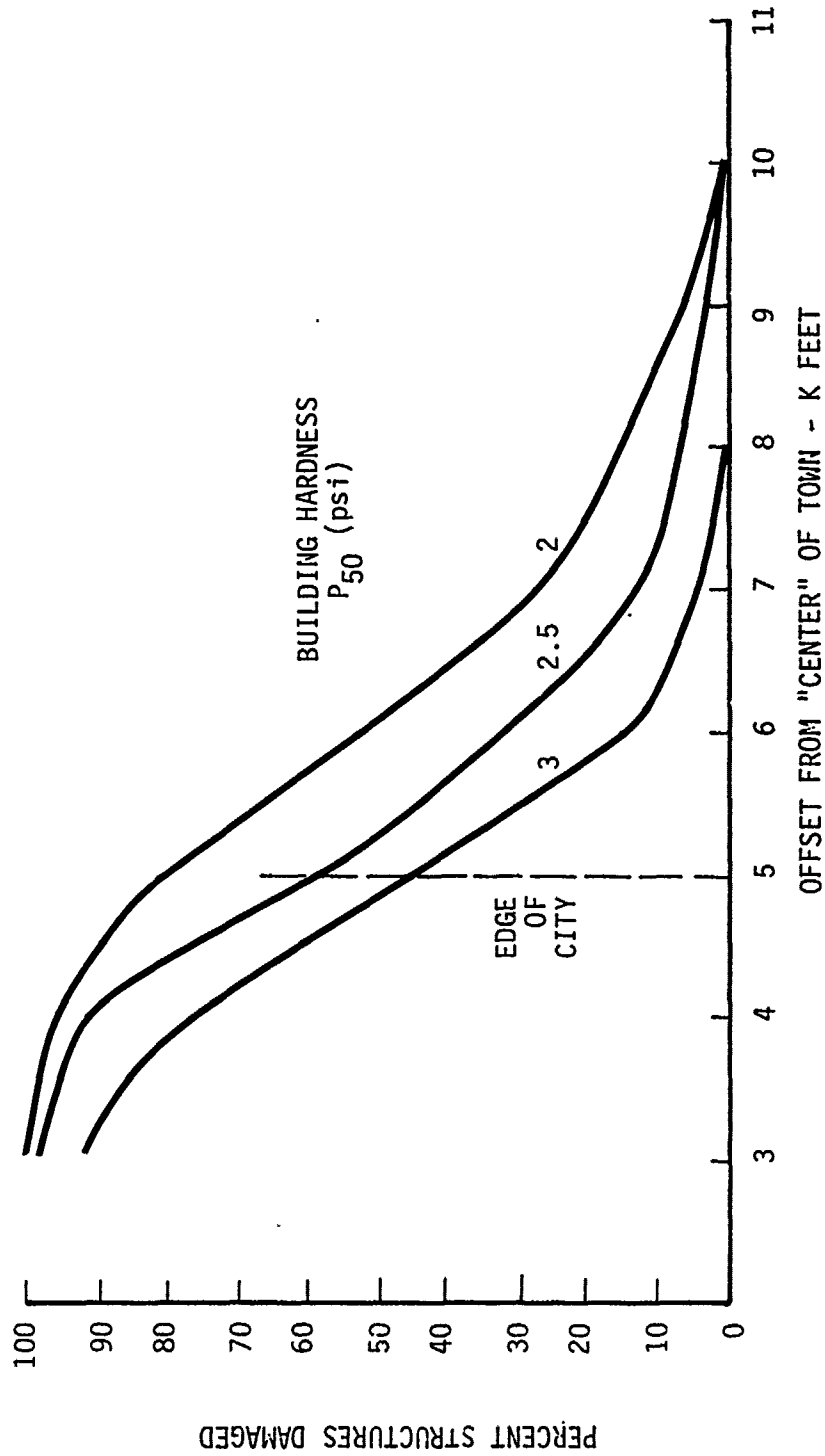


Figure 2.10 Significance of Vulnerability Variation to Structures in Core of City

CITY CORE
 DAMAGE FUNCTIONS
 10 KT SYSTEM
 - EAST -

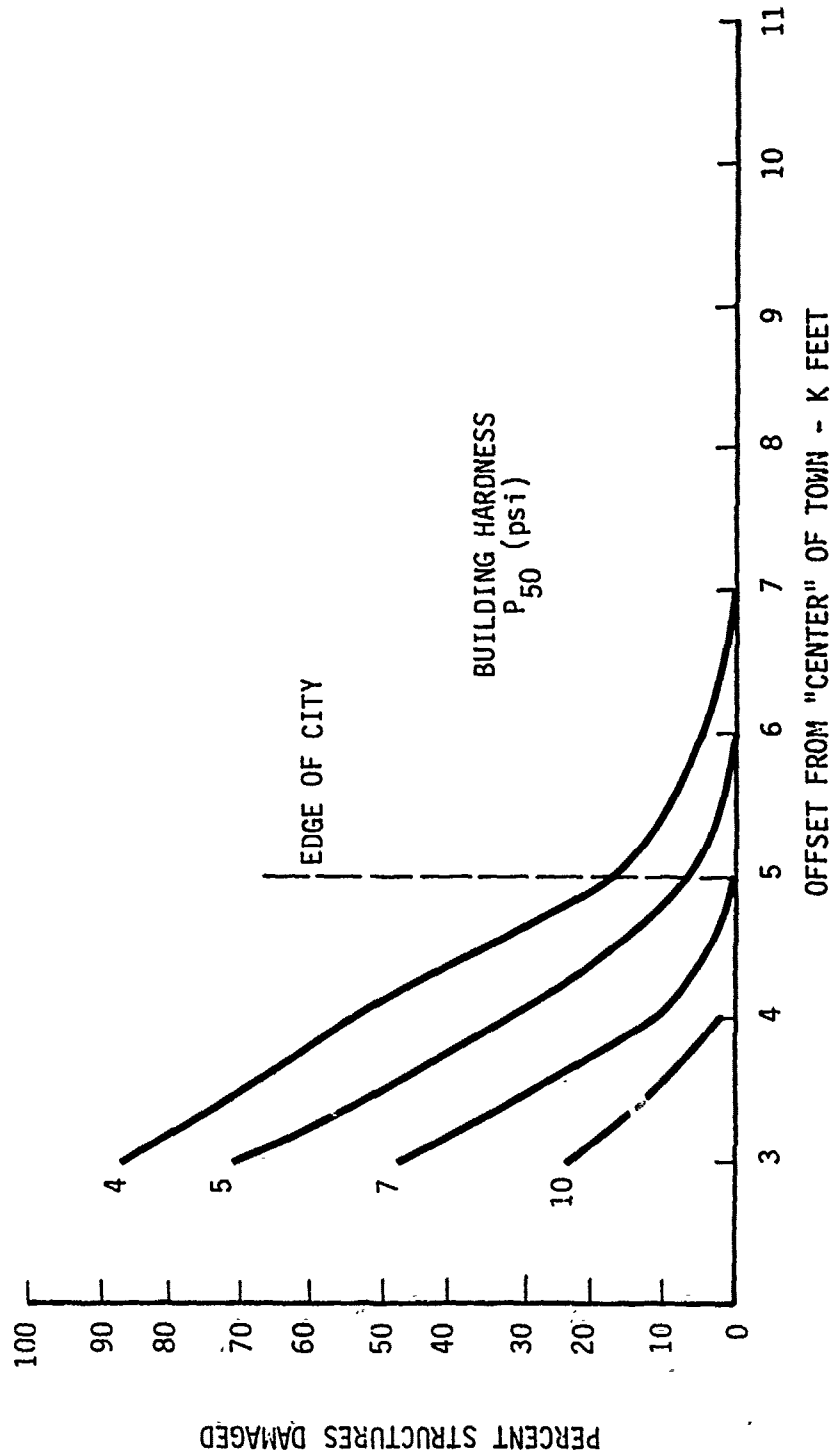


Figure 2.11 Significance of Vulnerability Variation to Structures in Core of City

The following two steps are intended to remove the core damage contribution, assessed at 2 psi, from this value and replace it with the contribution when the core is assessed at 4 psi. From Figure 2.10 about 80 percent of the core structures are damaged under this targeting scenario at a 2 psi vulnerability. From Figure 2.11 it is easy to determine that only about 18 percent of the core is damaged under identical targeting conditions but assessed at 4 psi hard. Therefore, the new city damage fraction for a 4 psi core and 2 psi structures in the suburbs is determined by,

$$T_f = 0.75 - (0.2 * 0.8) + (0.2 * 0.18) = 0.63 \quad .$$

2.5 IMPACT OF DAMAGE CRITERIA ON COLLATERAL DAMAGE

One of the most sensitive and subtle issues in the collateral damage area pertains to damage criteria. By its very definition, as presented in the FM 101-31⁶ series of documents, collateral damage is viewed in terms of undesirable civilian material damage or personnel injuries. Certainly, from a civilian viewpoint breakage of a single window pane could be considered as undesirable and excessive damage. Although as the military command would share this common concern there may be instances when it would be necessary to increase the civilian property risk to a greater degree of damage.

The possible subtlety of damage criteria relative to collateral damage occurs when a qualitative damage description is transformed to a damage probability prediction. The damage predictions are based upon an engineering vulnerability assessment which in turn reflects the damage criteria and building response characteristics. These damage probabilities are in fact a measure of the chance that the structure will be damaged to at least the level defined in the damage criteria. As such, a portion of these probabilities contain the chance that a far greater degree of damage may be realized. Also, although two qualitative damage definitions may be considerably different with regard to

physical damage the resultant vulnerability assessments could be quite close to one another. Accordingly, the difference in damage probabilities for the two damage criteria could be very small in a targeting context.

As a means to demonstrate the impact of different damage criteria to collateral damage predictions the following targeting analyses were performed. Three different damage criteria were used with assumed vulnerability assessments as interpreted from the Japanese data. These damage criteria, vulnerability assessments and targeting applications are summarized in Table 2.4.

As depicted in the following figures there is a very small difference between the superficial and roof collapse damage predictions. The potential problem depicted in these figures is that in a collateral damage context a seemingly low risk DGZ location, assessed in terms of superficial damage, could result in roof collapse to a large percentage of the buildings at risk.

Table 2.4 Targeting Parameter Variations to Assess Impact of Damage Criteria

Weapon System	Damage Criteria	Building Hardness		Direction/ Figure
		Core ^{P₅₀}	Suburbs (psi)	
1	Superficial	2.5	2.5	East/2.12
	Roof Collapse	4	3	North/2.13
	Wall Collapse	7	4	
10	Superficial	2.5	2.5	East/2.14
	Roof Collapse	4	3	North/2.15
	Wall Collapse	7	4	

CITY DAMAGE FUNCTIONS
 1 KT SYSTEM
 - EAST -

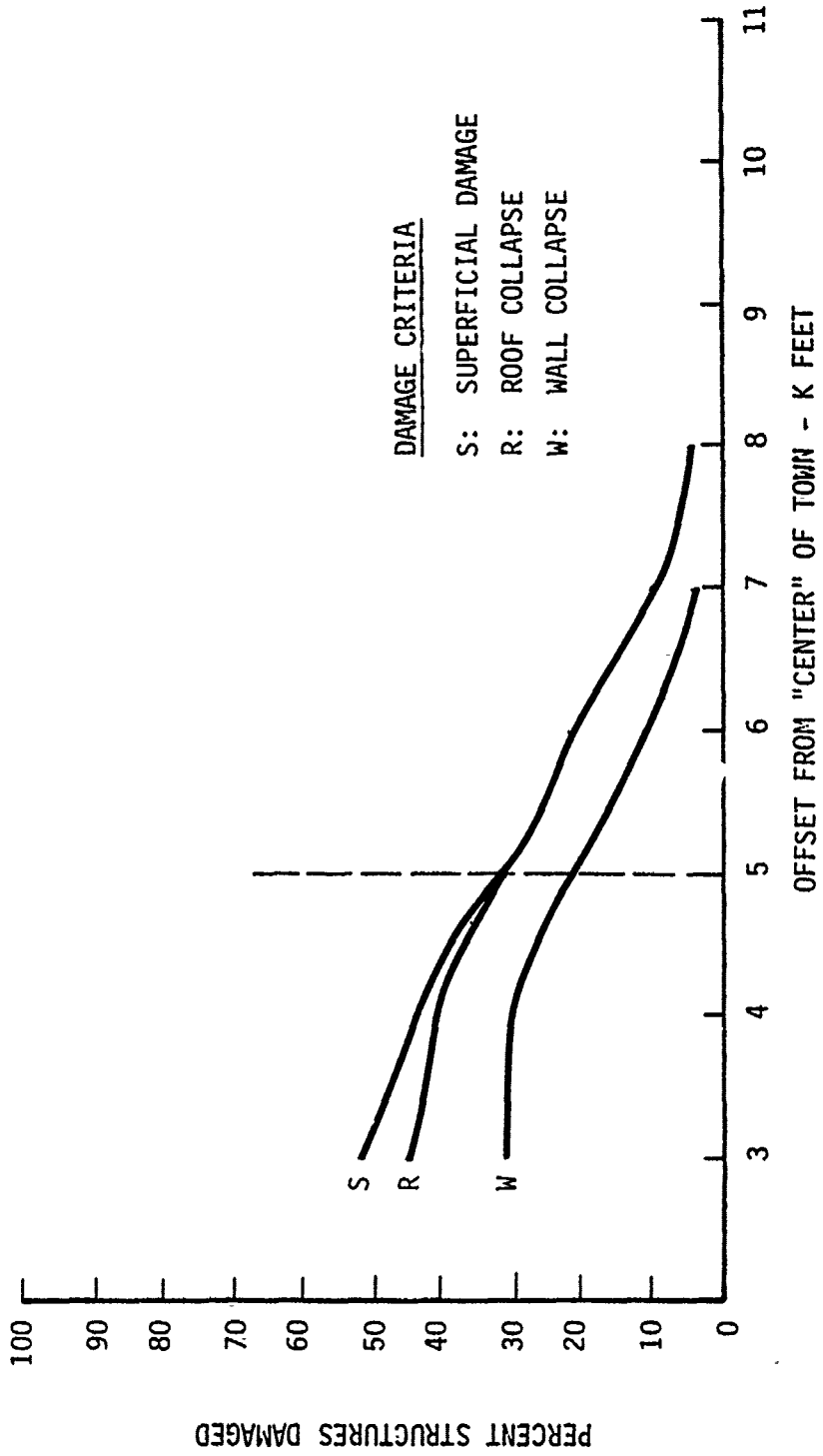


Figure 2.12 Significance of Damage Criteria to Collateral Damage Predictions

CITY DAMAGE FUNCTIONS
 1 KT SYSTEM
 - NORTH

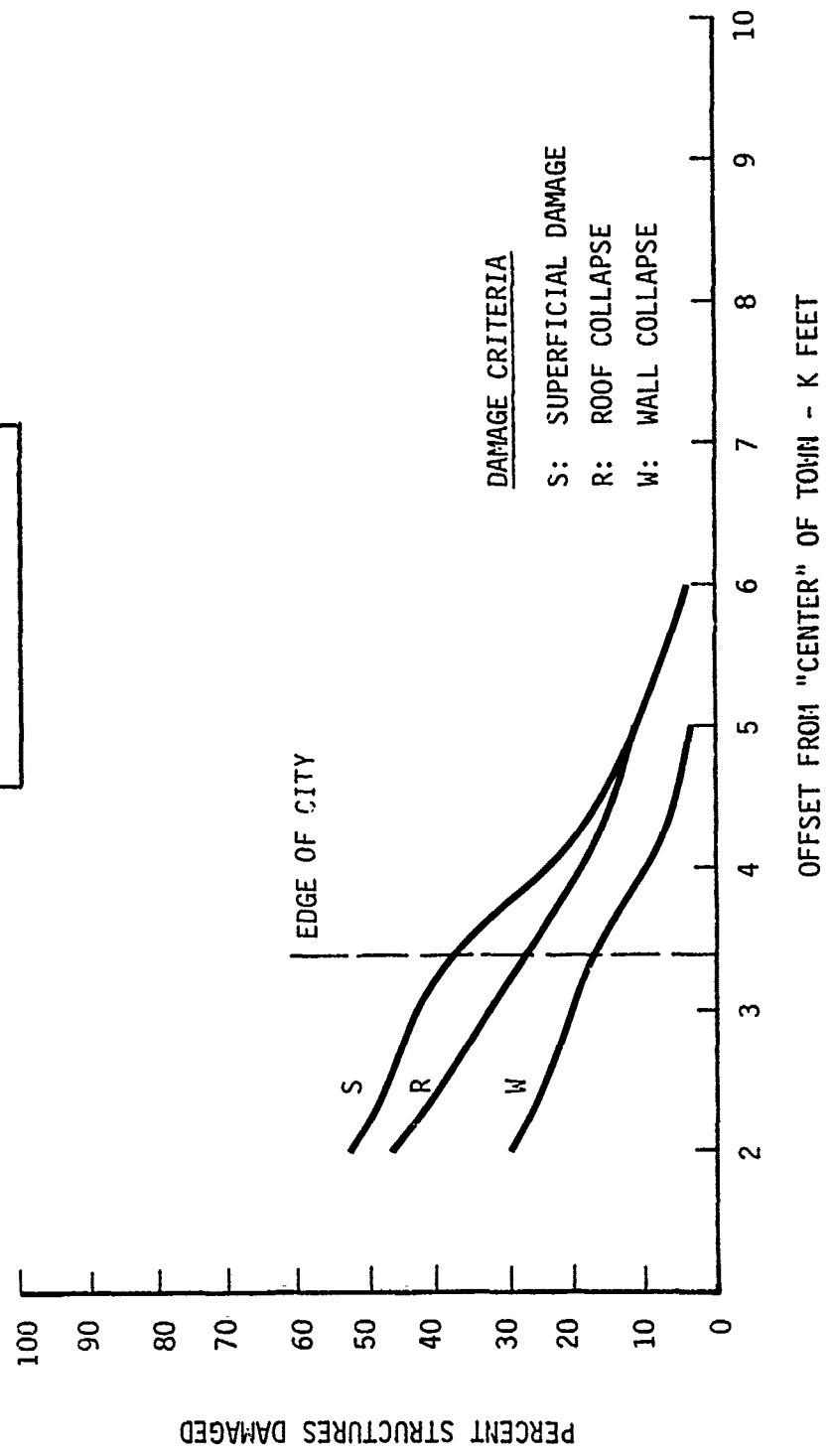


Figure 2.13 Significance of Damage Criteria to Collateral Damage Predictions

CITY DAMAGE FUNCTIONS
 10 KT SYSTEM
 - EAST -

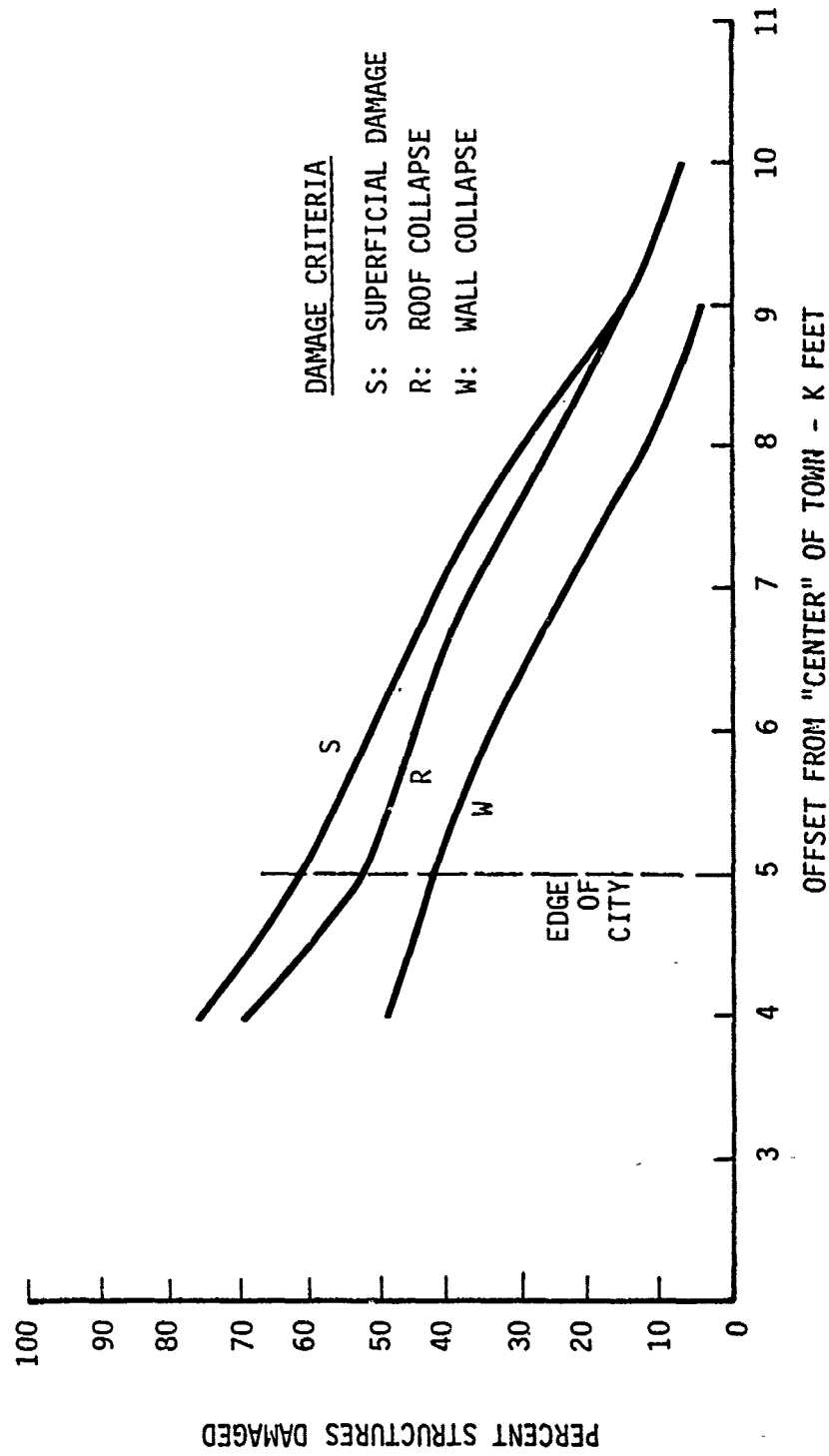


Figure 2.14 Significance of Damage Criteria to Collateral Damage Predictions

CITY DAMAGE FUNCTIONS
 10 KT SYSTEM
 - NORTH -

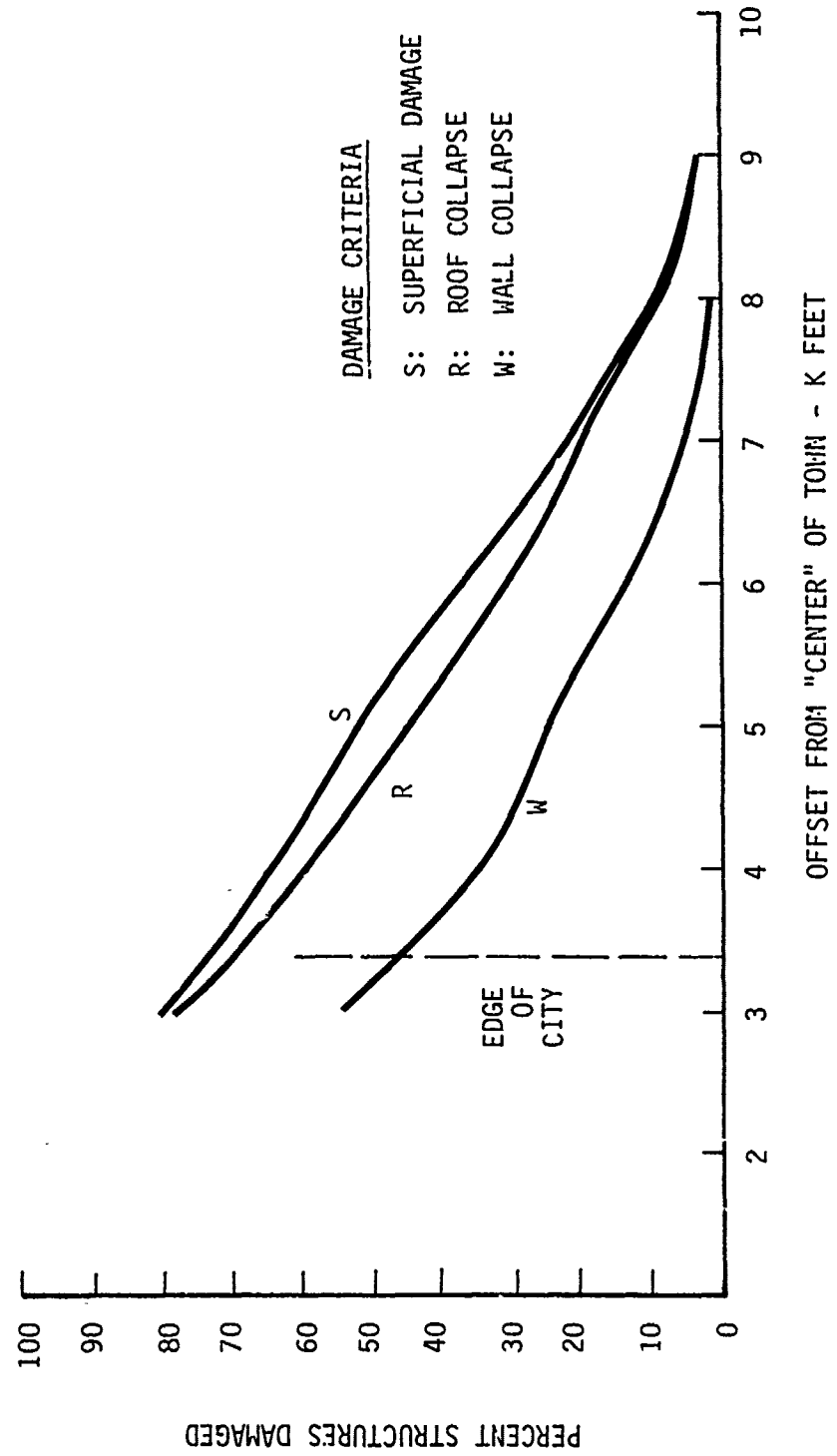


Figure 2.15 Significance of Damage Criteria to Collateral Damage Predictions

Although these example targeting calculations are based upon somewhat arbitrary vulnerability assessments, the trend in these city damage function curves to be relatively close to one another may be of serious concern to collateral damage issues.

2.6 SIGNIFICANCE OF DISTANCE DAMAGE SIGMA VALUES IN COLLATERAL DAMAGE PREDICTIONS

The mathematical damage prediction model currently being used in most nuclear weapon targeting analyses is the so-called log normal cumulative distribution function. In targeting applications the parameters of this function are often presented in terms of the weapon radius, WR, and the distance damage sigma, σ_d . This sigma term, a dimensionless value, is intended to convey a measure of the shot-to-shot variation in the weapon-produced environment, and the structure-to-structure variation in target hardness. Specifically, the mathematical expression for σ_d is,

$$\sigma_d^2 = 1 - \exp \left[-(\beta_E^2 + \beta_R^2)/n^2 \right], \text{ where}$$

β_E = a measure of shot-to-shot variation in the weapon produced damaging agent

β_R = structure-to-structure variation in hardness

n = rate at which the damaging agent is changing with ground range.

This distance damage sigma may, more intuitively, be thought of as a measure of the slope of the distance damage function. Figure 2.16 depicts this distance damage function for several values of σ_d including the limiting case when $\sigma_d = 0$. In the context of collateral damage the concern for adequately specifying the σ_d value is reflected by the "tail" of the damage function. As may be observed in Figure

2.16 increasing the value of σ_d increases the damage prediction values in the tail of the function. Given that the targeter will attempt to select DGZ regions so as to minimize the extent of collateral damage, adequate evaluation of this term could be an important consideration. If this term is underestimated the targeter may inadvertently exceed maximum acceptable collateral damage guidelines. Conversely, if this parameter value is overestimated the targeter may be unnecessarily restricting acceptable DGZ regions.

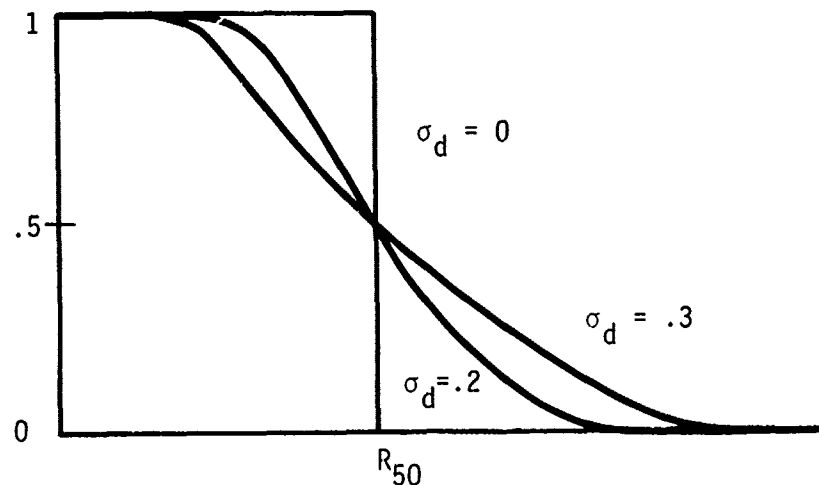


Figure 2.16 Impact of σ_d on Shape of Distance Damage Function

As a means to demonstrate the significance of this parameter in a collateral damage context four sets of city damage functions were constructed for three values of σ_d . Table 2.5 summarizes these targeting parameter variations. The corresponding city damage functions follow immediately.

Table 2.5 Targeting Parameters Used to Assess Impact of σ_d Values

Weapon System (KT)	Building Hardness P_{50} (psi) - all structures -	σ_d Values Demonstrated	Direction/ Figure No.
1	2.5	0, 0.2, 0.3	East/2.17
1	7	0, 0.2, 0.3	East/2.18
10	2.5	0, 0.2, 0.3	East/2.19
10	7	0, 0.2, 0.3	East/2.20

As depicted in these figures, variation in σ_d values does not necessarily generate significant differences in the predicted damage values. In fact, as demonstrated in these figures there are DGZ locations where variation in σ_d has no measurable impact. Also, there are locations, such as at 3000 feet in Figure 2.19, where smaller σ_d values result in increased damage predictions values. The primary reason for this behavior is the building distribution throughout the city. As depicted in Figure 2.1 there are many regions within the city which have no structures and regions where the spacing between structures is quite large. Even though a SIGMA-30 damage function has an extended tail it obviously can have no impact in areas where there are no structures.

The second reason for this behavior also attributable in part to the building distribution, is due to the size of the weapon yield and building hardness values. The family of curves in Figure 2.19 is the only set in the 4 presented where the σ_d value has any real impact, and only in excess of about 9000 feet from the town center. The trend being observed at this range and beyond is due to the fact that the structures at risk "appear" uniformly distributed (and dense) in terms of the damage function.

CITY DAMAGE FUNCTIONS
 1 KT SYSTEM
 - EAST -

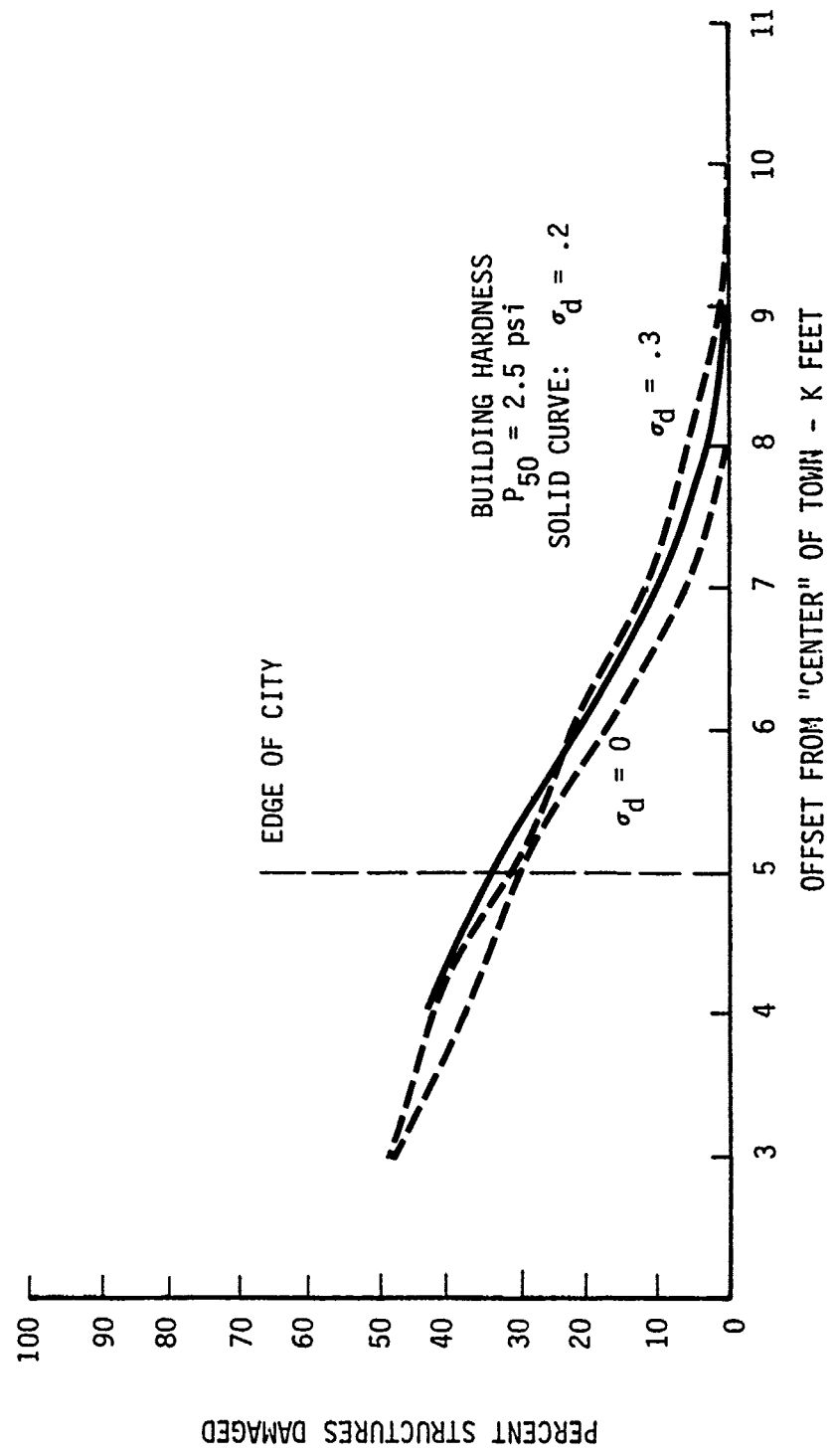


Figure 2.17 Significance of Distance Damage Sigma to Collateral Damage Predictions

CITY DAMAGE FUNCTIONS
 1 KT SYSTEM
 - EAST -

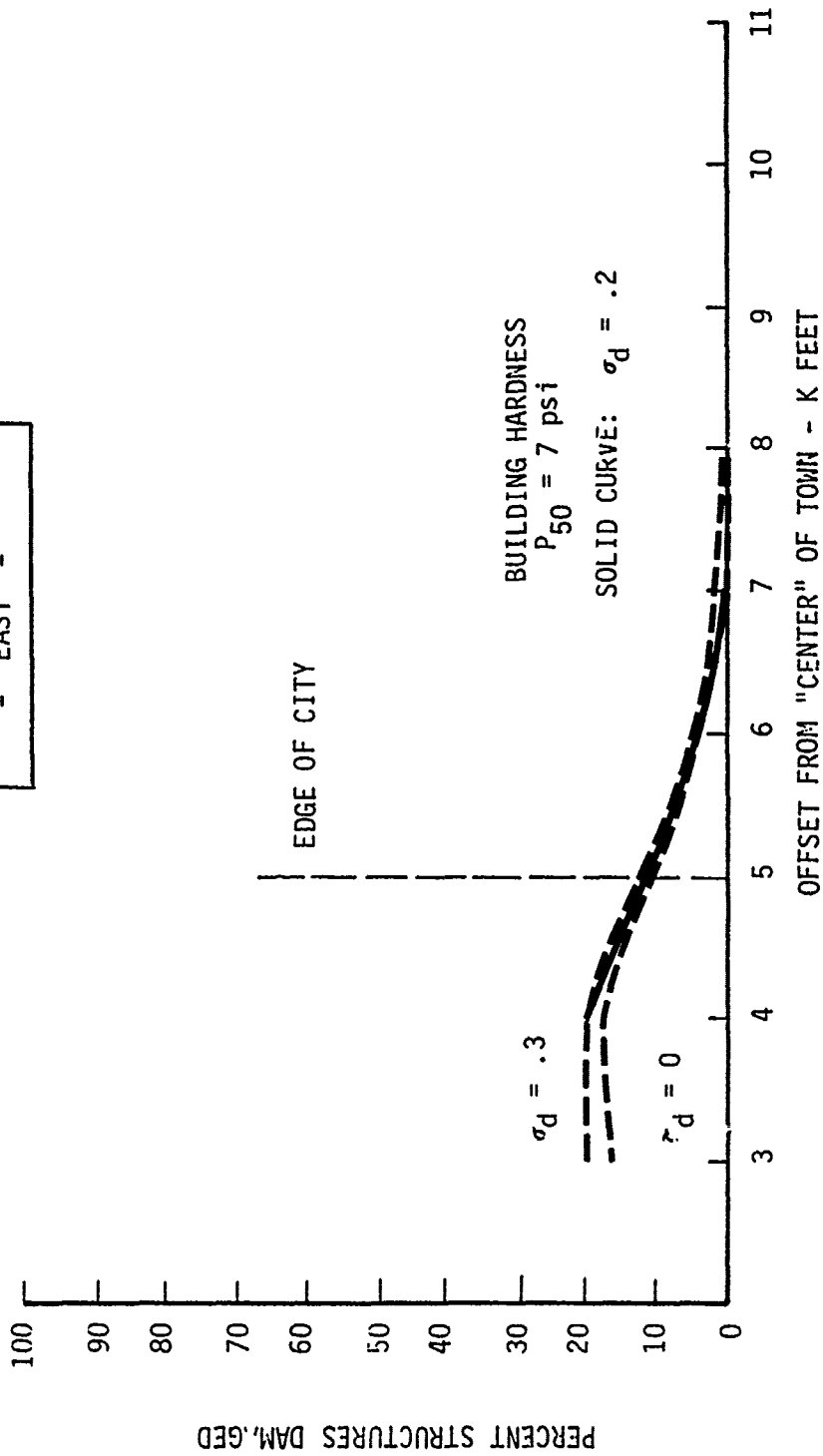


Figure 2.18 Significance of Distance Damage Sigma to Collateral Damage Predictions

CITY DAMAGE FUNCTIONS
 10 KT SYSTEM
 - EAST -

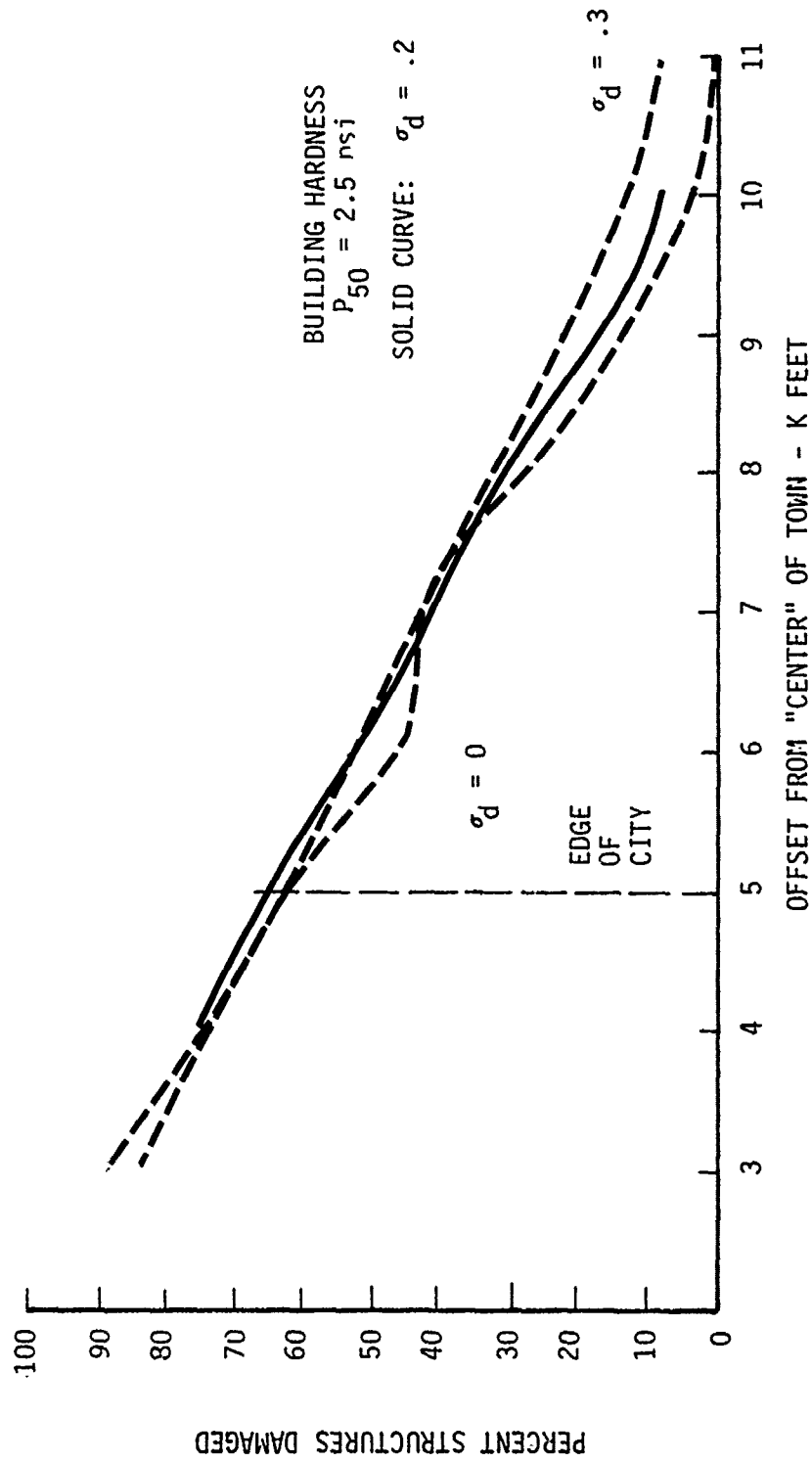


Figure 2.19 Significance of Distance Damage Sigma to Collateral Damage Predictions

CITY DAMAGE FUNCTIONS
 10 KT SYSTEM
 - EAST -

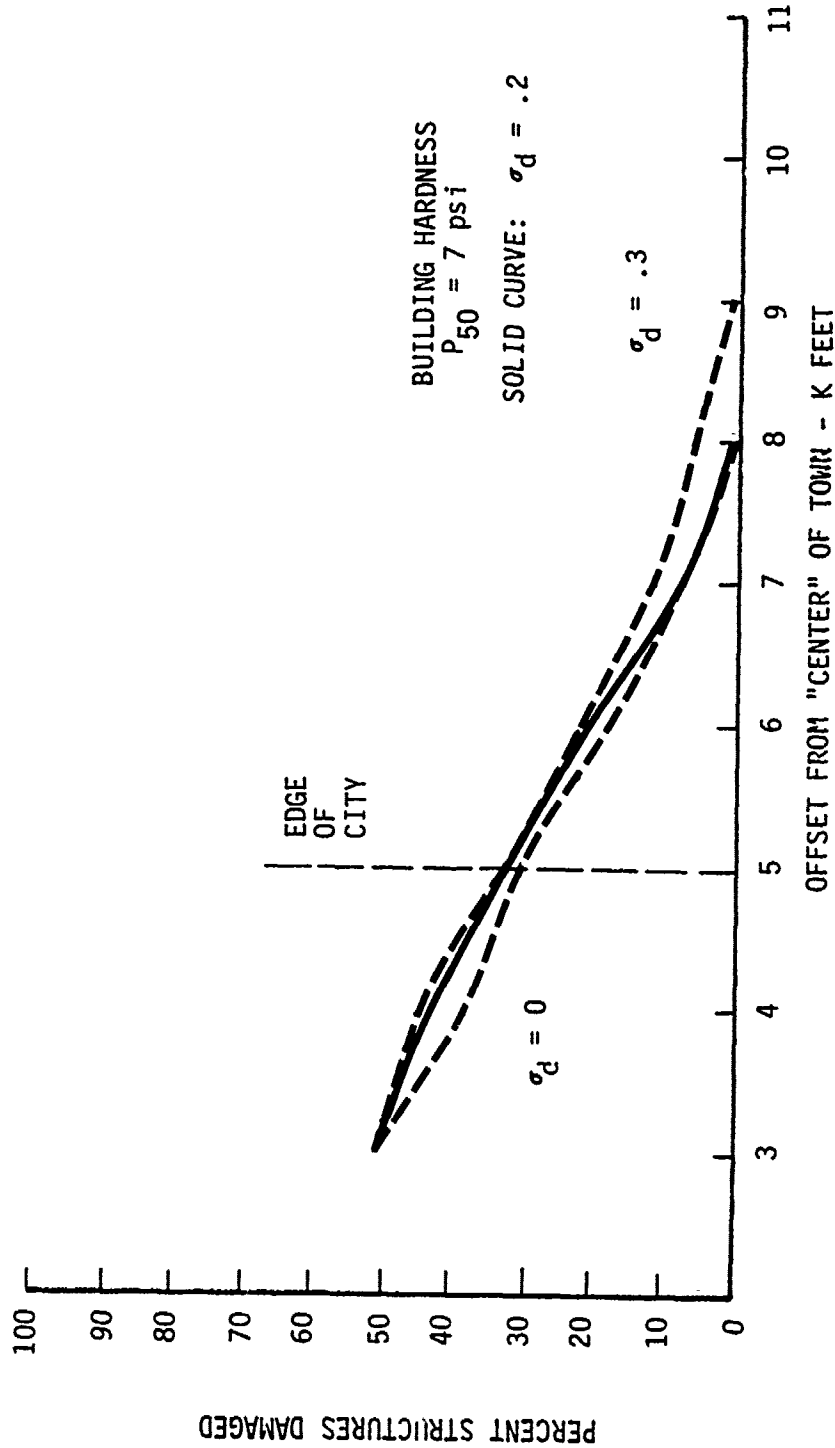


Figure 2.20 Significance of Distance Damage, Sigma to Collateral Damage Predictions

Adequate definition of the appropriate σ_d value may or may not be important to collateral damage predictions. As demonstrated in these example targeting applications weapon yield, building hardness, and building distribution can combine in many instances to suppress the importance of this sigma value. Although this parameter may be more important to collateral damage issues than is the case in other targeting scenarios and objectives, this parameter appears to remain a second order term relative to defining median (P_{50} , psi) vulnerability values.

2.7 IMPACT OF SHIELDING ON PREDICTING COLLATERAL DAMAGE

The Defense Nuclear Agency is currently sponsoring research in the area of blast wave shielding and its significance relative to collateral damage. Physical experiments have been performed with scale model structures to assess blast wave behavior within clusters of residential structures typical to western Europe. A preliminary interpretation of this data with regard to structural response and building vulnerability is anticipated within the near future.

The objective for performing the targeting analysis exhibited later in this section is to provide the vulnerability engineer with a measure for assessing the significance of the experimental data interpretation in a targeting context. This measure consists of a series of city damage function curves based upon somewhat arbitrary assumptions as to what the consequence of shielding might be with regard to predicting collateral damage. Given these damage function curves, the assumptions upon which they were generated, and the experimental results, the vulnerability engineer may have sufficient information for deciding the direction of further research efforts. It should be noted that these assumptions were made independent of experimental or calculational information. Also, the manner in which these assumptions are extended to a targeting context may not necessarily conform with the underlying physics of the shielding phenomenon. The objective of this analysis was not to necessarily model the inherent physics but

rather to assess the possible consequences of shielding with regard to predicting collateral damage.

The assumptions made in this targeting analysis to assess the consequence of shielding are given below.

1. The structures in the example city are primarily vulnerable to peak surface overpressure. The resultant impact of shielding on the blast environment is to perturb the peak effect. No consideration was given to the manner in which the pulse shape may be perturbed or the consequence of such an effect.
2. The peak surface overpressure is uniformly perturbed throughout a cluster of structures. That is, the consequence of shielding on the peak effect is the same at the edge of the cluster as would occur at the center of the cluster.
3. This perturbation is applied in the form of a multiplicative factor to the predicted free field environment. As stated, this factor is held constant throughout a specific cluster. For example, if ΔP (peak surface overpressure) is predicted to be 2 psi at the cluster boundary point normal to the blast wave, and the factor is 1/2, the perturbed value of ΔP is assessed to be 1 psi. Likewise, a free field ΔP prediction at an interior point of this cluster would also be reduced by 50 percent.
4. The value of this multiplicative factor is a function of the cluster density. Building vulnerability and the magnitude of ΔP do not influence the value of this factor.
5. The building density in the core of the example town, as delineated in Figure 2.21 is sufficient to perturb ΔP by as much as ± 50 percent.

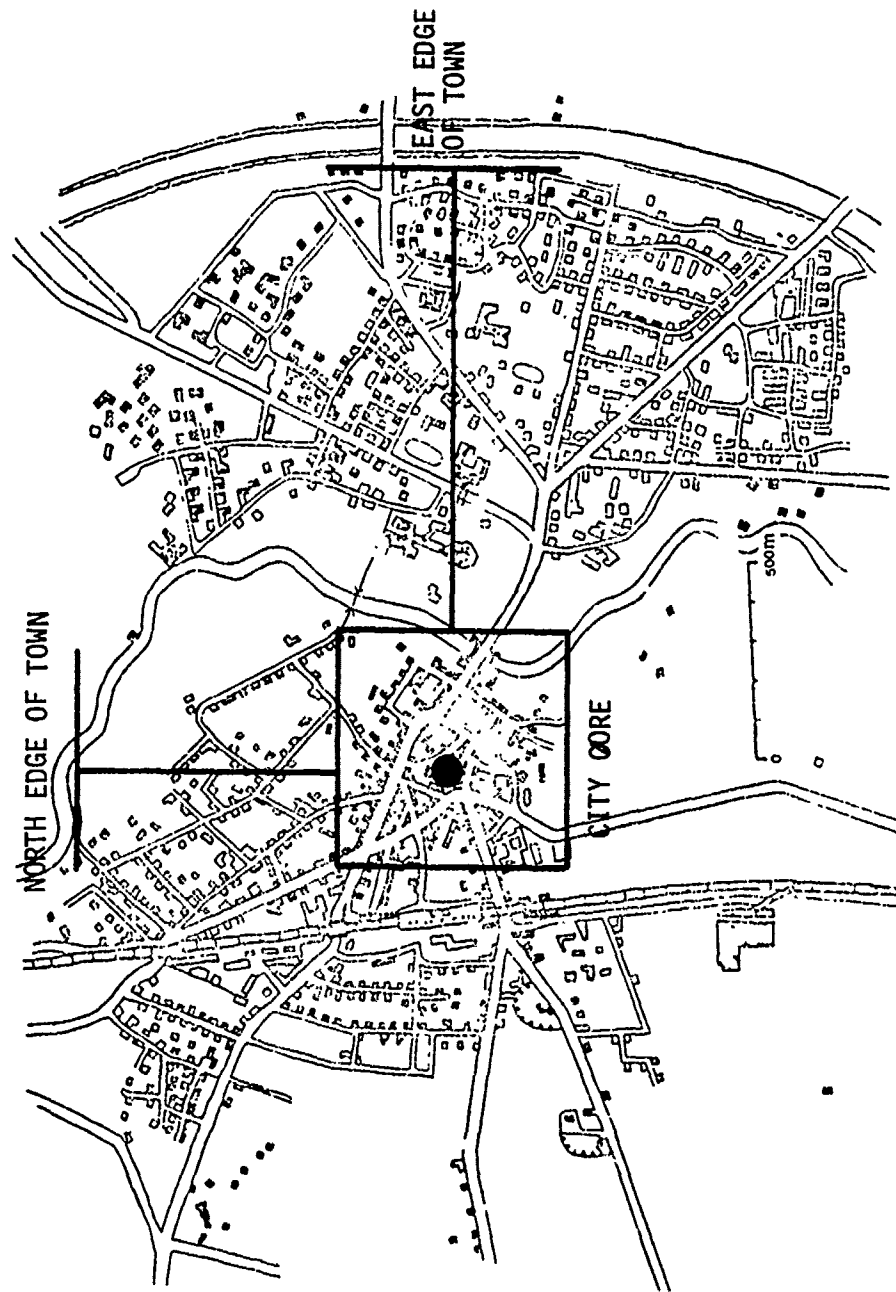


Figure 2.21 Example Town

6. The density of the building clusters distributed about the suburbs is constant. This density is sufficient to perturb ΔP by as much as ± 25 percent. Only 1/2 of these buildings are contained in clusters. The remaining structures are sufficiently separated so as to preclude the consequence of shielding. These clusters are uniformly distributed over the city.

Tables 2.6a and 2.6b summarize the targeting variations performed to demonstrate the possible consequence of shielding to predicting collateral damage. For convenience to the reader the targeting variations are described in these charts in terms of the shielding consequence with regard to building vulnerability. Figures 2.22 through 2.27 depict the targeting results obtained along the east axis. Similar targeting analyses performed along the north axis are contained in Appendix A of this report.

As demonstrated in these city damage function curves the assumed impact of shielding may not necessarily be a major factor to collateral damage predictions. It must be emphasized, however, that these calculations are primarily for determining the course of further research. It is quite possible that the final empirical data evaluation will conclude dramatically different consequences of shielding with regard to building vulnerability than has been used to develop these calculations.

2.8 RANDOM UNCERTAINTY INHERENT TO DAMAGE PREDICTIONS

Historically, the nuclear targeting community has relied almost exclusively on an expected value damage estimate for purposes of planning weapon allocation and evaluating the effectiveness of targeting strategies. This measure is used for both strategic and theater nuclear weapon targeting plans whether the targeter is evaluating deliberate damage objectives or assessing the possibility of undesirable collateral damage. In fact, current tactical targeting guidelines to

Table 2.6a Parameter Variations to Assess Impact of Assumed Shielding Consequences

WEAPON SYSTEM (KT)	IMPACT OF SHIELDING ON VULNERABILITY*			BUILDING HARDNESS P ₅₀ (psi)		DIRECTION/ FIGURE NUMBER
	N	D	I	CORE	1/2(CORE) ^c	
1	X			2.5	2.5	NORTH/A.11 EAST/ 2.22
		X		5	2.5	
			X	1.7	2	2.5
1	X			4	2.5	NORTH/A.12 EAST/2.23
		X		8	2.5	
			X	2.6	2	2.5
1	X			4	4	NORTH/A.13 EAST/2.24
		X		8	5.3	
			X	2.6	3.2	4

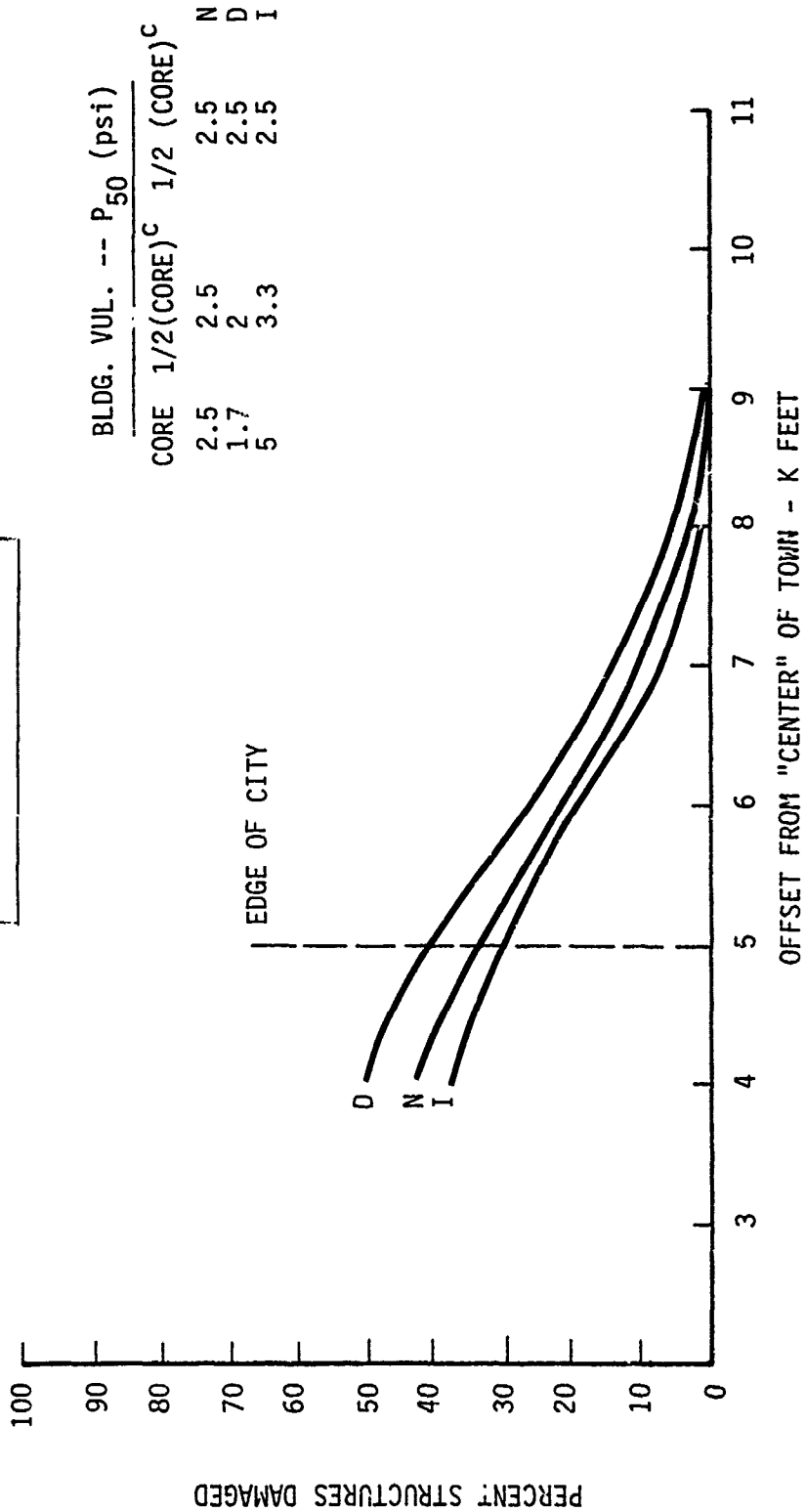
*
 { N = NO CHANGE
 D = DECREASE
 I = INCREASE
 (CORE)^c = SUBURBS

Table 2.6b Parameter Variations to Assess Impact of Assumed Shielding Consequences

WEAPON SYSTEM (KT)	IMPACT OF SHIELDING ON VULNERABILITY*			BUILDING HARDIENESS P ₅₀ (psi)		DIRECTION/ FIGURE NUMBER
	N	D	I	CORE	1/2 (CORE) ^C	
10				2.5	2.5	NORTH/A.14
	X			5	3.3	EAST/2.25
			X	1.7	2	
10				4	2.5	NORTH/A.15
	X			8	3.3	EAST/2.26
			X	2.6	2	
10				4	4	NORTH/A.16
	X			8	5.3	EAST/2.27
			X	2.6	3.2	

{ N = NO CHANGE
 * D = DECREASE
 I = INCREASE
 (CORE)^C = SUBURBS

CITY DAMAGE FUNCTIONS
 1 KT SYSTEM
 - EAST -



BLDG. VUL. -- P ₅₀ (psi)	
CORE	1/2 (CORE) ^C
2.5	2.5
1.7	2
5	3.3

PERCENT STRUCTURES DAMAGED

Figure 2.22 Impact of Shielding on City Damage Predictions

CITY DAMAGE FUNCTIONS
 1 KT SYSTEM
 - EAST -

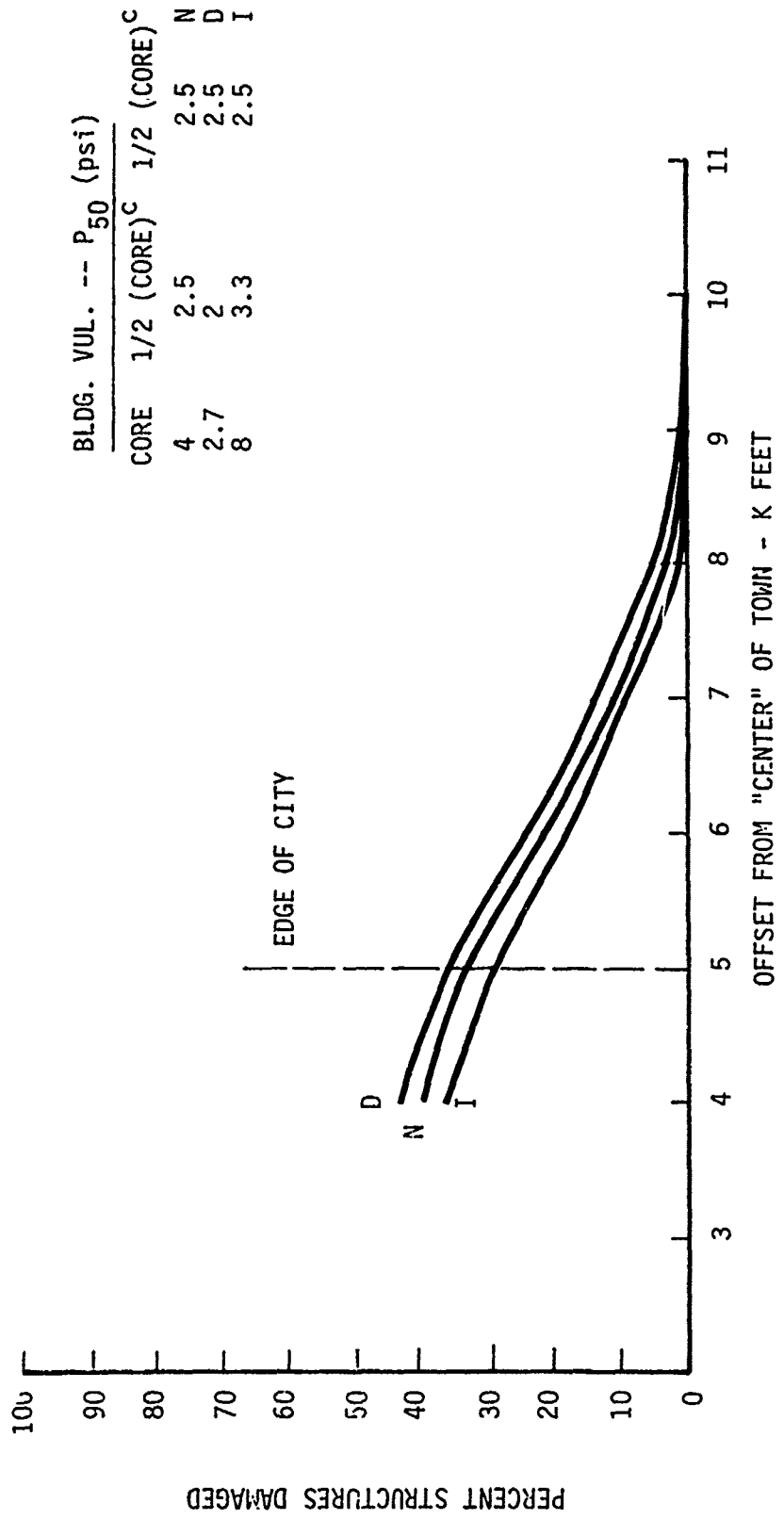
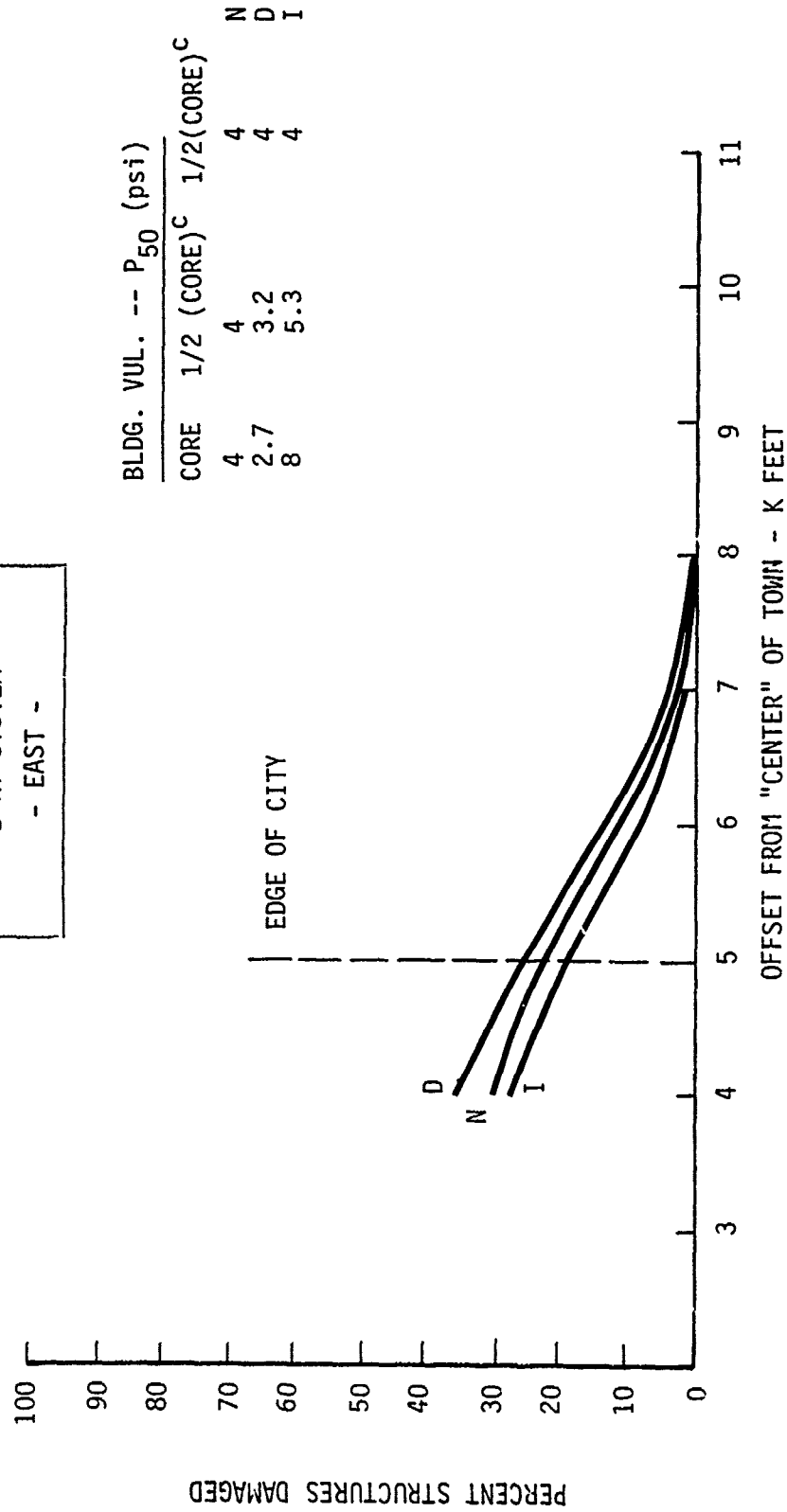


Figure 2.23 Impact of Shielding on City Damage Predictions

CITY DAMAGE FUNCTIONS
 1 KT SYSTEM
 - EAST -



BLDG. VUL. -- P_{50} (psi)		
CORE	$1/2$ (CORE) ^C	$1/2$ (CORE) ^C
4	4	4
2.7	3.2	4
8	5.3	4

N
D
I

Figure 2.24 Impact of Shielding on City Damage Predictions

CITY DAMAGE FUNCTIONS
 10 KT SYSTEM
 - EAST -

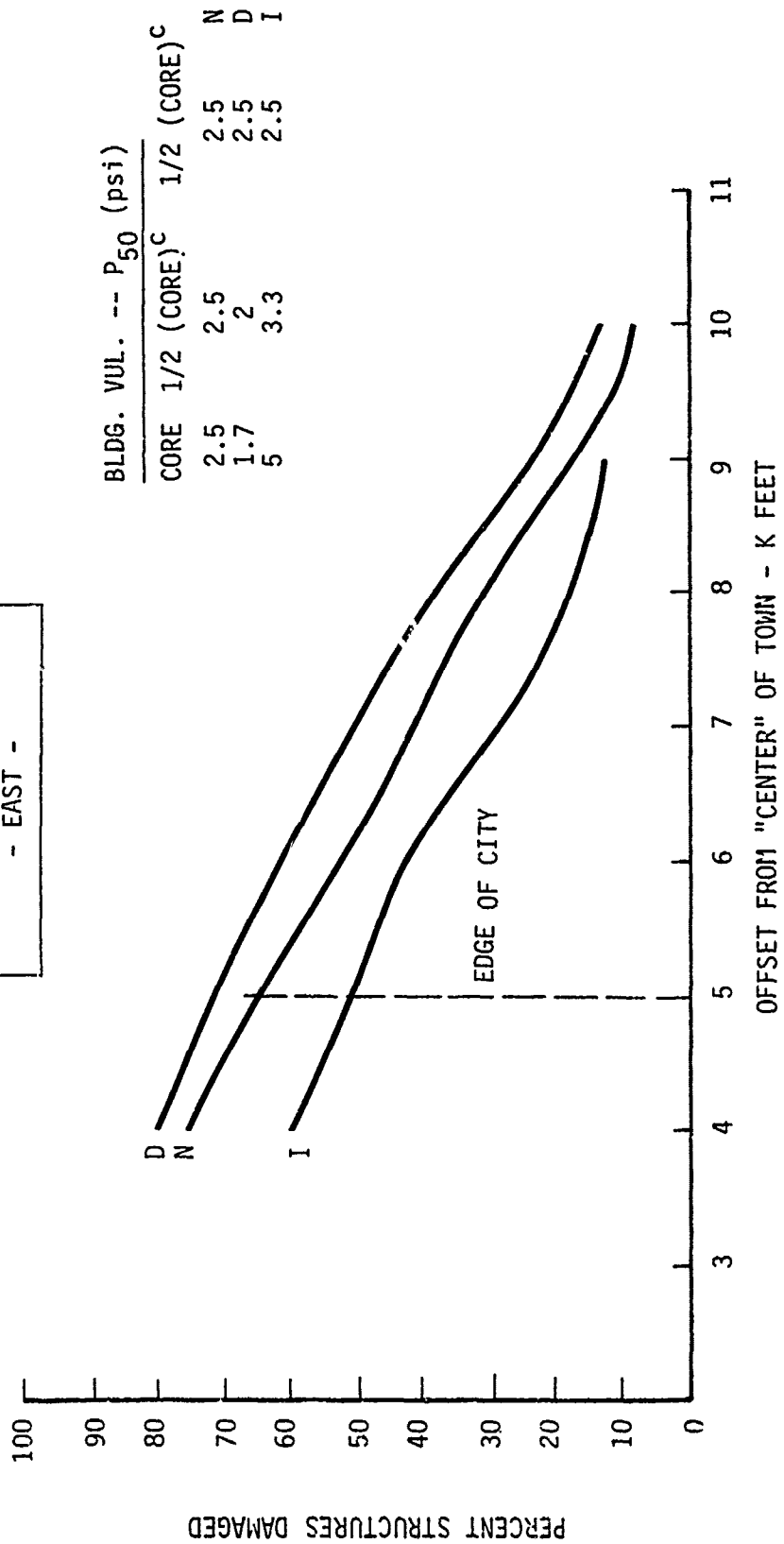


Figure 2.25 Impact of Shielding on City Damage Predictions

CITY DAMAGE FUNCTIONS
 10 KT SYSTEM
 - EAST -

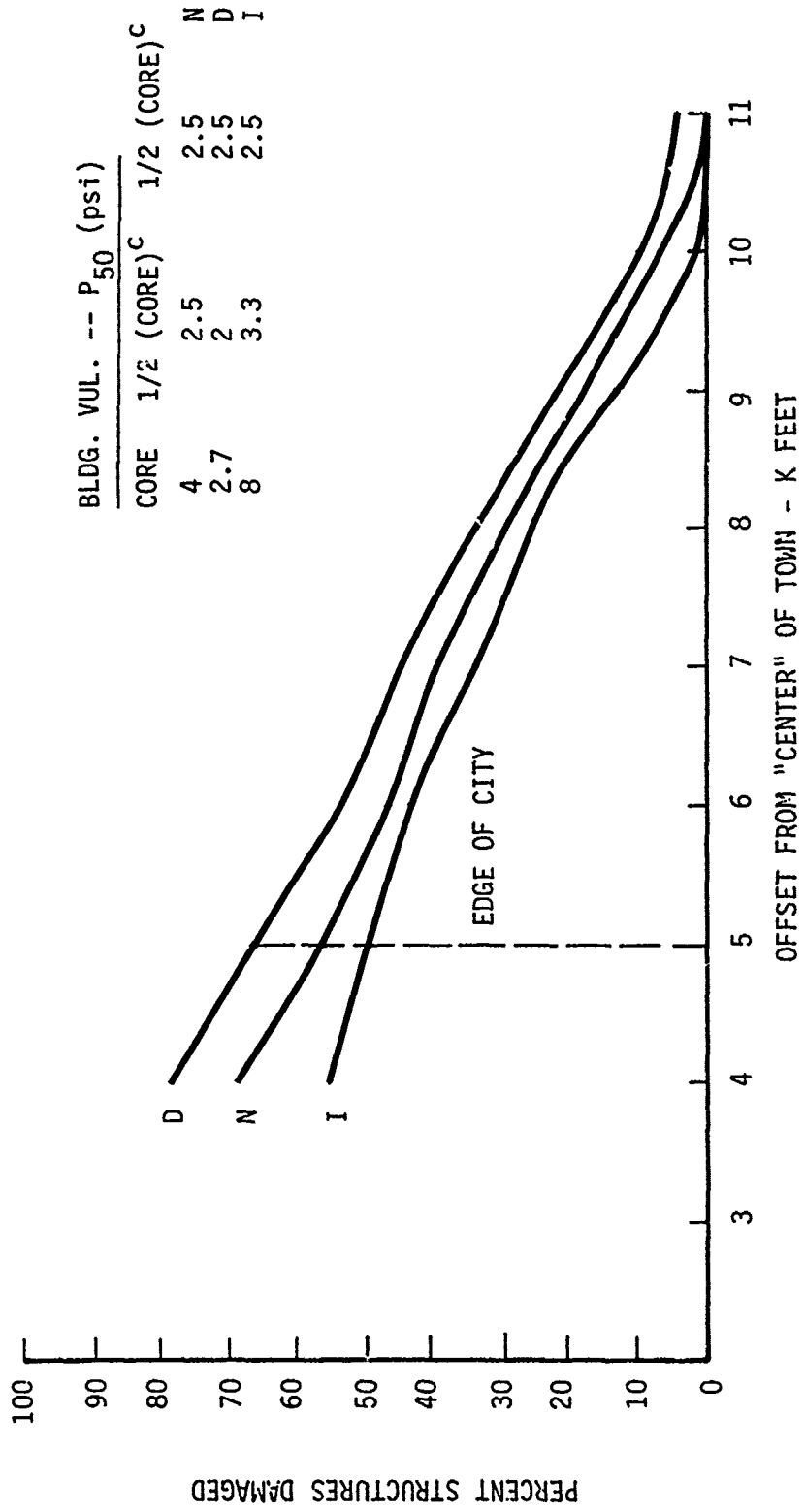


Figure 2.26 Impact of Shielding on City Damage Predictions

CITY DAMAGE FUNCTIONS
 10 KT SYSTEM
 - EAST -

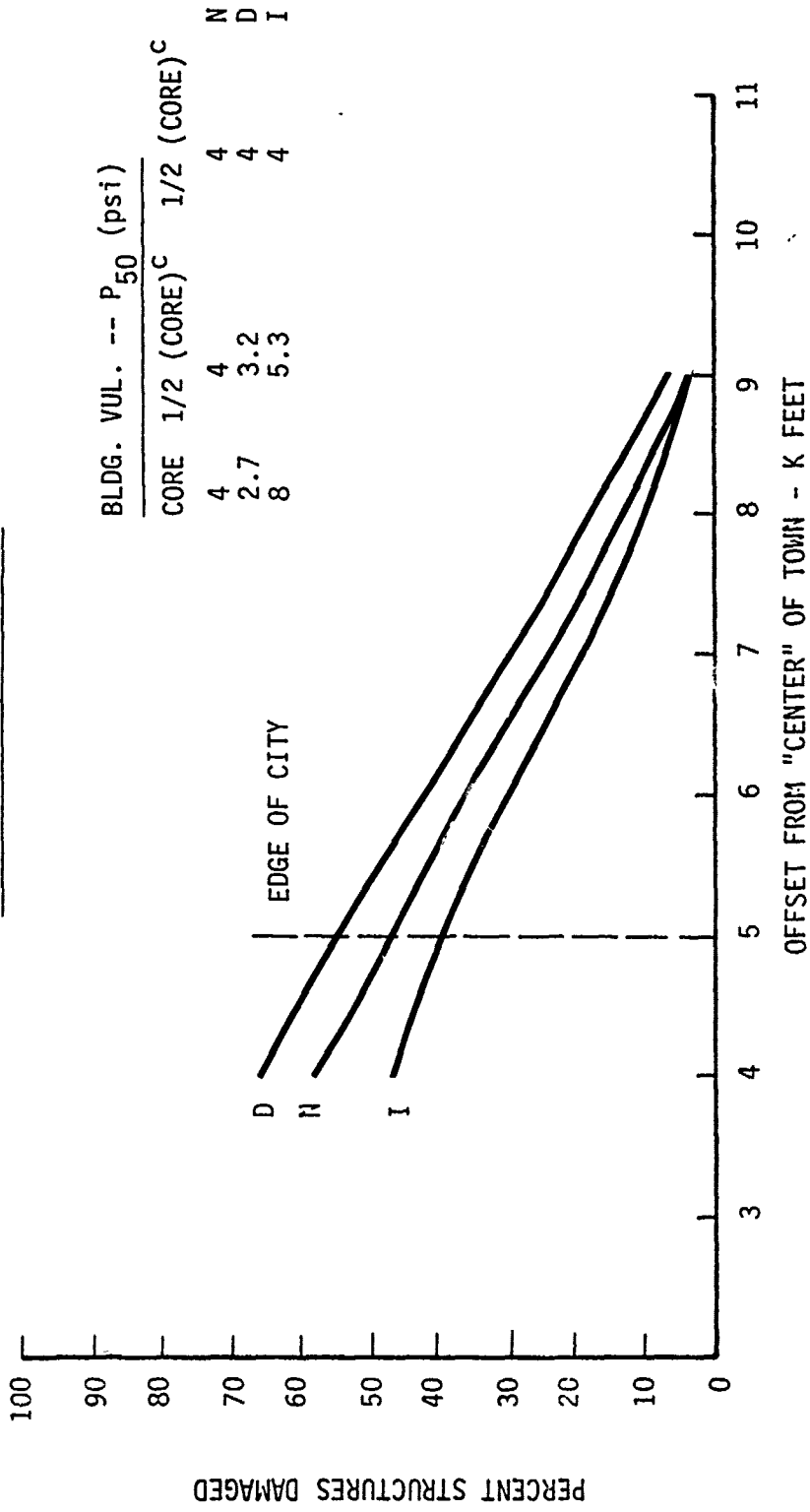


Figure 2.27 Impact of Shielding on City Damage Predictions

ensure minimal collateral damage to population centers is formulated in terms of a standoff distance such that the expected structural damage at the edge of town does not exceed 5 percent.

There are several reasons why this estimator has received almost exclusive attention in targeting applications. The first, and possibly most important reason involves ease in computation and the fact that in a normalized format this estimator may be easily tabulated in handbooks for virtually any targeting scenario. A second justification is derived from the probabilistic concepts fundamental to the law of large numbers. Many of these targeting analyses involve the employment of many weapon systems against a very large target base. Accordingly, even though the expected value may not be realized for any one single event, over the entire operation involving many events the error about the expected value is suspected to be small.

Although an expected damage estimate may be an adequate estimator for a large scale deployment it is not clear that this term provides sufficient collateral damage information for deciding to release tactical nuclear weapons. The shortcoming of this information to the decision process is of course that the command authority has no quantitative appreciation for the actual range of possible outcomes. As a means toward demonstrating this additional information the following analysis is directed toward quantifying the random uncertainty inherent to damage predictions assessed for the example city.

The source of the random error used in this analysis is taken directly from the distance damage function and the error function used to model the distribution of possible weapon impact points. By definition, the random uncertainty included in the distance damage function model is intended to reflect shot-to-shot variation in the weapon produced environment, and structure-to-structure variation in response. This latter component is based upon design and structural variation between buildings within a category and orientation of the structure relative to the blast wave.

Expressed in a mathematical format the shot-to-shot weapon produced environment is modeled as a random variable, denoted by E , and the variation in structural resistance as a random variable, denoted by R . For a specified damage criteria, which in turn specifies the parameter values for R , the structure is considered to be damaged when $E > R$, otherwise not. Since both E and R are random variables the targeter does not know the exact outcome for any single event but rather must rely on a probability measure to predict what could happen.

A similar kind of uncertainty prevails for assessing where the weapon will actually impact. To account for this uncertainty in a targeting methodology an analyst will often characterize this error through a circular Gaussian distribution model. This single parameter model, often characterized by a CEP value, provides the targeting analyst with a method for weighting the target damage prediction so as to reflect all possible impact points.

A Monte Carlo sampling routine was used in this analysis to generate the distribution of possible outcomes about the expected value. The fundamental logic followed in this sampling routine are indicated below.

- Given a DGZ and CEP the sampling algorithm randomly selects an azimuth and range for positioning the impact point relative to the DGZ coordinates. A uniform distribution model, defined in the interval $(0, 2\pi)$, was used to select the azimuth. A Rayleigh distribution model was used for sampling the range of the impact point from the DGZ.
- An airblast range-to-effect correction factor was randomly selected from a log normal distribution with parameters $(\text{median}, \beta_p) = (1, 0.2)$. This correction factor was applied to the pressure-range relationship defined in DASA 2506.

- For each structure a vulnerability correction factor was randomly selected from a log normal distribution with parameters (median, βr) = (1, 0.3). This correction factor was applied to the hardness estimate to determine an actual resistance value for each structure.
- On a structure-to-structure basis the algorithm determined if the peak surface overpressure exceeded the structural resistance. This damage evaluation was performed for each structure to determine the total number of structures damaged.

These steps constitute a single targeting iteration. This process was repeated about 500 times, the results of which were plotted in a histogram format. These particular β -values indicated in the logic of this analysis were deliberately selected for consistency with the vulnerability methodology for P-type targets, i.e., a distance damage sigma value of about 0.2.

Figure 2.28 depicts the results of this analysis for an example targeting application. The dashed curves in this figure represent one standard deviation of random error measured about the expected value. The outside solid curves represent the 10th and 90th percentile values. The lack of symmetry of the bounding curves about the expected damage results are attributable to the skewness in the log normal damage function, and the fact that the building distribution is discrete and non-uniform over the city. Figure 2.29a exhibits the damage distribution histogram obtained from the outcome of simulated results for Figure 2.28 at 8000 feet from the center of town. Figure 2.29b depicts the cumulative frequency function derived directly from the damage histogram. As depicted in this figure 50 percent of the results exceeded the expected value and approximately 17 percent exceed the mean plus 1 standard deviation.

The interpretation of these curves at any given ground range is as follows.

CITY DAMAGE FUNCTIONS
 10 KT SYSTEM
 - EAST -

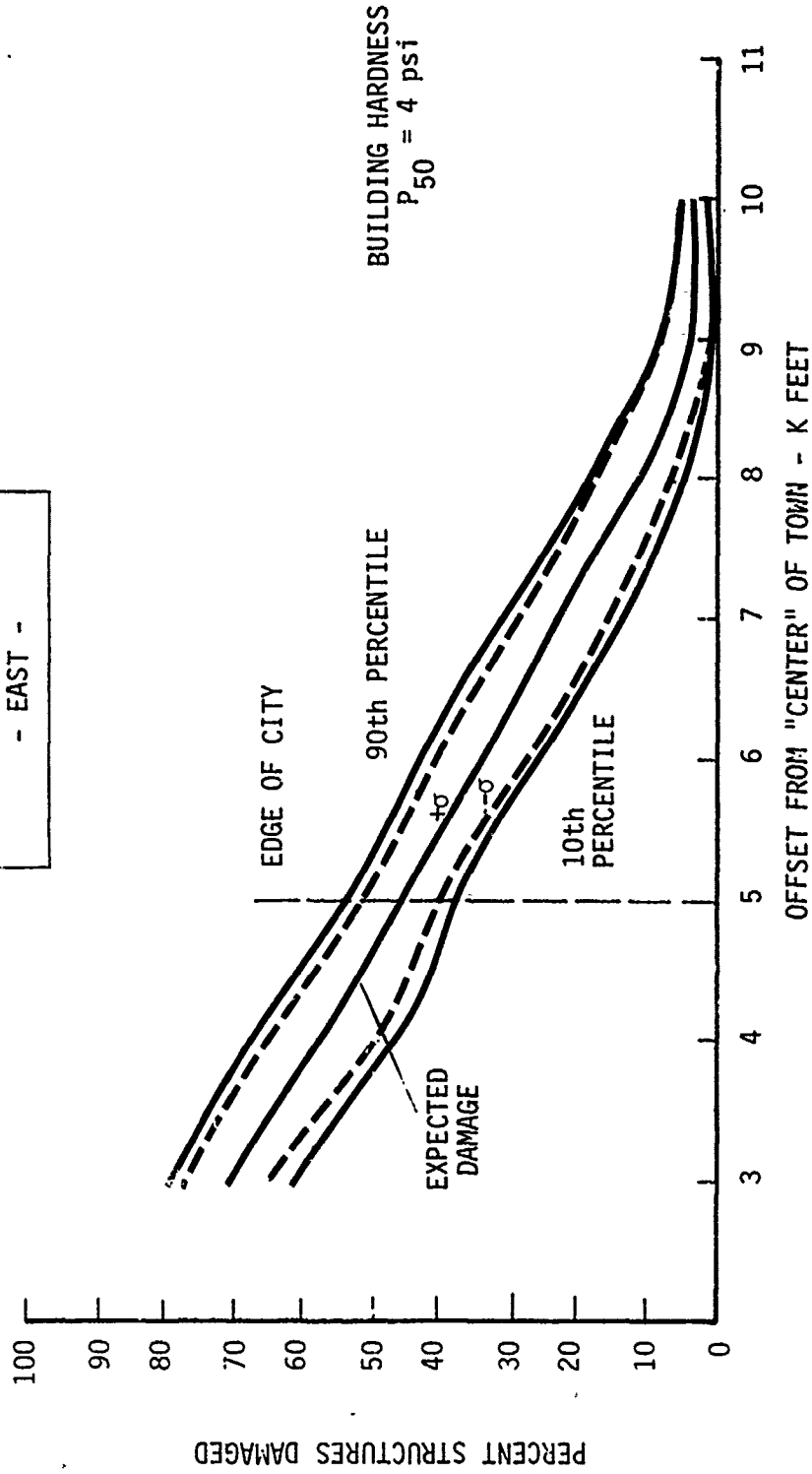


Figure 2.28 Impact of Random Error on City Damage Predictions

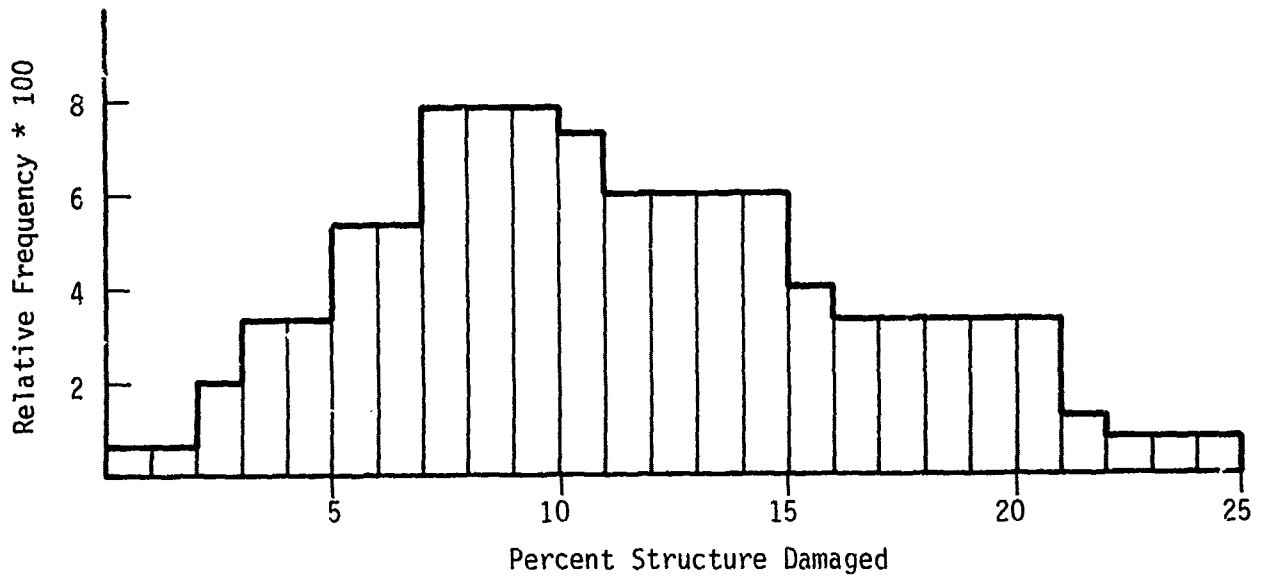


Figure 2.29a Distribution of Outcomes

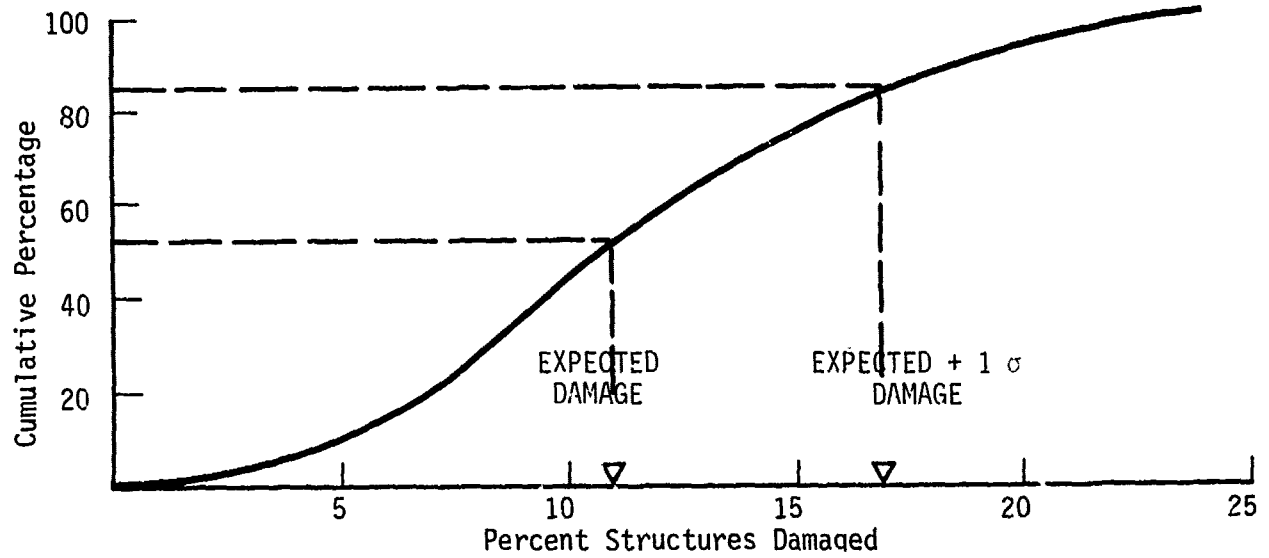


Figure 2.29b Cumulative Distribution

- Over a large number of repeated trials the average damage will tend in probability to the expected damage results calculated from the targeting mathematics and exhibited in these city distance damage curves.
- Given that the actual damage to be realized at a given offset distance, is a random variable there is a 10 percent chance that the damage will exceed the 90th percentile value. Similarly, there is a 10 percent chance that it will be less than the 10th percentile value.

If desired, probability distributions may also be constructed for the ordinate values in Figure 2.28. For example, a collateral damage constraint may specify that no more than 10 percent of all structures are to be damaged. Given this constraint on the percent damage it is possible to determine the distribution of ground range over which this particular percentage could occur.

As depicted in Figure 2.28 random uncertainty could be a very important factor with regard to minimizing collateral damage. It should be apparent from this figure that the expected damage may be an insufficient measure toward realizing this goal when it is used apart from this auxiliary damage information.

Section 3

SHOOT-LOOK-SHOOT

3.1 OBJECTIVE AND SCOPE

The objective of examining this targeting strategy is to investigate the utility of real time battlefield management toward reducing collateral damage. Obviously, the most effective strategy for minimizing collateral damage from nuclear weapon effects is to not deploy nuclear weapons. If this strategy is not feasible, the second best strategy is to use only the number of weapons necessary to achieve the targeting objective. The basic concept of a shoot-look-shoot approach to targeting is, of course, an integral part of this strategy.

The following application of the shoot-look-shoot targeting strategy is very simplistic and is in no way intended to represent an in-depth analysis. No consideration is given to problems of collecting and performing damage assessment analyses on intelligence information. It is recognized that obstacles inherent to this problem could limit the effectiveness of this strategy, and independent of this consideration the method may not be applicable for time sensitive critical targets. The obvious benefit of this strategy toward realizing a minimum collateral damage objective, however, would seem to support at least an exploratory investigation of its potential impact toward achieving this goal.

3.2 PROBABILISTIC MODELS FOR BASIC TARGETING PROBLEMS

A fundamental reason for using a shoot-look-shoot strategy is to ensure realization of the targeting objective without wasting weapon resources. As indicated by the phrase "shoot-look-shoot" this goal is intended to be realized by evaluating the results of an attack and subsequently deploying additional forces if the targeting objective was not attained. This method of targeting is particularly well suited for point

or small area targets that require multiple weapons under the current strategy. This strategy consists of specifying the number of weapons required to attain a high probability of achieving the specified damage. The mathematical model frequently used for this strategy is of the form

$$P^* = 1 - (1 - P)^n \quad , \text{ where}$$

P is a single weapon damage probability, P^* is the desired probability, and n is the number of weapons required to achieve P^* given the value P . Basically, this strategy consists of expending a fixed number of weapons and allowing the outcome to be a random variable. That is, the target may or may not be damaged as predicted by the probability value P^* .

In contrast to the "blind" targeting strategy, the shoot-look-shoot concept is modeled on the premise that the required weapon count to achieve with certainty the desired target damage is a random variable. That is there is random uncertainty inherent to the actual number of weapons which will be expended against the target. The principal advantage of this strategy over the blind targeting method is that damage assessment information collected during the "look" phase will preclude further deployment of unnecessary weapons. The net result is that a lesser number of weapons is expected to be expended with this dynamic method than would be used with the blind targeting strategy.

The simplest deployment strategy under this targeting method is to follow a pattern of shoot/look/shoot...(i.e., SLS). Under this targeting scheme the expected number of weapons to be expended is

$$E(N) = \frac{1}{P}$$

where N is the random variable for the weapon count and P is the probability of killing the target with a single weapon. The expression

for the variance of N is simply,

$$\text{Var } (N) = (1 - P)/P^2 .$$

These moments are based upon the random variable N following a geometric distribution. That is,

$$\text{Pr } (N = n) = P (1 - P)^{n-1} .$$

where $\text{Pr } (N = n)$ is the probability of the first success occurring on the n th trial.

It is a relatively straight forward procedure to modify this basic model to account for, say, time urgent targeting problems. For example, if it was determined that two weapons should be expended prior to evaluating the damage, and then follow a shoot-look-shoot targeting scheme (i.e., SSLSL), the expected value of N and its variance are,

$$E (N) = 2 + (1 - P)^2/P ,$$

$$\text{Var } (N) = \left(\frac{1-P}{P}\right)^2 * (1 + P - P^2) .$$

These moments were derived from the probability mass function

$$\text{Pr } (\bar{X} = n) = \begin{cases} 1 - (1 - P)^2 & , n = 1 \\ P (1 - P)^n & , n = 2, 3... \end{cases}$$

where $\text{Pr } (\bar{X} = n)$ is the probability of the first success occurring on the n th event.

For simple comparison purposes assume that the blind approach required a damage probability of at least 0.9 for a point target. Table 3.1 compares the fixed number of weapons to be expended under this method, for selected values of P, with the expected number determined from these two versions of shoot-look-shoot.

Table 3.1 Weapon Number Requirements,
Blind Method vs. Shoot-Look-Shoot

P-single weapon Probability of Kill	Number of Weapons Deployed				
	n-blind method	E(N) $\sqrt{\text{Var} (N)}$ (SLSL)		E(N) $\sqrt{\text{Var} (N)}$ (SSLSL)	
.3	7	3.3	2.8	3.6	2.6
.4	5	2.5	1.9	2.9	1.7
.5	4	2	1.4	2.5	1.1
.6	3	1.6	1.1	2.3	.7
.7	2	1.4	.8	2.1	.5

It is apparent from this table of comparisons that for certain targeting problems a shoot-look-shoot approach for weapon deployment could result in fewer numbers of weapons being expended compared to the blind method, to achieve the same damage objective. Accordingly, the extent of collateral damage to civilian dwelling units may be reduced under this alternative weapon deployment scheme. There are additional benefits. The reduced number of weapons that would be required under the SLS approach would tend to suppress escalation, as well as conserve weapon resources in any prolonged conflict such as is described in Soviet strategic literature. Despite the fact that real-time nuclear battle management is not within the current state-of-the-art, there is a practical need for such a capability, and the attainment of the required technology in the near term is not implausible.

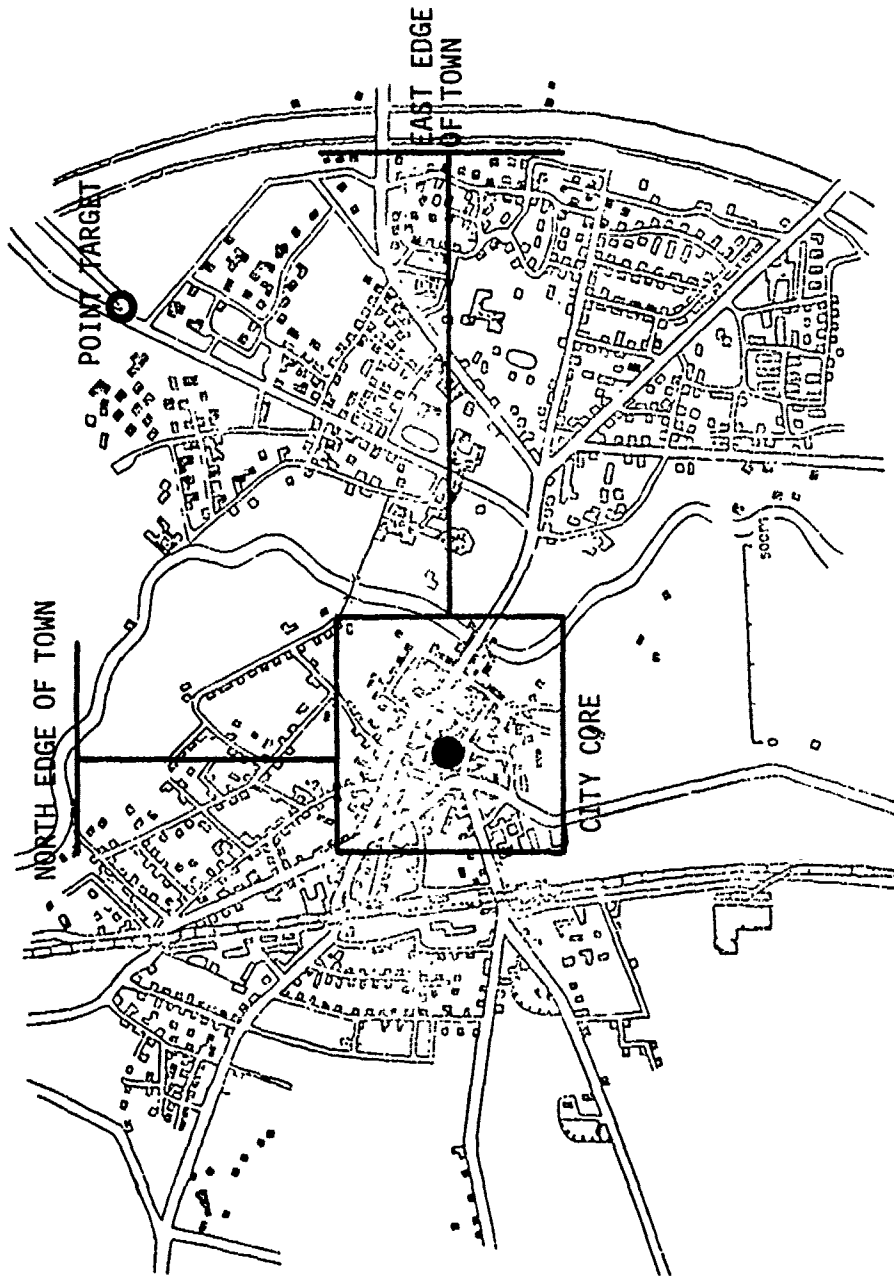


Figure 3.1 Example Town

3.3 COMPARISON OF COLLATERAL DAMAGE PREDICTIONS FOR A SHOOT-LOOK-SHOOT STRATEGY VS. THE "BLIND" METHOD

The purpose of this targeting analysis is to demonstrate the impact of these two strategies on collateral damage predictions. For the purpose of these example calculations it is assumed that there is a military target located along the road-side about 4700 feet north-east from the center of the example city. This target is depicted on the city map in Figure 3.1. Assume also that the single shot probability of kill (SSPK) against this target with the 1 KT weapon system is 0.5. Given that the desired probability of target kill is set at 0.9 the "blind" targeting strategy would necessarily require expending 4 weapons. Under a SLS strategy the information in Table 3.1 indicates that the expected number of weapons to be expended is 2 and the standard deviation about this value is about 1.4. Table 3.2 summarizes this information along with 2 alternative vulnerability descriptions for the structures in the city.

Table 3.2 Targeting Parameters and Strategy, Blind vs. SLS

<u>TARGETING PARAMETERS</u>	<u>SCENARIO 1</u>	<u>SCENARIO 2</u>
Weapon	1 KT System	1 KT System
SSPK	0.5	0.5
Desired Damage Probability	0.9	0.9
Vulnerability of all City Buildings -P ₅₀ -	2.5 psi	4 psi
<u>TARGET STRATEGY</u>		
<u>"Blind" Method</u>		
number weapons expended	4	4
<u>Shoot-Look-Shoot</u>		
expected number weapons expended	2	2
standard deviation	1.4	1.4

Figures 3.2 and 3.3 exhibit the impact of these two strategies on collateral damage predictions for scenario 1 and 2, respectively.

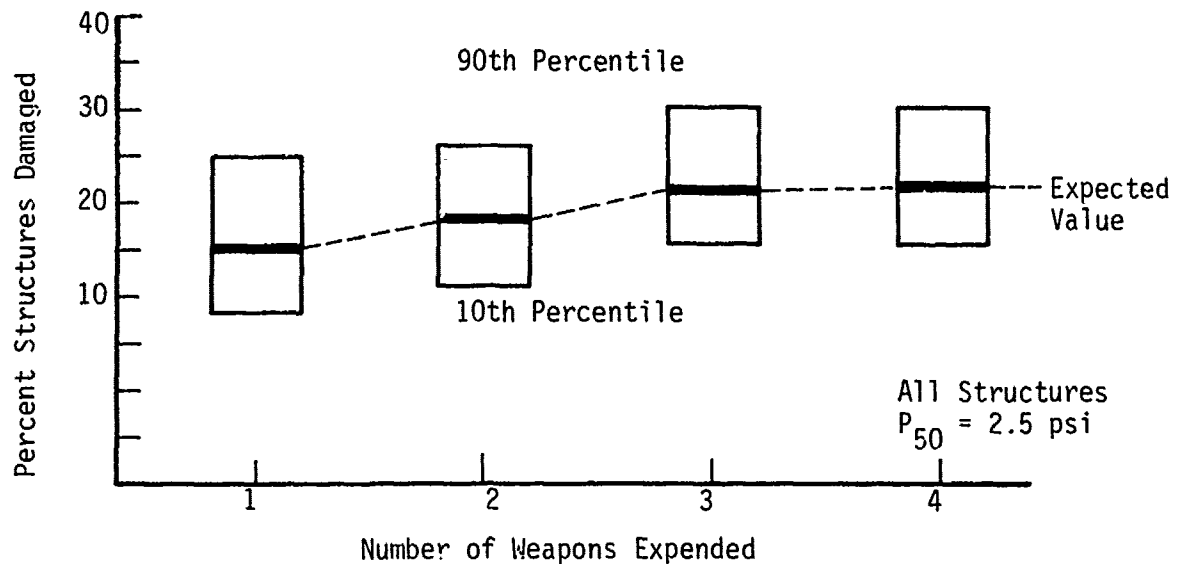


Figure 3.2 Collateral Damage Predictions vs. Weapons Expended

As shown in Figure 3.2 the "blind" targeting strategy, i.e., expending 4 weapons, would result in an expected collateral damage fraction of about 0.24. The 10th and 90th percentile values of the underlying damage distribution are approximately 0.17 and 0.3, respectively. These percentile values are the result of random uncertainty in building response, and random uncertainty in the location of weapon impact. The former uncertainty is that error reflected in the shape of the distance damage function. For each of these example calculations as σ_d value of 0.2 was used. The interpretation of these damage fractions is that although the expected outcome is 0.25 there is a 20 percent probability that the actual damage fraction will exceed 0.3, or will be less than 0.17. Under the SLS targeting strategy the expected

number of weapons to be expended is 2. Conditioned upon realizing this weapon count the expected collateral damage fraction is 0.2. The corresponding 10th and 90th percentile values are approximately 0.14 and 0.28 respectively.

Figure 3.3 depicts the collateral damage predictions for the case when all structures are evaluated at a P_{50} value of 4 psi. Under the "blind" strategy the expected collateral damage fraction is about

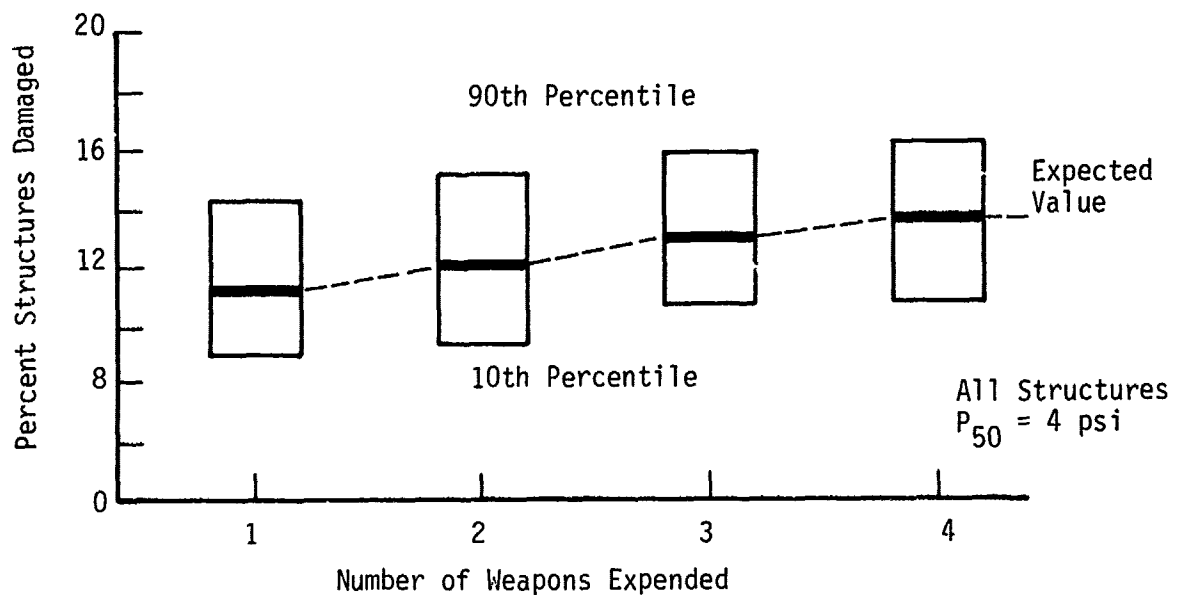


Figure 3.3 Collateral Damage Predictions vs. Weapons Expended

0.13, with 10th and 90th percentile values of approximately 0.1 and 0.16, respectively. Alternatively, realization of the expected weapon count under the SLS strategy would generate an expected collateral damage fraction of 0.11, with 10th and 90th percentile values of approximately 0.08 and 0.14, respectively.

As demonstrated in these two targeting examples the impact on the collateral predictions appears to be minimal for the two targeting strategies. Although these calculations were based upon a hypothetical example it may very well be true that the greatest impact on collateral damage is realized from the first weapon. As such, an SLS targeting strategy may not necessarily offer a high return in terms of reducing collateral damage. A subtle but important measure not adequately reflected in this targeting information, however, suggests that the SLS strategy should not be completely discounted. Table 3.3 contains the city wide damage information generated from 500 Monte Carlo iterations. The term $\sigma_T/E(T)$ (coefficient of variation) is a measure of the random uncertainty in the possible outcome relative to the expected outcome. As demonstrated in this table the $\sigma_T/E(T)$ decreases with number of weapons expended. In theory, this measure will approach

Table 3.3 Collateral Damage Statistics for 1000 Structures

Number of Weapon	$P_{50} = 2.5 \text{ psi}$		$P_{50} = 4 \text{ psi}$	
	expected total damaged	$\sigma_T/E(T)$	expected total damaged	$\sigma_T/E(T)$
1	184	.28	104	.25
2	207	.25	115	.22
3	230	.24	128	.20
4	236	.23	130	.19

a value of zero as the weapon count becomes increasingly large. The message conveyed in this measure, of course, is that the probability of realizing a substantially lesser degree of damage than expected approaches zero as the weapon count increases. As such, the potential payoff in terms of reduced collateral damage offered by the SLS strategy tends to be suppressed under the "blind" method. Or equivalently, the random error tends to average out as the number of weapons increases.

Section 4

A PROTOTYPE ALGORITHM FOR PREDICTING COLLATERAL DAMAGE

4.1 BACKGROUND

Prior to granting approval for the release of nuclear weapons, a command authority must evaluate civilian risk to collateral damage. The purpose of this evaluation is to ensure that undesirable civilian material damage or personnel injuries produced by the effects of nuclear weapons is held to a minimum. In a tactical nuclear operation, the recommended planning strategy toward this goal is to constrain weapon aim points to regions removed from a buffer zone defined about a given town. The span of this buffer zone, measured from the "edge" of a town is formulated upon weapon yield, weapon system accuracy (CEP), vulnerability to nuclear effects, and a measure of damage probability. The net result of this methodology is a minimum stand off distance such that the probability of achieving a specified damage level does not exceed 5 percent at the edge of town. Expressed in mathematical notation,

$$\text{BUFFER DISTANCE (measured from edge of town)} \geq R_{05} + M \cdot \text{CEP},$$

where R_{05} is the ground range assessed from the weapon to which there is a 5 percent chance of causing a specified level of damage. The multiplier, M , applied to the weapon system CEP may be used to provide an additional level of assurance toward realizing this damage avoidance goal.

The mechanics for defining this buffer distance, or collateral damage distance (CDD), is a straight forward application of information contained in the FM 101-31 series of documents. Extensively tabulated charts are provided for the targeter to determine a CDD value for virtually all possible combinations of weapon system, height of burst, and nuclear vulnerability. Accordingly, for most any targeting

scenario a targeter may refer to a collateral damage avoidance table for an R_{05} value and subsequently calculate the span of the buffer zone. This tabulated information, however, does not provide damage information if it is necessary to position a weapon aim point within the buffer zone. In the event of this possibility, the targeter may refer to additional charts in the FM 101-31 series that provide solutions to expected fraction of a target area to be damaged for a specified targeting scenario.

There are, in fact, two methods available to the targeter for estimating collateral damage when the aim point is positioned inside the buffer zone. The first method provides the targeter with a visual description of the area at risk. This is accomplished by a series of templates that allow the targeter to strike an arc through that portion of a town which will be at risk to a specified probability of damage. The second method is used for target areas which can be represented by a series of circles. Once the location and size of the circles are determined the targeter may estimate the expected fractional area damaged for each circle and any given weapon system. In this second method it is not necessary that the desired weapon placement (DGZ) coincide with the center of a circle, but only that the target area be represented by a set of circles.

While both of these methods can provide the targeter with valuable insight toward evaluating collateral damage, both of these methods have individual as well as common limitations. For example, the risk of introducing human error into the targeting analysis may increase substantially when these tools are used for large and complex targeting problems. As a means toward improving these targeting analysis tools, the Defense Nuclear Agency (DNA) has directed an effort to develop an algorithm suitable for evaluating collateral damage to small towns. A prototype algorithm has been developed toward this requirement. Documentation of this algorithm, including the underlying mathematics and a demonstration of its utility, is detailed in the remainder of this section, and also in Appendix B of the report.

4.2 COLLATERAL DAMAGE ALGORITHM REQUIREMENTS

The purpose for developing this algorithm was to provide the targeter in the field with a simplistic and rapid technique for predicting collateral damage to residential and commercial areas. Although the algorithm is primarily intended for structural damage predictions in small towns, the program logic and mathematics are applicable to a wide range of target types and operational scenarios. The basic design requirements for the algorithm included the capability to predict area damage for towns of any given geometry. Additionally, this criterion was to be achieved without requiring the user to be dependent upon a computational facility, i.e., the algorithm must not be so complex as to require the user to be dependent upon a large scale sophisticated computer. Considering the mathematical complexity of even a simple targeting application, however, it was assumed that the user would have access to a hand held calculator.

Additional design requirements, deliberately oriented toward the user, included ease in operation, versatility toward a wide range of targeting scenarios, and a sufficient degree of accuracy relative to more rigorous and complicated damage prediction codes. Toward this last requirement, an obvious and pertinent question concerns definition of tolerable error. In order to satisfy the all inclusive geometry requirement, yet not exceed the capability of a hand held calculator, simplifying assumptions were necessarily required. The extent to which these assumptions may effect the computational accuracy of the damage prediction, however, may vary as a function of the accepted measure for comparison. For example, the area target damage prediction curves presented in FM 101-31 are of near perfect precision in their own right. This high level of precision for an idealized target geometry, however, is not necessarily invariant when extended to an actual targeting situation. Consequently, toward this issue of algorithm accuracy, the selected approach was to demonstrate agreement of results obtained from both an idealized model and the results obtained from a

discrete element enumeration of a target area. For this latter comparison, the algorithm was applied to the example town used in the sensitivity analysis presented in the previous section. The results of these damage prediction comparisons are presented later in this section.

4.3 ALGORITHM ASSUMPTIONS

The damage prediction algorithm used for the sensitivity analyses evaluated each known structure on an individual basis in order to assess the total (city wide) expected damage. This total enumeration of structures was desirable for the expressed purposes of the sensitivity analysis, but would probably not be practical for general targeting applications. In lieu of a total building enumeration, most targeting procedures model a town as a continuum of structures distributed over the definite or idealized boundary conditions. The purpose and objective of this building distribution model is, of course, to facilitate ease in damage prediction computation without significantly degrading the results one would obtain from a discrete enumeration analysis.

The geometric distribution models most frequently used to describe building dispersion over specified areas are the so-called uniform and circular Gaussian distributions. While one of these models may appear more appropriate for a given city, or sub-region of a city, it has yet to be ascertained if either of these models is most appropriate for describing cities in general. In fact, the particular model used for a given targeting problem is usually based upon the computational resources available to the targeter to perform a damage prediction analysis.

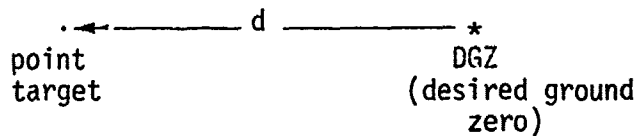
In consideration of the user requirements previously stated, the following area targeting algorithm is based upon a uniformly continuous distribution of structural elements. That is, over any specified area, the structural elements are assumed dense and evenly distributed. Accordingly, over an area A , the fraction of total structures

contained in a subset of A, say A*, would be determined by evaluating the expression,

$$A^{-1} \int_{A^*} dA = \text{fraction of structures in area } A^*.$$

An additional assumption of this algorithm, common to most targeting methodologies, ascribes a constant vulnerability assessment within disjoint sub-regions of the total town area. In the context of this document, the interpretation of vulnerability assessment is intended to be synonymous with that of a vulnerability value in the VN-T-K system. This assumption greatly facilitates ease in overall damage prediction computations and, at least heuristically, should not be a major source of error in the targeting algorithm.

The third assumption results in a simplified description of the damage function used to determine area damage. The point target, distance damage function common to most existing targeting methodologies is derived from the integration of a cumulative log normal distribution over the region of probable weapon impact. For convenience to the targeter, this damage function has been evaluated for virtually every conceivable targeting situation and is often presented in a format similar to that of Figure 4.1. The method by which a targeter would use this information is demonstrated in the following example. The precise meaning of these terms will be explained in subsequent paragraphs.



- WR(weapon radius) = 2000 feet; a measure of weapon yield, height of burst, and target vulnerability
- CEP (circular probable error) = 500 feet; the parameter of a circular Gaussian distribution - describes dispersion of probable weapon impact locations

$d = 2000$ feet; distance between target and DGZ

the ratios, $\left(\frac{d}{\text{CEP}}, \frac{\text{WR}}{\text{CEP}}\right) = (4,4)$

To determine the probability of target damage - locate $\frac{d}{\text{CEP}} = 4$ on the abscissa of Figure 4.1, extend a vertical line from this point to the curve designated $\frac{\text{WR}}{\text{CEP}} = 4$, and read across to the ordinate to determine a damage probability of 0.4.

These damage function curves, developed for point targets, are also used to predict damage to area targets. This is accomplished by integrating the appropriate damage function over the target area. For example, given that the vulnerability of the target area is expressed in terms of the weapon radius (WR), and the damage function is represented in some functional form $f\left(\frac{d}{\text{CEP}}; \frac{\text{WR}}{\text{CEP}}\right)$, then the expected total area damaged can be derived from the expression

$$\text{area damage} = \int_A f\left(\frac{r}{\text{CEP}}; \frac{\text{wr}}{\text{CEP}}\right) dA .$$

To perform this integration on a small calculator it is usually necessary to approximate the analytical form of the damage function. There are polynomial expressions that have been demonstrated to give excellent approximations, however, they tend to require a large number of coefficients which may exceed the capability of most hand held calculators. To alleviate this possible restriction, and improve computational efficiency, a simplified approximation to the damage functions depicted in Figure 4.1 was developed. This simplification is based upon a trend in the damage function curves depicted in Figures 4.1 and 4.2. For each of these two families of curves (SIGMA-20, SIGMA-30), the damage function tends to be a straight line on the probability X linear scale representation when $\frac{\text{WR}}{\text{CEP}}$ equals or exceeds a value of 3. This trend in the shape of the curves suggests that a cumulative

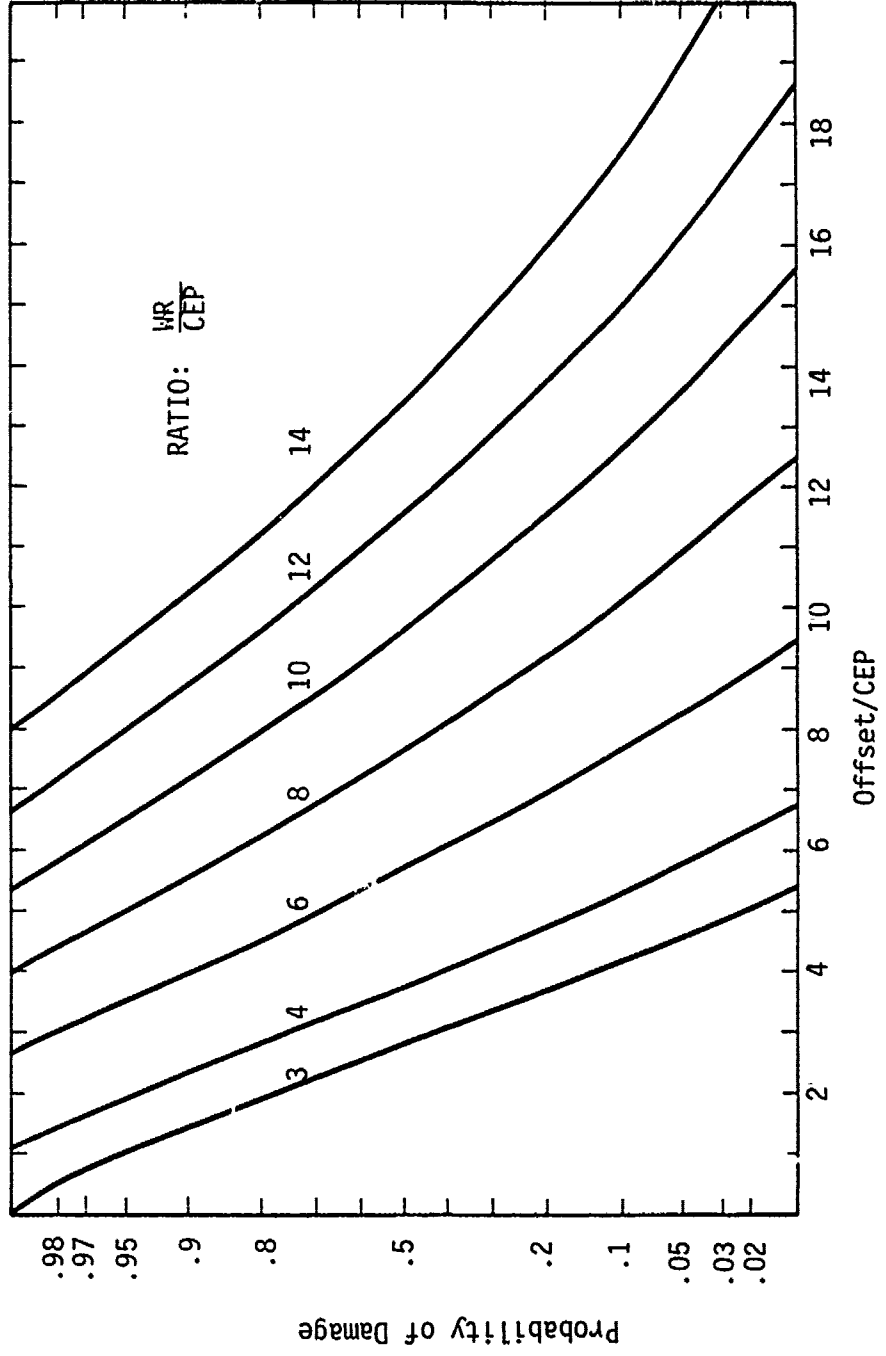


Figure 4.1 Probability of Damage to Point Targets ($\sigma_D = 0.2$)

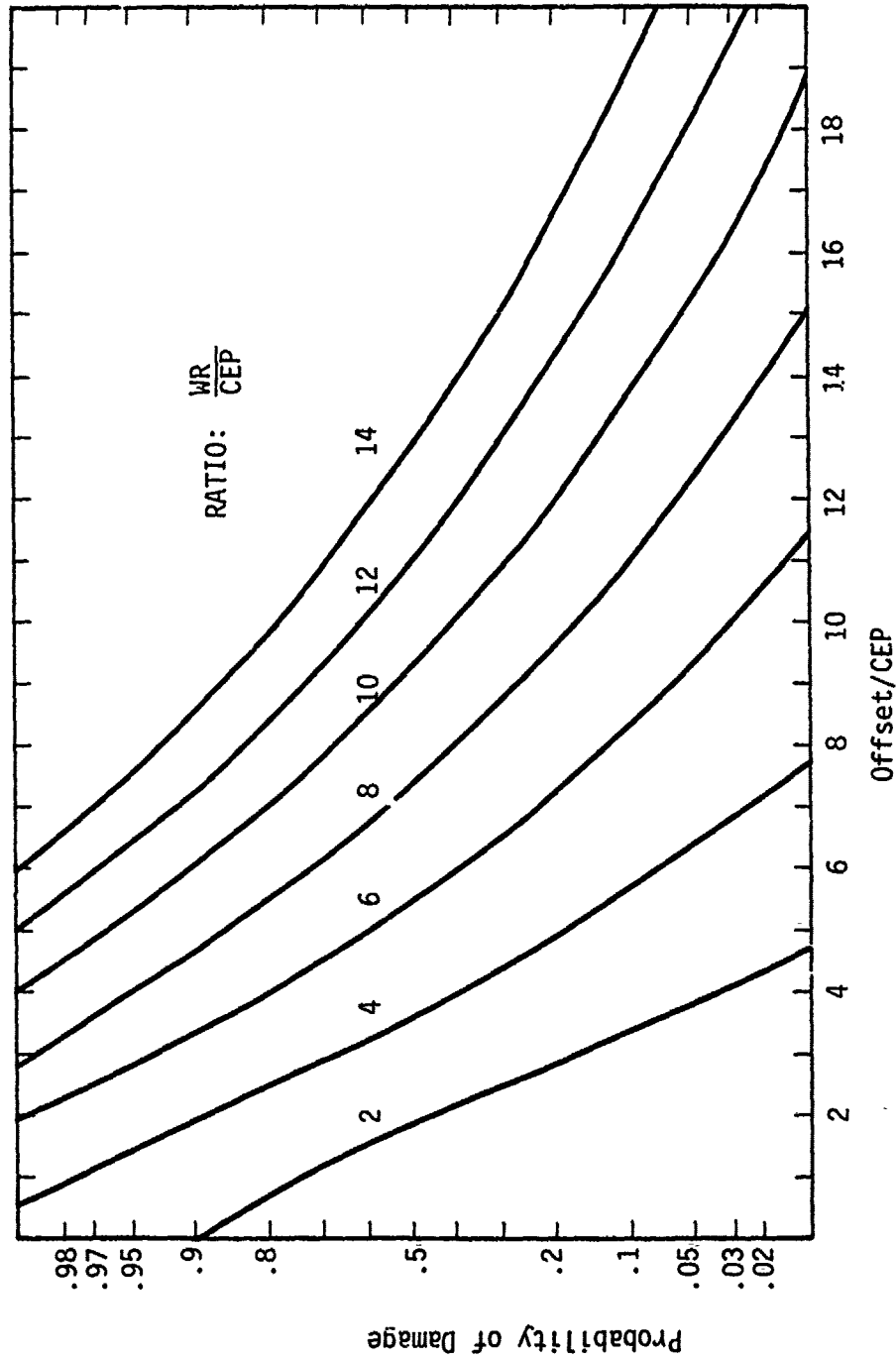


Figure 4.2 Probability of Damage to Point Targets ($\sigma_D = 0.3$)

normal distribution may be used to approximate the damage function when $\frac{WR}{CEP} \geq 3$. This approximation to the damage function is especially attractive for computational purposes since the cumulative normal distribution function can be represented by a 5th order polynomial. Accordingly, the demand on computational capability is considerably less than with other approximations. Using this simplified approximation, target area damage may be estimated by evaluating the expression,

$$\text{target area damage} = \int_A \left[1 - F \left(\frac{r}{CEP} ; \frac{WR}{CEP} \right) \right] dA,$$

where $F(\cdot)$ is a cumulative normal distribution function. The requirement that $\frac{WR}{CEP} \geq 3$ is not believed to be a serious limitation when predicting collateral damage to residential/commercial structures in a tactical targeting scenario. These structures are thought to be relatively soft. Also, since tactical weapon systems tend to have a small CEP, relative to the weapon radius, there should be very few, if any, situations when this ratio would be less than a value of 3.

4.4 MATHEMATICS OF COLLATERAL DAMAGE PREDICTION ALGORITHM

As previously stated, the purpose for developing this algorithm is to provide a targeter with a convenient method for predicting collateral damage to residential/commercial structures dispersed over a small town. A major obstacle to developing the algorithm was the requirement that the program be able to evaluate areas of any configuration. Additionally, the mathematics used for generating these area damage predictions must not be of such detail as to exceed the capability of a hand held calculator.

As a means of achieving these algorithm design goals, it was necessary to make some simplifying assumptions. The single most important simplification was the analytical form of the distance damage

function used to approximate the targeting mathematics detailed in the DIA publication, DI-550-27-74. The mathematical damage prediction model presented in this document, is the compliment of a cumulative log-normal distribution. The general shape of this damage prediction model is depicted in Figure 4.3. As a target damage prediction model, this distribution is often characterized by two parameters; the weapon radius (WR) and the distance damage sigma (σ_d).

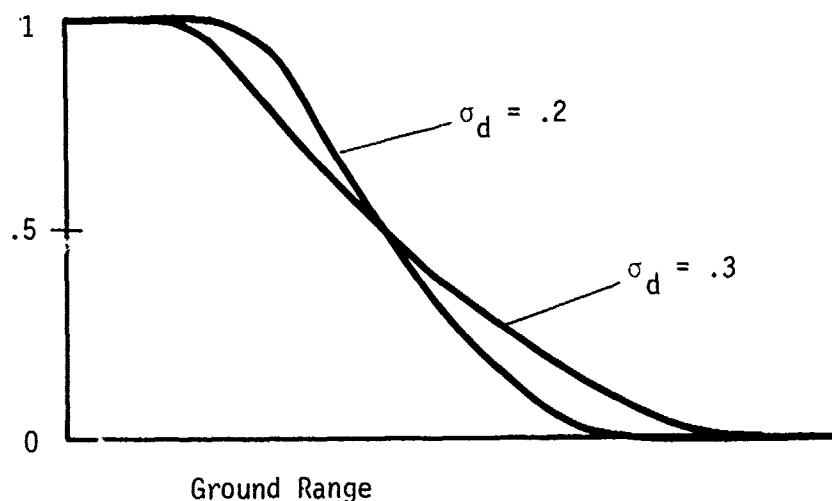


Figure 4.3 Targeting Distance Damage Function

The weapon radius is, by definition, the radius of a circle originating at ground zero and measured over an infinite array of uniformly distributed like targets, such that, there will be as many targets undamaged (to a specified level) inside the weapon radius as there will be damaged targets outside the weapon radius. Expressed mathematically this definition is equivalent to the expression,

$$\int_0^{2\pi} \int_0^{WR} (1-P_d(r)) r dr d\theta = \int_0^{2\pi} \int_{WR}^{\infty} P_d(r) r dr d\theta .$$

The purpose of the distance damage sigma (σ_d) is to provide a measure of the shot-to-shot random variation, in target response and the associated variation in the weapon produced damaging effect(s). With reference to Figure 4.3, the physical significance of this damage sigma is reflected in the slope of the damage function.

The two damage function parameters are, in fact, merely variations of two parameters often used to characterize a log-normal distribution. If we define R_{50} to be the ground range at which there is a 50 percent chance of achieving a specified damage level then,

$$WR \cdot (\text{Weapon Radius}) = R_{50} * \exp\left(\frac{\beta^2}{2}\right)$$

and

$$\sigma_d \text{ (damage sigma)} = \sqrt{1 - \exp(-\beta^2)} .$$

The term, β^2 , is the variance of a random variable $Y = \log_e \bar{X}$, where \bar{X} is a so-called log normally distributed variate.

The family of curves exhibited in Figures 4.1 and 4.2 are obtained by integrating the log normal damage function, $P_d(r)$, over the probable area of weapon impact.

That is,

$$f(d) = \int_A P_d(r) dA \quad , \text{ where } d \text{ is the distance between the}$$

point target and the DGZ.

As discussed previously, this point target damage prediction function may be integrated over a target area to assess the expected total area damage. It is for this targeting problem that the algorithm was developed, hence, the cumulative normal distribution function is used to approximate the function $f(\cdot)$ as defined in DIA publication, DI-550-27-74. Accordingly, the mathematics of this algorithm is built upon the relationship

$$\int_A [1-F(r)] dA \approx \int_A f(r) dA$$

where A is the target area.

In order for the approximating function, $1-F(r)$, to be of some utility to the targeter, there must exist a procedure for inserting the individual target parameters into this damage prediction function. That is, given specific values for WR , CEP , and separation between target and DGZ, there must exist some technique for inserting this information into the approximating function to arrive at a point target damage prediction. The approach used to resolve this issue was also based on the observation that the family of curves in Figures 4.1 and 4.2 tend to follow a cumulative normal distribution. For any given value of $\frac{WR}{CEP}$, knowledge of the mean and standard deviation of the underlying normal variate is sufficient information for predicting target damage at any offset distance. Analysis of these curves identified a linear relationship between $\frac{WR}{CEP}$ and the mean and standard deviation. The development and resulting linear expressions are discussed in the following paragraphs.

Toward developing these functional relationships among $\frac{WR}{CEP}$, mean, and standard deviation, extensive use was made of two characteristics of the normal distribution. The first is that the mean and median (50th percentile) of a normal distribution coincide. The second feature is that the standard deviation may be determined from the relationship

$$\sigma \text{ (standard deviation)} = \frac{\text{90th percentile} - \text{mean}}{1.28}$$

To demonstrate the functional relationships between $\frac{WR}{CEP}$ and the mean and standard deviation, a member of the family of curves in Figure 4.1 is depicted in Figure 4.4. As may be observed in this exhibit, the mean and standard deviation may easily be derived according

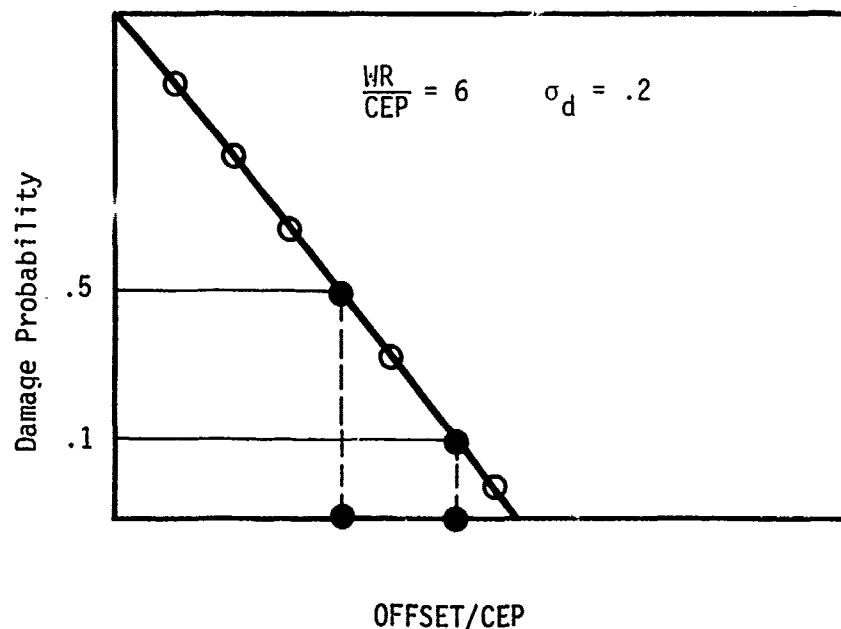


Figure 4.4 Damage Function Parameters

to the relationships,

$$\hat{\mu} = \left(\frac{d}{\text{CEP}}\right) 50 = 5.75$$

$$\hat{\sigma} = \frac{\left(\frac{d}{\text{CEP}}\right) 90 - \hat{\mu}}{1.28} = \frac{7.75 - 5.75}{1.28} \approx 1.6$$

Insertion of these parameter values into the approximating damage function, $1-F\left(\frac{d}{\text{CEP}}; \hat{\mu}, \hat{\sigma}, \frac{WR}{\text{CEP}} = 6, \sigma_d = .2\right)$, results in damage prediction estimates as demonstrated by the open circles in Figure 4.4.

The parameter evaluations described in the previous paragraph were performed on each of the curves exhibited in Figure 4.1. The parameter values obtained from this analysis are shown in Table 4.1. The respective values for $\hat{\mu}$ and $\hat{\sigma}$ are plotted in Figure 4.5.

Table 4.1 Damage Function Parameters, SIGMA-20

$\frac{WR}{\text{CEP}}$	$\hat{\mu}$	$\hat{\sigma}$
3	2.8	1.09
4	3.7	1.25
6	5.7	1.56
8	7.7	1.88
10	9.7	2.27
12	11.6	2.66
14	13.4	3.28

as a function of $\frac{WR}{\text{CEP}}$. The mathematical equations used to fit the apparent linear relations between $\frac{WR}{\text{CEP}}$ and $\hat{\mu}, \hat{\sigma}$ are as follows:

$$\hat{\mu} = 0.968 * \left(\frac{WR}{\text{CEP}}\right) - 0.09$$

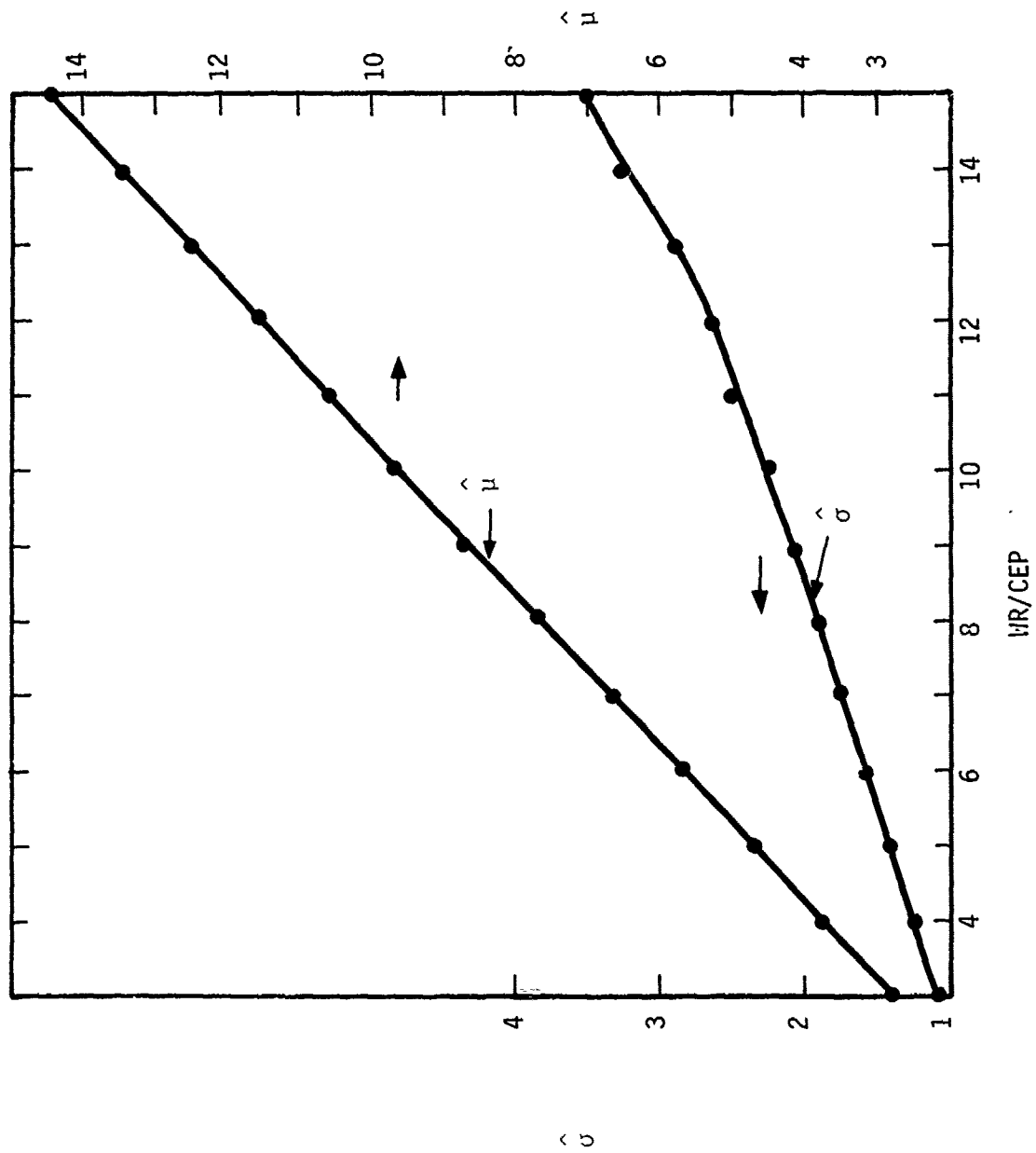


Figure 4.5 Relationship Between Damage Function Parameters (SIGMA-20)

$$\hat{\sigma} = \begin{cases} 0.1737 * \left(\frac{WR}{CEP}\right) + 0.5418, & \text{for } 3 \leq \frac{WR}{CEP} \leq 12 \\ 0.297 * \left(\frac{WR}{CEP}\right) - 0.922, & \text{for } \frac{WR}{CEP} > 12 \end{cases}$$

Similar relations were developed between $\frac{WR}{CEP}$, $\hat{\mu}$, and $\hat{\sigma}$ for the curves shown in Figure 4.2. The values obtained for $\hat{\mu}$ and $\hat{\sigma}$ are tabulated in Table 4.2 and plotted in Figure 4.6 opposite the corresponding $\frac{WR}{CEP}$ values.

Table 4.2 Damage Function Parameters, SIGMA-30

$\frac{WR}{CEP}$	$\hat{\mu}$	$\hat{\sigma}$
4	3.6	1.64
6	5.5	2.19
8	7.3	2.81
10	9.2	3.44
12	10.9	4.14
14	12.8	4.48

The mathematical equations used to describe these functional relationships between $\frac{WR}{CEP}$, $\hat{\mu}$, and $\hat{\sigma}$ are as follows:

$$\hat{\mu} = 0.916 * \left(\frac{WR}{CEP}\right) - 0.0126$$

$$\hat{\sigma} = 0.3034 * \left(\frac{WR}{CEP}\right) + 0.3987$$

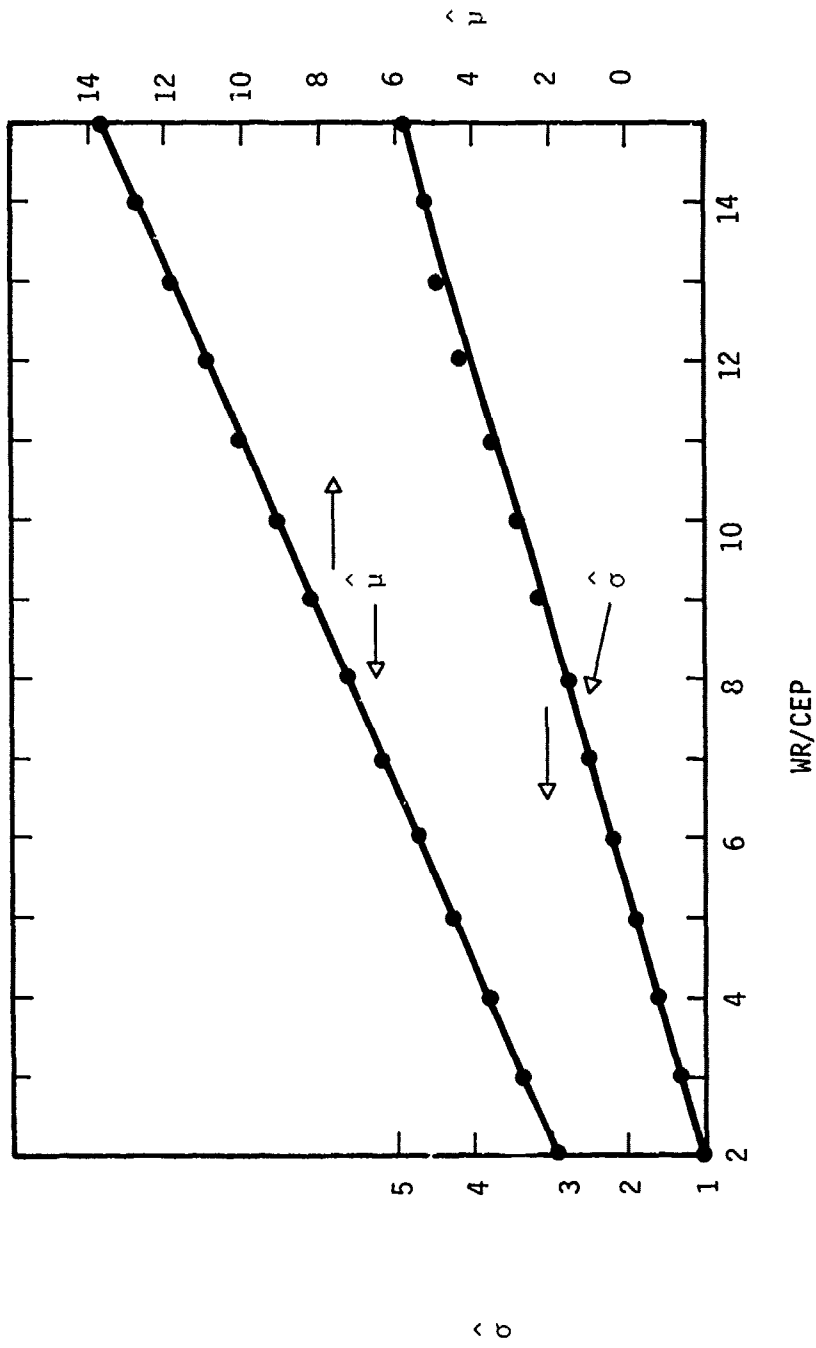


Figure 4.6 Relationship Between Damage Function Parameters, (SIGMA-30)

Given these functional forms for $\hat{\mu}$ and $\hat{\sigma}$, and the damage prediction function $1-F(r)$, predicting damage to a point target now requires a far less complicated mathematical expression to evaluate. The following example demonstrates how this method can be applied to a targeting problem.

Given a point target with parameters:

$$WR = 2000 \text{ FT}$$

$$\sigma_d = 0.2$$

$$CEP = 500 \text{ FT}$$

$$d \text{ (DGZ offset)} = 2000 \text{ FT}$$

The objective is to evaluate the probability of damage. The procedure is as shown in the following steps.

Step 1

Determine $\frac{WR}{CEP}$ and $\frac{d}{CEP}$

$$\frac{WR}{CEP} = 4, \quad \frac{d}{CEP} = 4$$

Step 2

Determine $\hat{\mu}$ and $\hat{\sigma}$

$$\begin{aligned}\hat{\mu} &= 0.968 * \left(\frac{WR}{CEP}\right) - 0.09 \\ &= 3.78\end{aligned}$$

$$\begin{aligned}\hat{\sigma} &= 0.1737 * \left(\frac{WR}{CEP}\right) + 0.5418 \\ &= 1.24\end{aligned}$$

Step 3

Evaluate damage probability

$$\left(\begin{array}{c} \text{Probability} \\ \text{of} \\ \text{Damage} \end{array} \right) = 1 - F\left(\frac{d}{\text{CEP}}; \hat{\mu}, \hat{\sigma} \right)$$

where

$$F\left(\frac{d}{\text{CEP}}; \hat{\mu}, \hat{\sigma} \right) = \int_{-\infty}^{\frac{d}{\text{CEP}}} \frac{\exp\left(-\frac{1}{2} \left(\frac{x - \hat{\mu}}{\hat{\sigma}}\right)^2\right)}{\hat{\sigma} \sqrt{2\pi}} dx$$

$$= \int_{-\infty}^{\left(\frac{d}{\text{CEP}} - \hat{\mu}\right)/\hat{\sigma}} \frac{\exp\left(-\frac{1}{2} x^2\right)}{\sqrt{2\pi}} dx$$

$$= \int_{-\infty}^{0.18} n(x; 0, 1) dx$$

$$\therefore \left(\begin{array}{c} \text{Probability} \\ \text{of} \\ \text{Damage} \end{array} \right) = 1 - \int_{-\infty}^{0.18} n(x; 0, 1) dx$$

$$= \int_{0.18}^{\infty} n(x; 0, 1) dx$$

$$= .43$$

For this example, the integral expression given above was evaluated using a standard normal distribution table. In the targeting algorithm developed for a hand held calculator this integral expression is approximated by a 5th order polynomial. This polynomial approximation is further discussed in the following paragraphs.

This point target damage function is also applicable for predicting the total damage to an area array of point targets. For example, integration of this damage prediction function over the inhabited regions of a city will provide an estimate as to the expected fraction of damaged structures resulting from a specific targeting scenario. The target area modeling method selected for this collateral damage prediction algorithm assumes a continuously uniform distribution of structures described in the shape of a wedge. This particular shape was selected to facilitate the damage prediction over the target area. A pictorial representation of this method for describing the target area is exhibited in Figure 4.7.

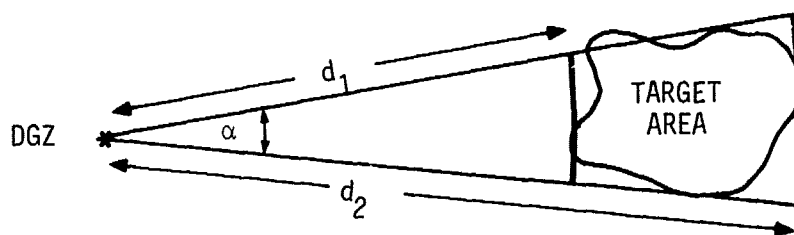


Figure 4.7 Target Area Representation

Given the target area representation as described in Figure 4.7 the expected area damaged is evaluated by the expression,

$$\begin{aligned} \text{Area Damage} &= \int_0^\alpha \int_{d_1}^{d_2} [1-F(r)] \, r \, dr \, d\theta \\ &= \alpha \int_{d_1}^{d_2} [1-F(r)] \, r \, dr \end{aligned}$$

In most targeting applications, however, the analyst is primarily concerned with the expected fractional area damage, not the total area damage. To obtain this fractional damage prediction measure it is only necessary to divide the total area damage estimate, given above, by the target area. Accordingly, the expected fractional area damage is determined from the expression,

$$\begin{aligned} \left(\frac{\text{Fractional Area}}{\text{Damage}} \right) &= \frac{\text{Area Damage}}{\int_0^\alpha \int_{d_1}^{d_2} r \, dr \, d\theta} \\ &= \frac{\int_{d_1}^{d_2} [1-F(r)] \, r \, dr}{\frac{1}{2} [d_2^2 - d_1^2]} \end{aligned}$$

It is of interest to note that the angle of integration cancels out in the expression for fractional area damage. As such, the only additional information required by the target analyst to evaluate an area target, over that for a point target, are the values d_1 and d_2 , the distances from the DGZ to the "front" and "back" edges of the town, respectively.

4.5 APPLICATION OF ALGORITHM TO AREA TARGETS

The purpose of the following analysis is to demonstrate the utility of this prototype algorithm for predicting damage to area-type targets. As shown in the previous examples the agreement between this algorithm and the log normal model is very good for point targets provided the ratio $WR/CEP \geq 3$. The purpose for developing this algorithm, however, was primarily as a tool for predicting damage to a large number of discrete elements which could be represented by an area distribution model. The following examples demonstrate application of this algorithm for area-type targeting problems. The first demonstration is for an idealized target area description such as found in targeting handbooks. The second example demonstrates an application to predicting collateral damage to the small town used for the targeting analyses presented in the previous sections. In each of these examples the damage predictions obtained from this algorithm will be compared with the results obtained using a log normal targeting model.

4.5.1 Application of Algorithm to Circular Area Targets

The purpose for presenting this targeting example is to demonstrate consistency of results between this algorithm and information contained in targeting handbooks. In particular, the following example demonstrates application of this algorithm to a uniformly distributed circular target area, and compares the damage predictions with damage values contained in the handbooks. Given that this algorithm was deliberately developed for collateral damage targeting problems

the damage prediction comparisons will be demonstrated only for the case when the DGZ is removed from the center of the target area at least one multiple of the target radius (TR). Figure 4.8 depicts this constraint on the DGZ locations selected for this comparison of damage estimates. The label "d" in this figure denotes the 3 DGZ locations, expressed as a multiple of the target radius, used in the following examples

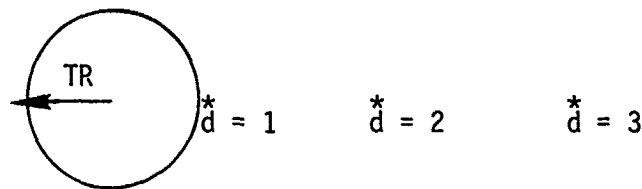


Figure 4.8 DGZ Locations for Comparing Damage Predictions

Circular target area damage predictions are based on the values of 4 variables.

- WR : Weapon Radius
- CEP : Circular Probable Error
- TR : Target Radius
- OFFSET : Distance From Center of Circle to DGZ

Since the following examples are deliberately intended to demonstrate area damage predictions at 3 specific DGZ locations these four variables can be reduced to 3 variables by normalizing the respective terms with respect to the target radius. The 3 variables are, (WR/TR, CEP/TR, $d = \text{OFFSET/TR}$). For each value of "d" in these targeting examples the term WR/TR will be the continuous variable. The impact of this continuous variable on damage prediction will be demonstrated for parameter values of CEP/TR equal to 1/10, 2/10, and 1/2. These seemingly small parametric values for CEP/TR were selected because tactical-type weapon systems tend to have small CEP values relative to the span of small towns and cities.

As explained previously in this section the algorithm models the target area in the geometry of a truncated wedge. This manner of characterizing the actual target area is primarily for ease in evaluating the integral of the damage function taken over the target area. As such, the algorithm will actually be evaluating the area damage as if the area of the circle were uniformly distributed within a circular annulus. This method of describing the target area is depicted in Figure 4.9. The distances, d_1 and d_2 , shown in this figure, are 2 of the 5 input variables to this algorithm. These 5 variables, presented in the order in which they are entered into the calculator, are (WR, CEP, d_1 , d_2 , σ_d).

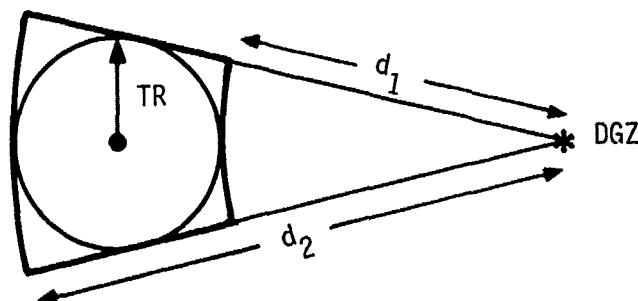


Figure 4.9 Target Area Representation

Figures 4.10a, 4.10b, and 4.10c depict the area damage predictions obtained from targeting handbooks and this prototype algorithm. As indicated by the residual error between the open circles, denoting the algorithm generated results, and the continuous curves the algorithm results tend to compare favorably with the precise calculations.

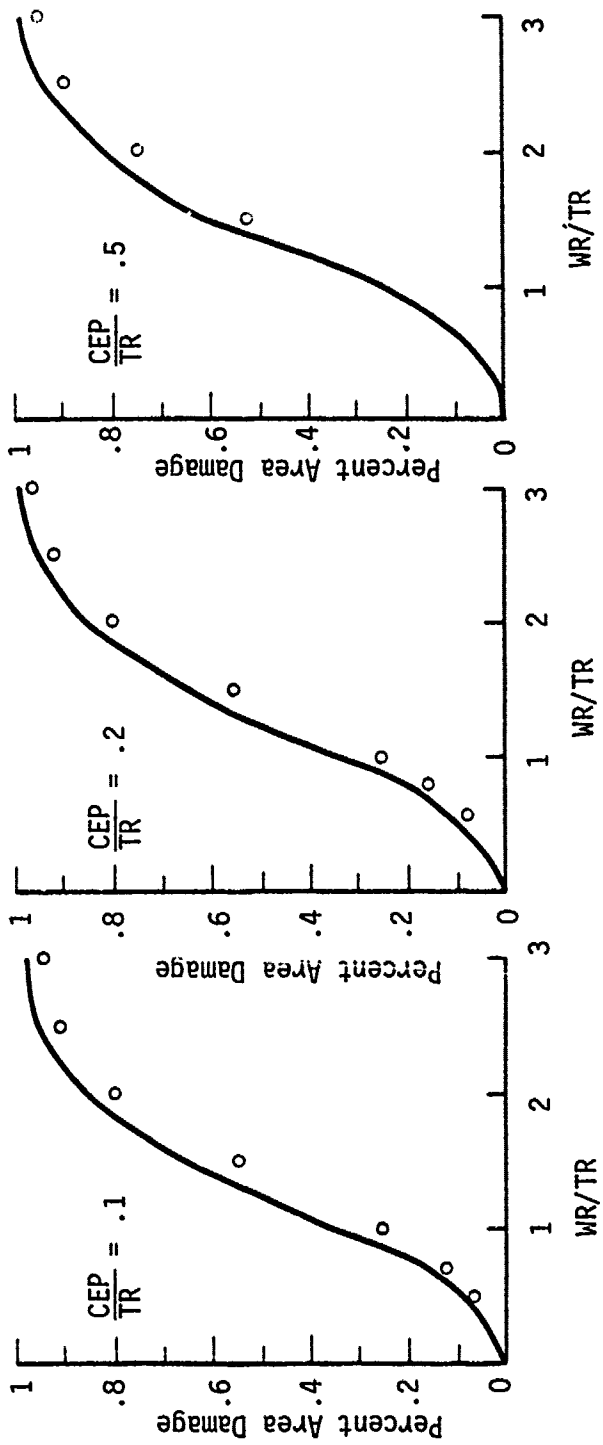


Figure 4.10a Damage Prediction Comparisons Circular Area Target, Offset/TR = 1 (SIGMA-20)

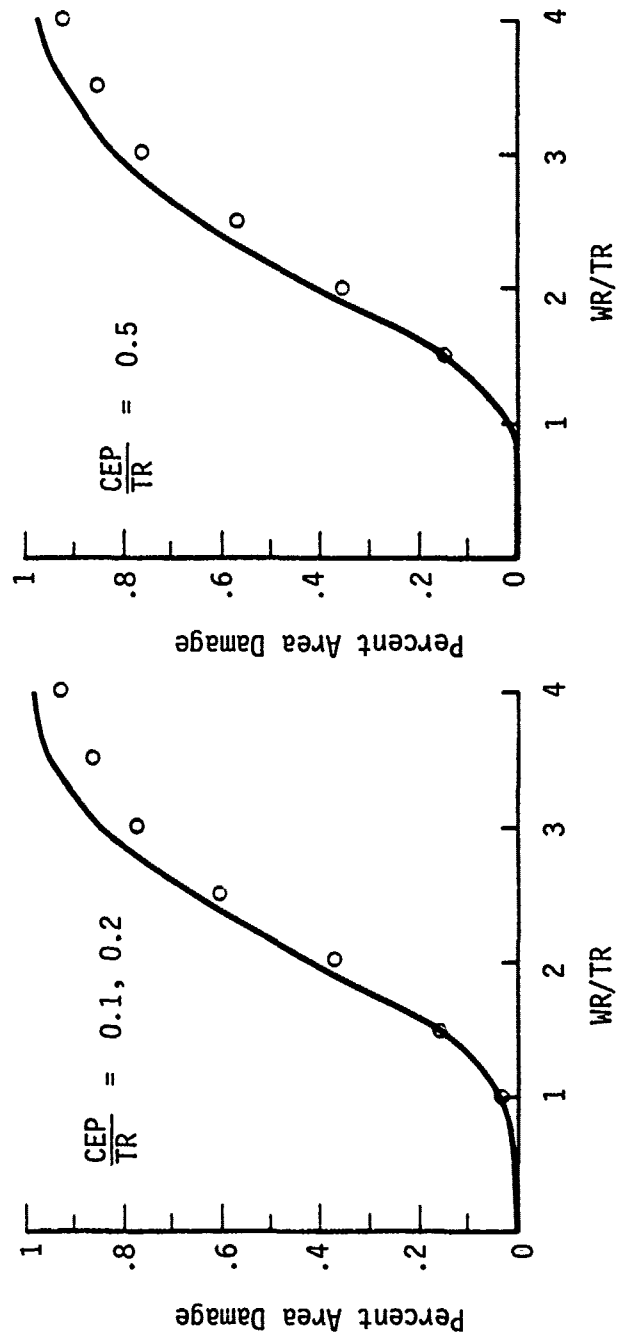


Figure 4.10b Damage Prediction Comparisons Circular Area Target, Offset/TR = 2 (SIGMA-20)

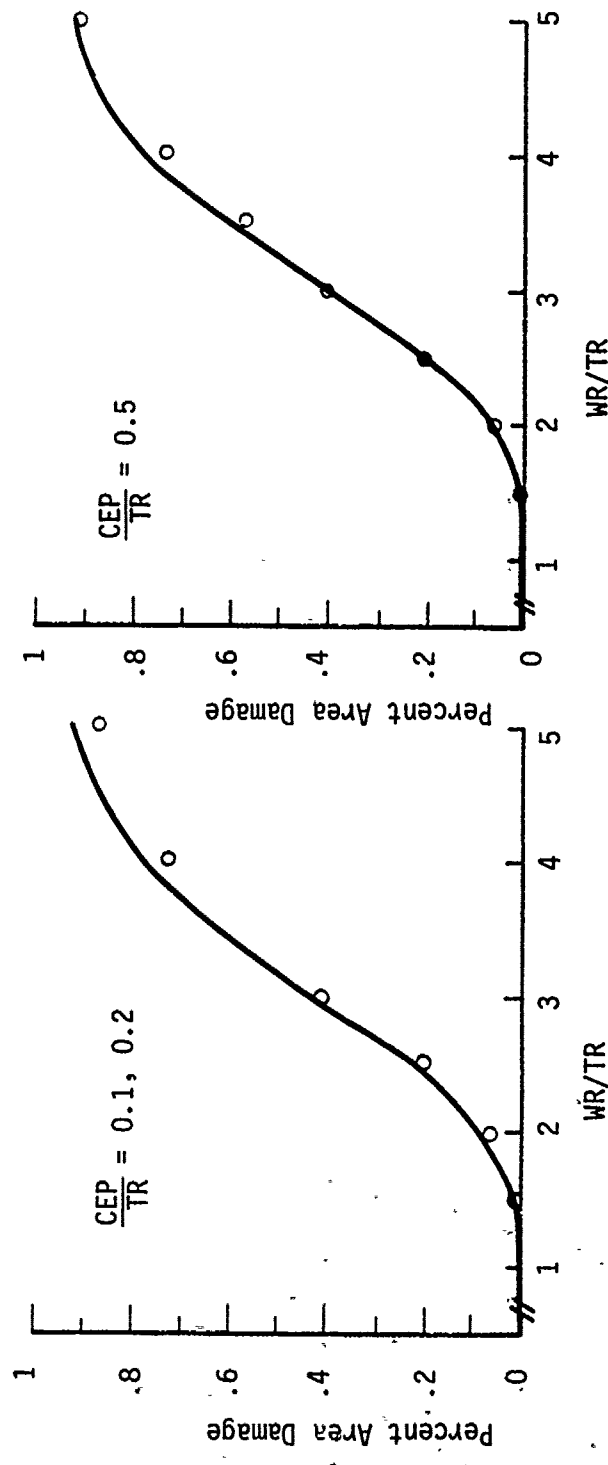


Figure 4.10c Damage Prediction Comparisons Circular Area Target, Offset/TR = 3 (SIGIA-20)

4.5.2 Application of Algorithm to an Actual Town

The city wide damage predictions exhibited in Section 2 of this document were derived by combining a log normal damage prediction model with a circular Gaussian model for weapon impact locations. This combined mathematical targeting model served as the tool for predicting damage to all residential/commercial structures on a building-by-building basis. As such, the city structures were not condensed into area distribution model. Although this total enumeration does provide the most precise means for predicting city wide damage it is probably not a practical, nor feasible, method for field operations. For the targeting analyst, performing calculations for many such towns, the distribution of structures in the town must necessarily be represented by an area description model. The following example demonstrates a comparison of damage prediction results obtained from a discrete building enumeration and the simplified area representation used in the prototype algorithm.

The two damage prediction curves depicted in Figure 4.11 were derived from a total enumeration of all known residential/commercial structures in the example town. The open circles depicted immediately adjacent to these respective curves denote the results obtained from the prototype algorithm. As demonstrated in this figure the predictions obtained from the algorithm agree quite closely with the results obtained from the more precise method. The targeting parameters used to generate these curves are summarized in Table 4.3.

Table 4.3 Targeting Parameters, Damage Prediction Comparisons

WEAPON SYSTEM (KT)	BUILDING VULNERABILITY P_{50} (psi) - ALL STRUCTURES -	DIRECTION FROM CENTER OF TOWN
1	2	East Axis
1	4	East Axis

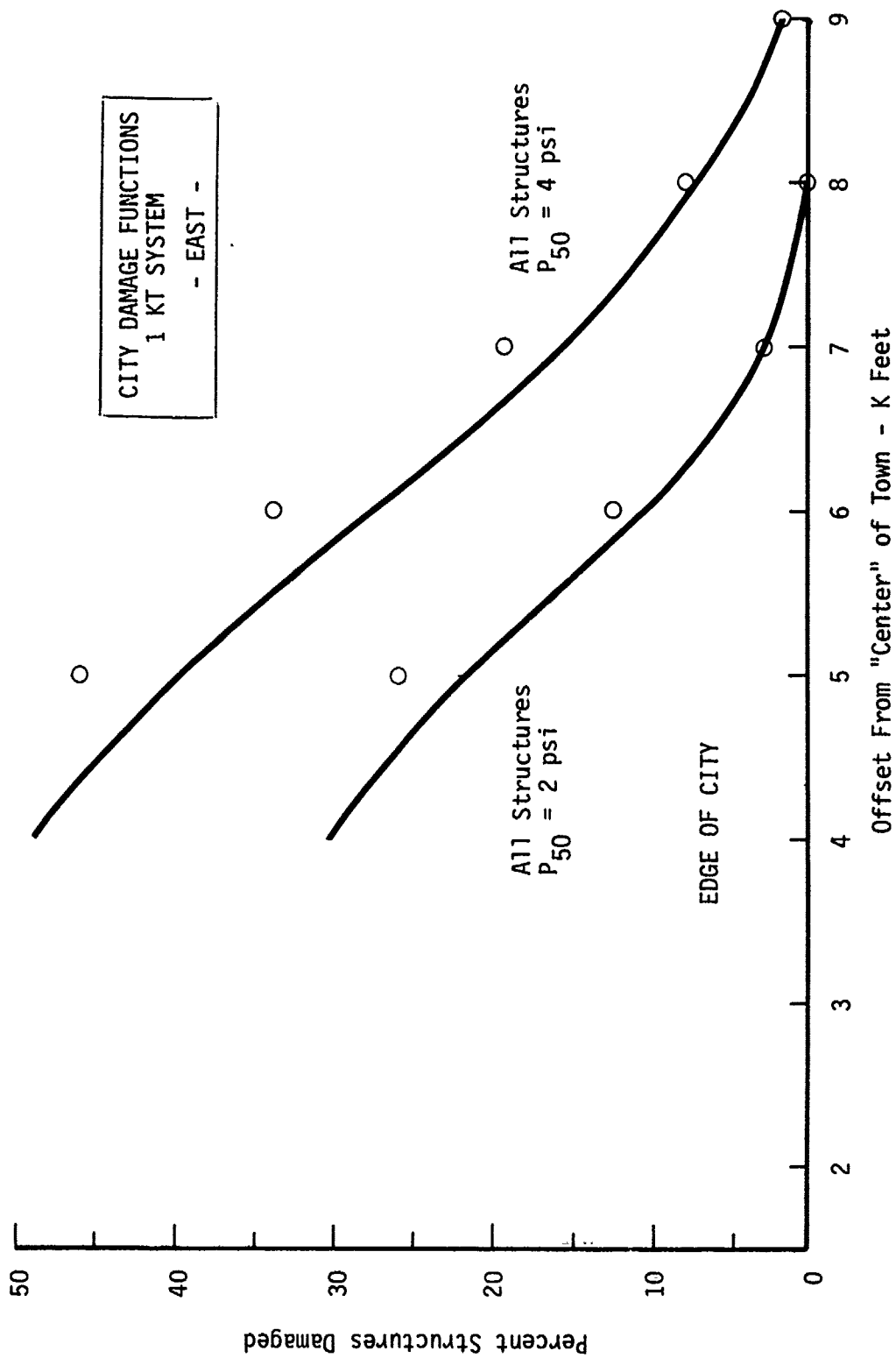


Figure 4.11 Comparison of Damage Predictions, Total Enumeration Vs. Prototype Algorithm

The data input to this algorithm used to generate the results presented in Figure 4.11 were derived in the following manner.

1. The city was divided into 2 sectors as depicted in Figure 4.12. The purpose for outlining these two sectors is to define the general regions where structures are located. Since this algorithm uses an area representation to model the distribution of structures it is important to eliminate the regions where there are no buildings. Failure to do so can generate a biased error in city wide damage predictions since the area representation is including structures which don't exist.

2. The distances between the DGZ location and the edges of the sectors were entered into the damage prediction algorithm along with the WR/CEP, and σ_d information. Each of the city sectors is evaluated separately by the algorithm. The area damage predictions for each sector are added together, external to the algorithm, and divided by 2. The reason for weighting these individual sector damage predictions by a factor of 1/2 is because each sector has about 1/2 of the total number of structures.

The actual data input to the algorithm and the results obtained are presented in Tables 4.4a and 4.4b for the 2 psi and 4 psi examples, respectively. For example, in Table 4.4a the data input and results for the DGZ located 7000 feet from the city center are:

		<u>SECTOR I</u>	
I N P U T	WR	=	3500 Feet
	CEP	=	150 Feet
	d_1	=	2000 Feet distance from DGZ to "front" edge of Sector I
	d_2	=	5000 Feet distance from DGZ to "back" edge of Sector I
	σ_d	=	0.2
O U T P U T	Fraction of Target Area Damaged	=	.39

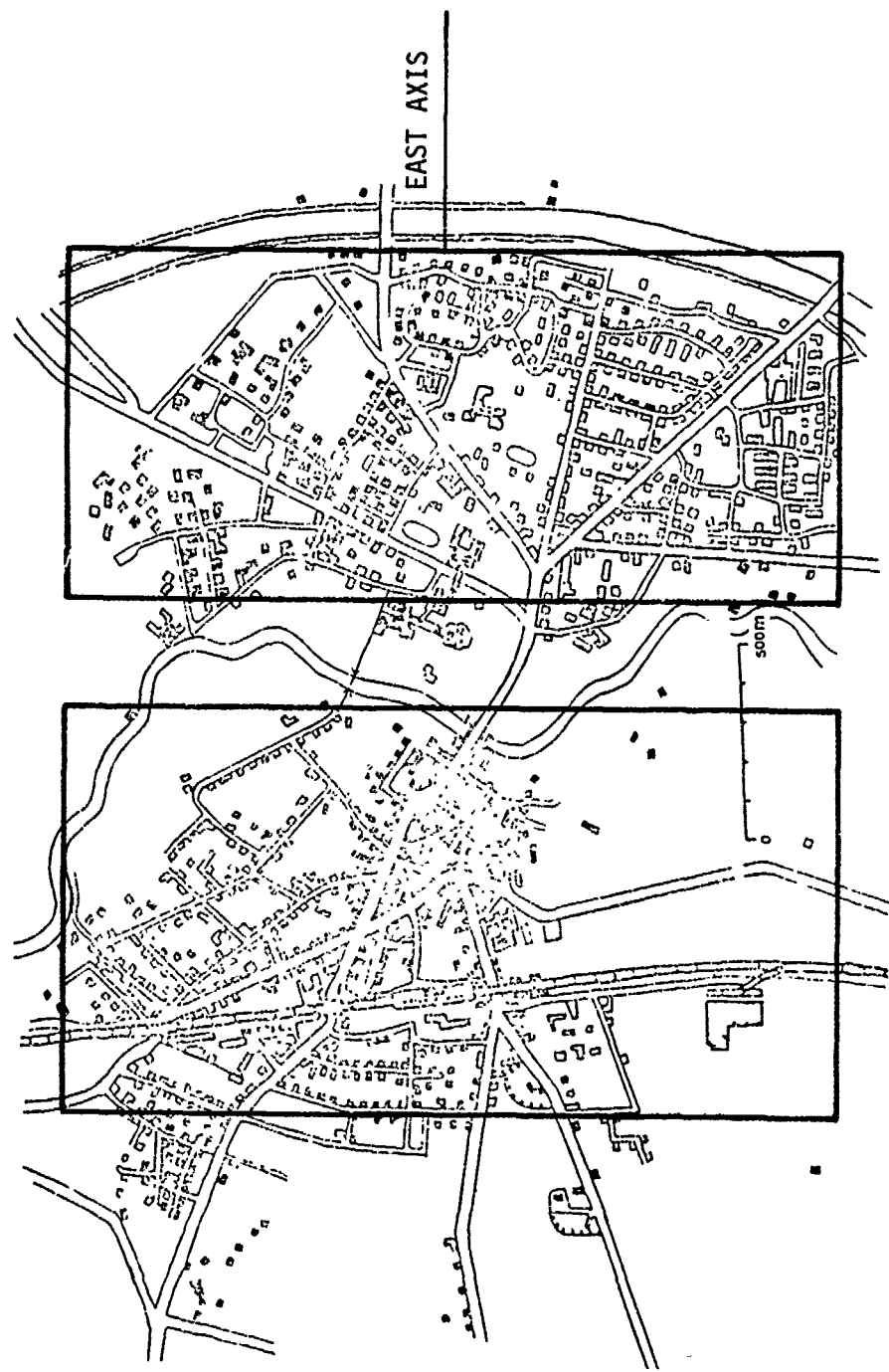


Figure 4.12 Example Town

Table 4.4a Data Input and Damage Prediction Results

DGZ OFFSET FROM CENTER OF CITY (FT)	WEAPON RADIUS (FT) - WR -	CEP (FT)	SECTOR I		SECTOR II		AVERAGE OF SECTOR RESULTS
			d_1 (FT)	d_2 (FT)	d_1 (FT)	d_2 (FT)	
5000	3500	150	0	3000	3900	7400	.46
6000	3500	150	1000	4000	4900	8400	.34
7000	3500	150	2000	5000	5900	9400	.2
8000	3500	150	3000	6000	6900	10400	.08
9000	3500	150	4000	7000	7900	11400	.01

* 1 KT Weapon Ssystem --- All Structures, $P_{50} = 2$ psi --- DGZ on East Axis
 $\sigma_d = 0.2$

Table 4.4b Data Input and Damage Prediction Results*

DGZ OFFSET FROM CENTER OF CITY (FT)	WEAPON RADIUS (FT) - WR -	CEP (FT)	SECTOR I		SECTOR II		AVERAGE OF SECTOR RESULTS		
			d ₁ (FT)	d ₂ (FT)	RESULTS	d ₁ (FT)		d ₂ (FT)	RESULTS
5000	2200	150	0	3000	.52	3900	7400	0	.26
6000	2200	150	1000	4000	.25	4900	8400	0	.12
7000	2200	150	2000	5000	.06	5900	9400	0	.03
8000	2200	150	3000	6000	0	6900	10400	0	0
9000	2200	150	4000	7000	0	7900	11400	0	0

* I KT Weapon System ---- All Structures, P₅₀ = 4 psi ---- DGZ on East Axis

- σ_d = 0.2 -

SECTOR II

I
N
P
U
T

O
U
T
P
U
T

WR	=	3500 Feet	
CEP	=	150 Feet	
d_1	=	5900 Feet	distance from DGZ to "front" edge of Sector II
d_2	=	9400 Feet	distance from DGZ to "back" edge of Sector II
σ_d	=	0.2	

Fraction of Target Area Damaged	=	0
---------------------------------	---	---

$$\text{Average of Sector Results} = \frac{0.39+0}{2} = 0.2$$

4.6 SUMMARY OBSERVATIONS

In the example demonstrations presented in the previous paragraphs the results of this targeting algorithm have compared favorably with results obtained from very precise and complex analytic methods. As detailed in Appendix B of this report the algorithm can easily be adapted to a programmable calculator such as the TI (Texas Instruments) 58/59 models.

The existing mathematical logic of this targeting algorithm does limit its application on the requirement that $WR/CEP \geq 3$. This bounding constraint, however, is not considered to be a problem for collateral damage applications since tactical weapons tend to have small CEP values relative to the building vulnerability values. Also, the inherent mathematics are tailored specifically for targeting situations when the DGZ is located at or beyond the boundaries of the urban area. Considering that this algorithm was developed for predicting collateral damage, however, this applications requirement should not be a significant handicap.

The discussion accompanying the application to the example city noted that a biased error could be introduced if the entire city area was treated as a single and uniform distribution of structures. For this reason the city was divided into two sectors so as to eliminate the large area void of structures. This concern and reference to the potential biased error is not unique to the logic of this particular algorithm. Any targeting methodology using some type of continuous area representation to describe the building distribution would be susceptible to a biased error in the damage prediction.

Section 5

SUMMARY REMARKS

The following paragraphs summarize the topics and concluding observations reported in this document. With regard to the Japanese structures data analysis the objective was to identify trends in the damage data relevant to current research efforts being sponsored by the Defense Nuclear Agency. This data analysis focused exclusively on load-bearing-wall structures. It is suspected that the damage data for this particular structure category may be the most relevant to the buildings of interest. Specifically, the data analysis was oriented toward the consequence of shielding on building damage, the impact of building orientation on the resultant damage, and vulnerability ranges for various damage criteria.

With regard to the questions of shielding and building orientation statistical trends could not be identified in the damage data to suggest that these factors significantly influenced the resultant damage. This is not to say, however, that these factors did not have some role toward influencing the eventual outcome of reported damage. As stated in the text of this document, there could be many factors which would tend to camouflage these damage data signatures. This is especially true for the question of shielding given the small sample size and limited information available in the damage survey. As such, the Japanese data base may not be an especially useful source of information for evaluating the impact of shielding to building damage.

Toward the question of building orientation, however, the absence of any data trend strongly suggests that the vulnerability of load-bearing-wall structures may not be very sensitive to building orientation relative to the approaching blast wave. The data set suitable for this analysis should be sufficiently large and evenly distributed over the area of risk to allow for the development of a

definite trend in the data. The absence of any data signature from this sample is probably a very good indicator that the resultant damage was not significantly influenced by building orientation.

The vulnerability ranges developed in this analysis are intended to represent and include the diversity of building characteristics that were reported in the damage survey information. It was not the intent of this analysis to identify any one single value as being the most appropriate vulnerability estimate for the structures of interest. Extrapolation of a best estimate from the Japanese data to European residential structures has yet to be validated. Arguing from a heuristic viewpoint, however, it may be appropriate to assume that the desired vulnerability estimates may be contained within the range of information extracted from the Japanese data.

The targeting analyses contained in this report demonstrate that vulnerability uncertainty within each of three range of values may not be especially critical to collateral damage concerns. The upper range of 5-10 psi contains the current preliminary vulnerability estimate for the structures of interest. Based upon the targeting analysis performed within this hardness interval the utility of refining this vulnerability estimate may be negligible in terms of goals oriented toward minimizing collateral damage.

An interesting and informative observation in the targeting analysis pertains to the significance of the distance damage function tail toward collateral damage. Example calculations demonstrate that this targeting parameter may not be as important to collateral damage concerns as currently suspected. The principal factor which tends to degrade the importance of this targeting parameter is the distribution of structures within a town. The structures tend to be contained in clusters distributed about the town. The separation between clusters is sufficiently great, relative to the weapon radius from tactical-type weapons, so as to suppress the importance of the damage function tail.

Also demonstrated in this targeting analysis is the significance of random error toward collateral damage predictions. Historically, this component of the targeting mathematics has been ignored or assumed unimportant. As demonstrated in this document, however, random error may be a very important factor in attempting to control and minimize collateral damage.

Included in this report is a prototype targeting algorithm developed for performing collateral damage predictions in the field. This algorithm easily fits on programmable hand-held calculators. The results obtained with this algorithm agree very favorably with the damage predictions obtained from more lengthy and complex mathematical targeting models. It is anticipated that this algorithm will greatly reduce the burden on targeting analysts when generating collateral damage predictions for large and complex targeting scenarios.

Section 6

REFERENCES

1. "The Effects of the Atomic Bomb on Hiroshima, Japan," Physical Damage Division, United States Strategic Bombing Survey, Volumes I, II, and III, May 1947.
2. "The Effects of the Atomic Bomb on Nagasaki, Japan," Physical Damage Division, United States Strategic Bombing Survey, Volumes I, II, and III, May 1947.
3. Daniels, R., and Johnson, G., "Statistical Analysis of Japanese Structural Damage Data," Final Report, DNA4213F on contract DNA001-76-C-0245, Lulejian and Associates, Inc., January 1977.
4. Binninger, G., Castleberry, P., and McGrady, P., "Mathematical Background and Programming Aids for the Physical Vulnerability System for Nuclear Weapons," Defense Intelligence Agency, November 1974.
5. Brode, H., "Height of Burst Effects at High Overpressures," DASA 2506, RM-6301, DASA, July 1970.
6. "Nuclear Weapons Employment Doctrine and Procedures," Department of the Army Field Manual, FM101-31-1, March 1977.

APPENDIX A

CITY DAMAGE FUNCTIONS ALONG NORTH AXIS

This appendix contains city wide and core damage functions. These damage functions were developed from DGZ locations along the north axis originating at the center of the example city. Figure A.1 depicts the example city and highlights the core region and north axis. These damage functions are presented for two weapons as defined in Section 2 of this document.

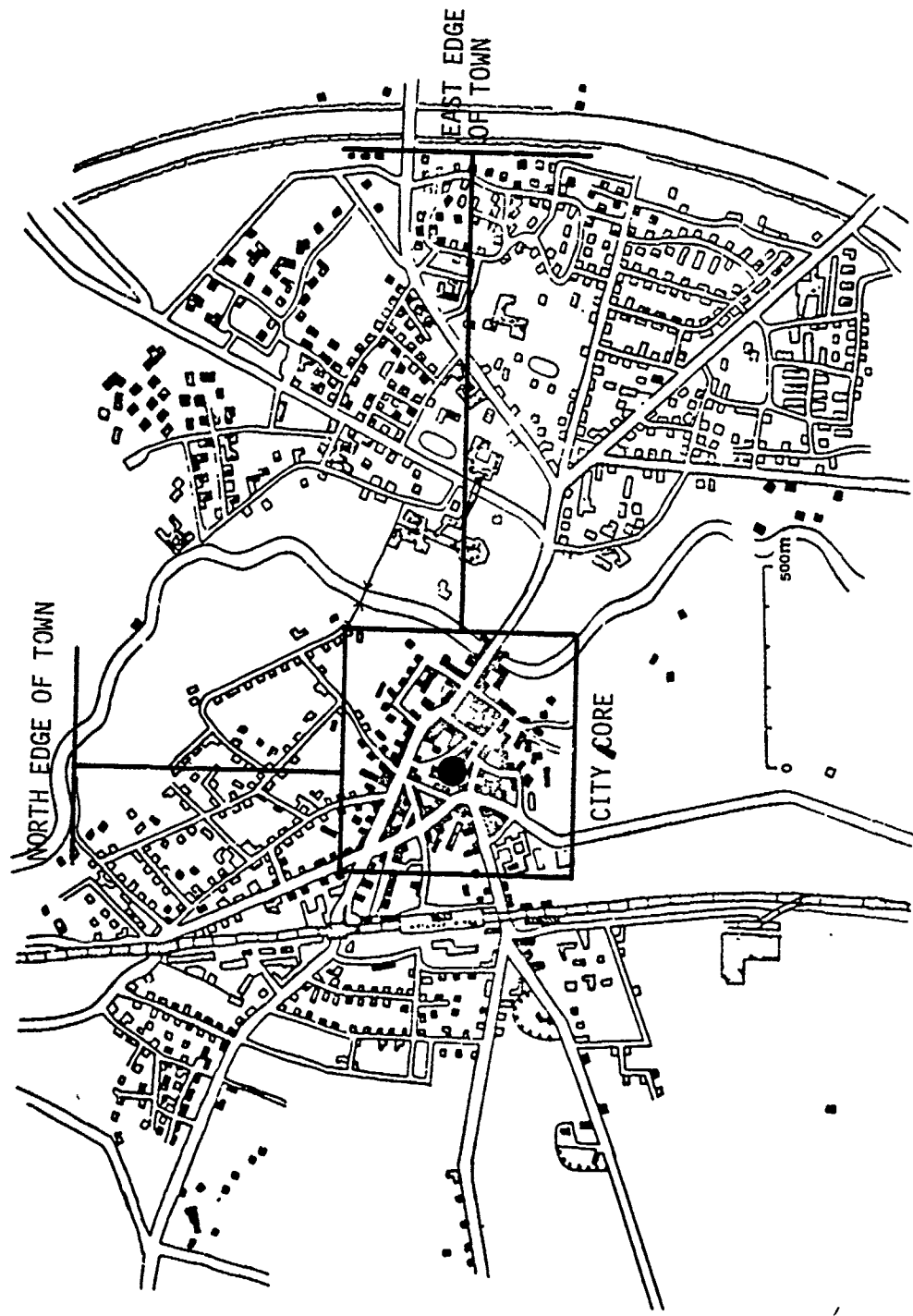


Figure A.1 Example Town

CITY DAMAGE FUNCTIONS
 1 KT SYSTEM
 - NORTH -

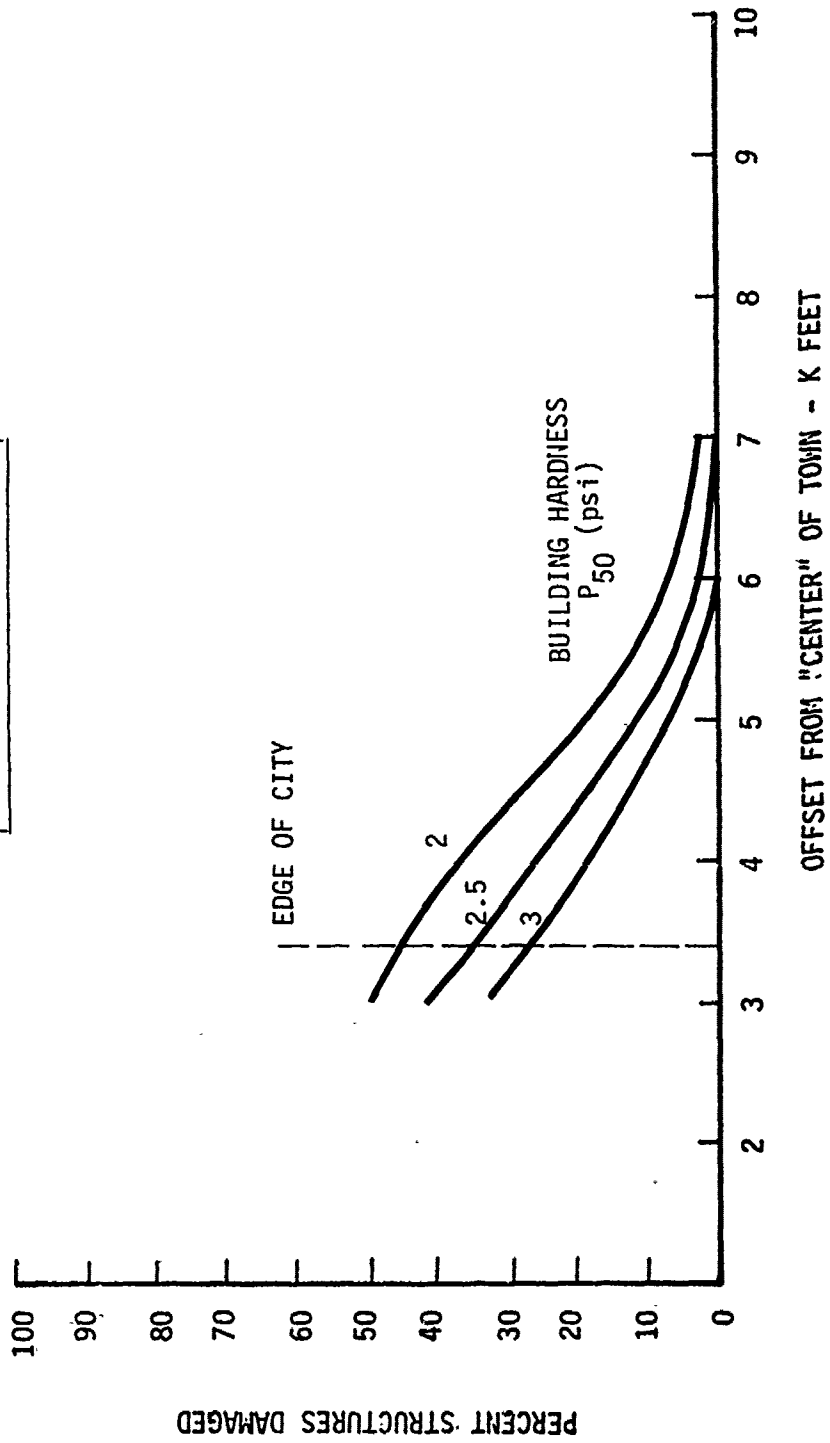


Figure A. 2 Significance of Vulnerability Uncertainty

CITY DAMAGE FUNCTIONS
 1 KT SYSTEM
 - NORTH -

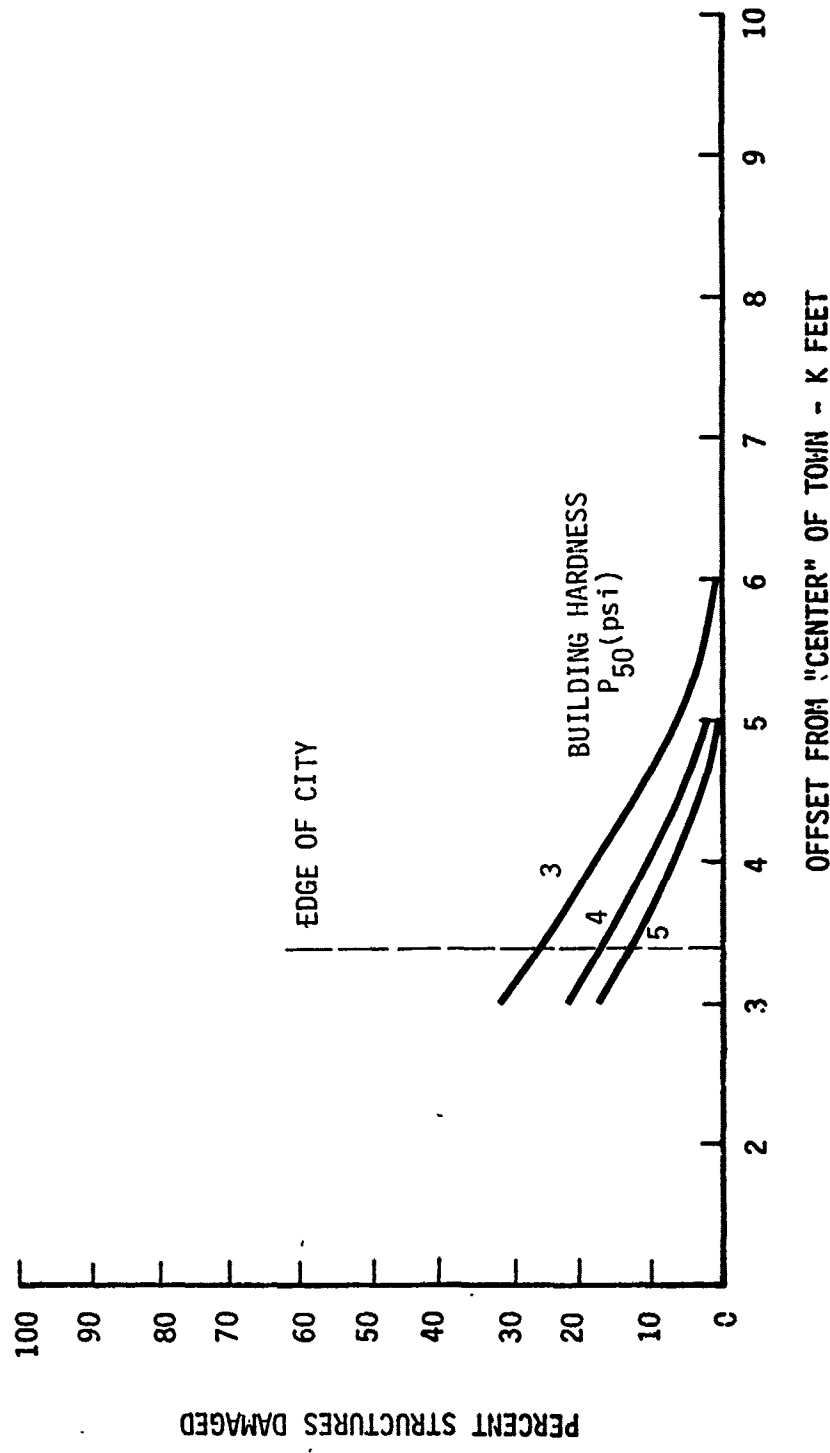


Figure A.3 Significance of Vulnerability Uncertainty

CITY DAMAGE FUNCTIONS
 1 KT SYSTEM
 - NORTH -

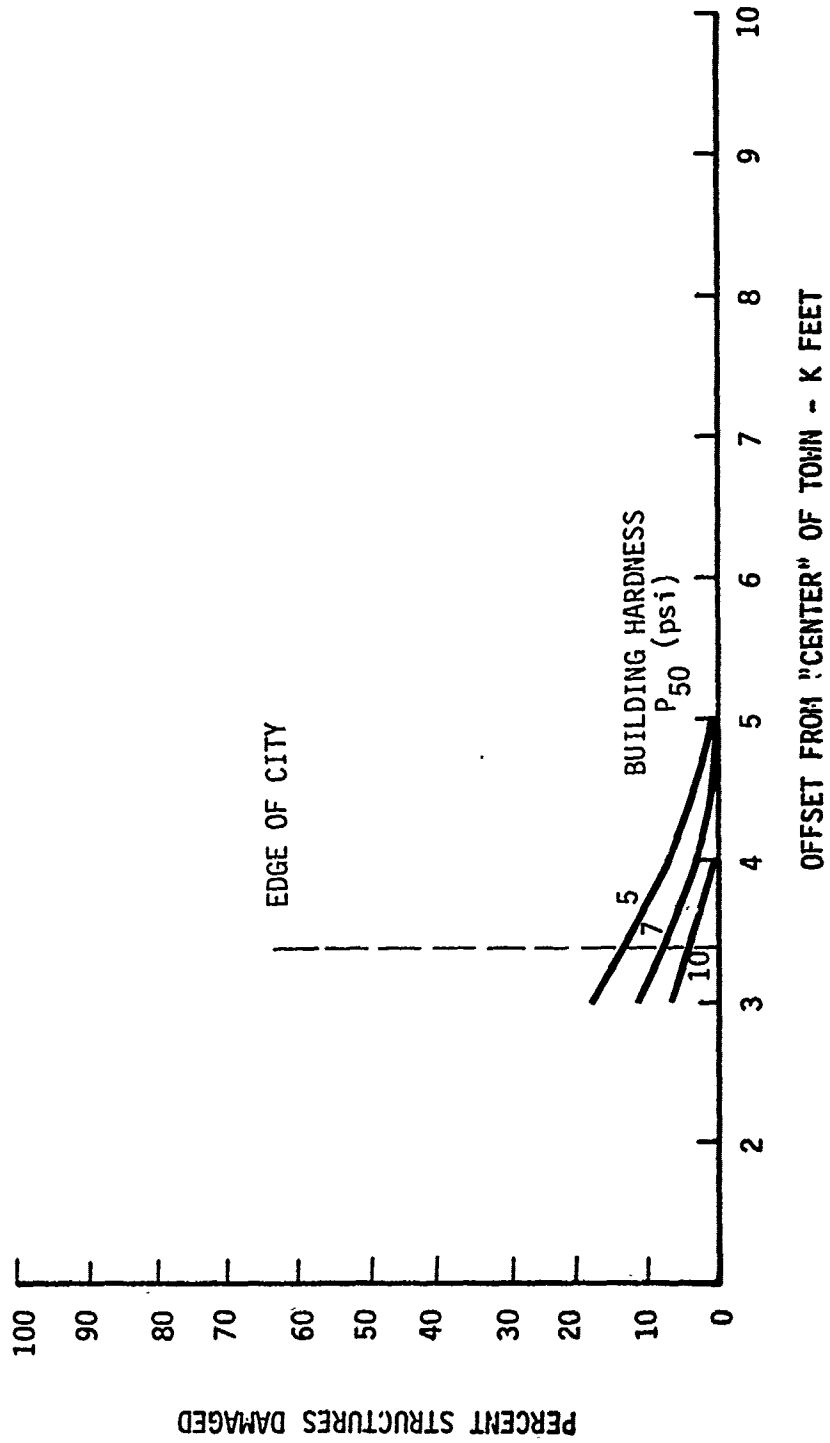


Figure A.4 Significance of Vulnerability Uncertainty

CITY DAMAGE FUNCTIONS
 10 KT SYSTEM
 - NORTH -

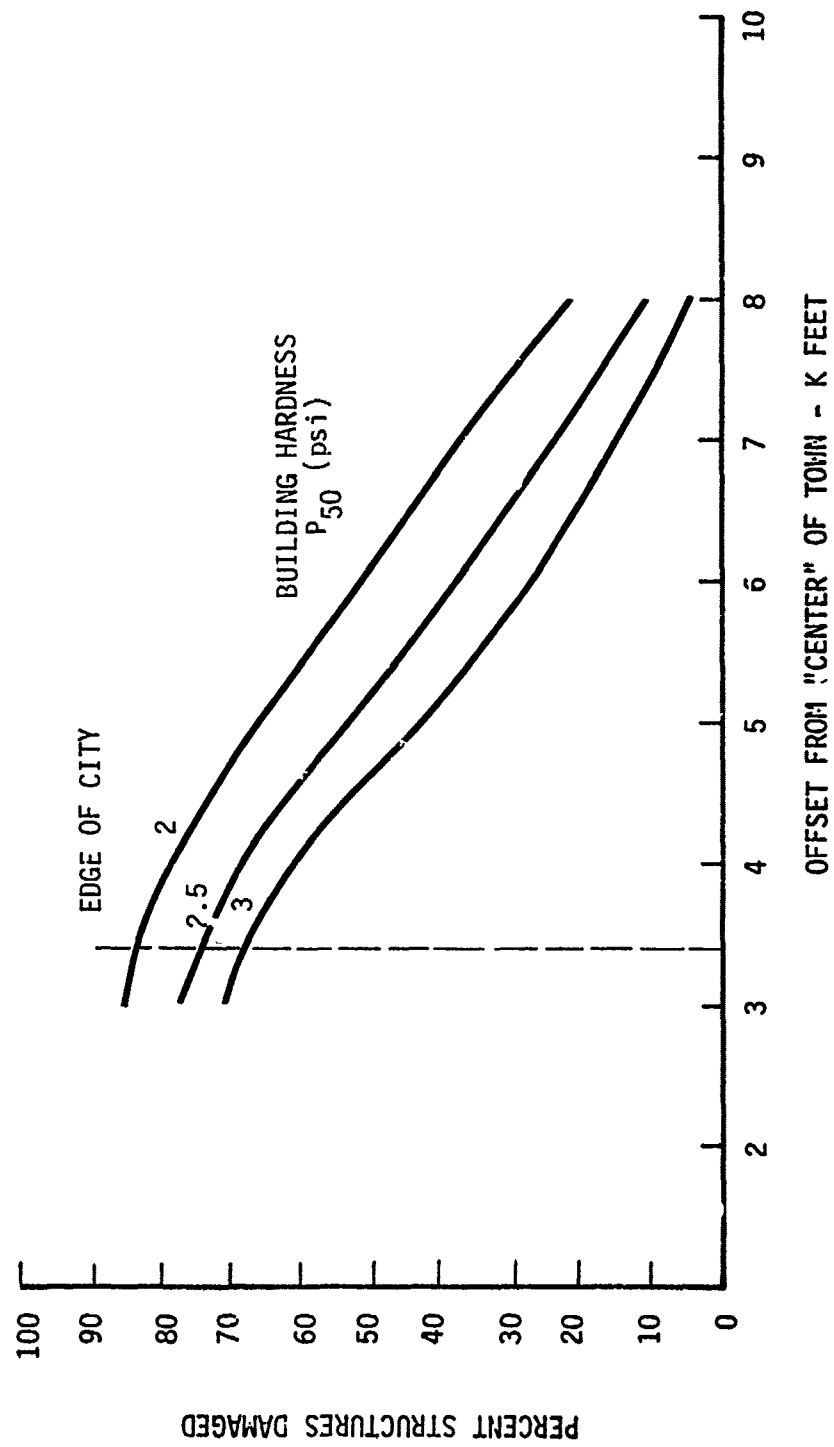


Figure A.5 Significance of Vulnerability Uncertainty

CITY DAMAGE FUNCTIONS
 10 KT SYSTEM
 - NORTH -

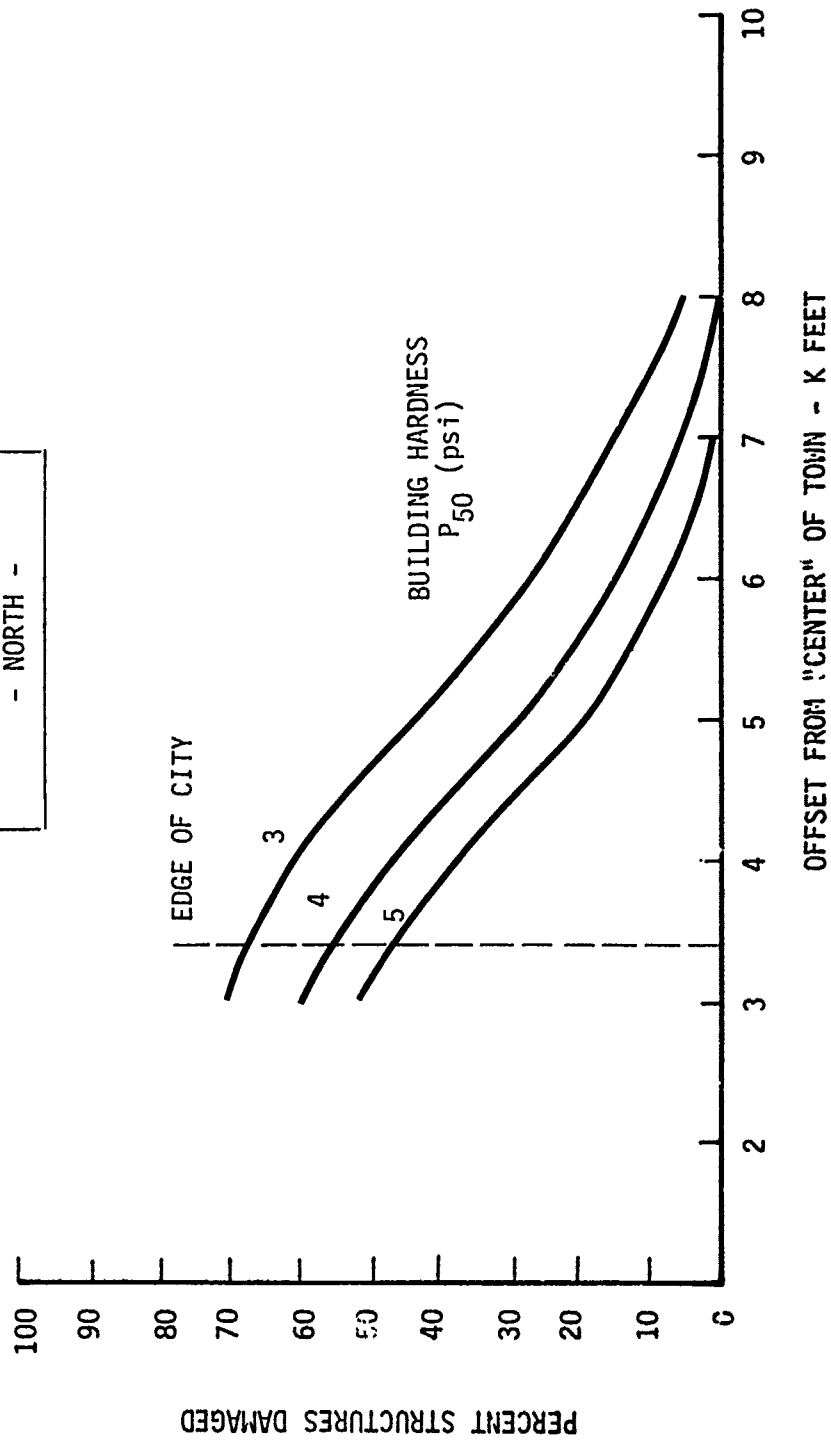


Figure A.6 Significance of Vulnerability Uncertainty

CITY DAMAGE FUNCTIONS
10 KT SYSTEMS
- NORTH -

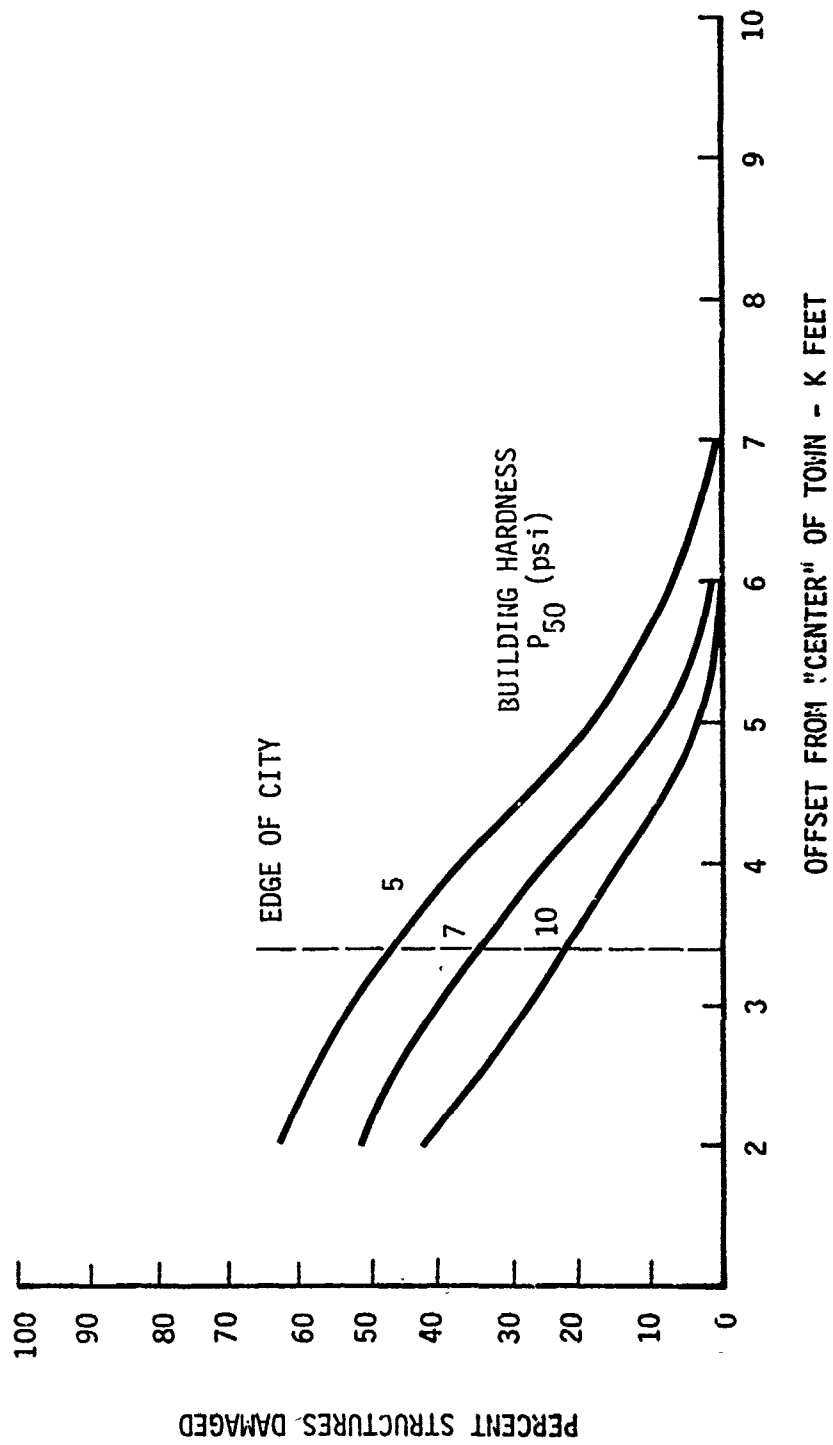


Figure A.7 Significance of Vulnerability Uncertainty

CITY CORE
 DAMAGE FUNCTIONS
 1 KT SYSTEM
 - NORTH -

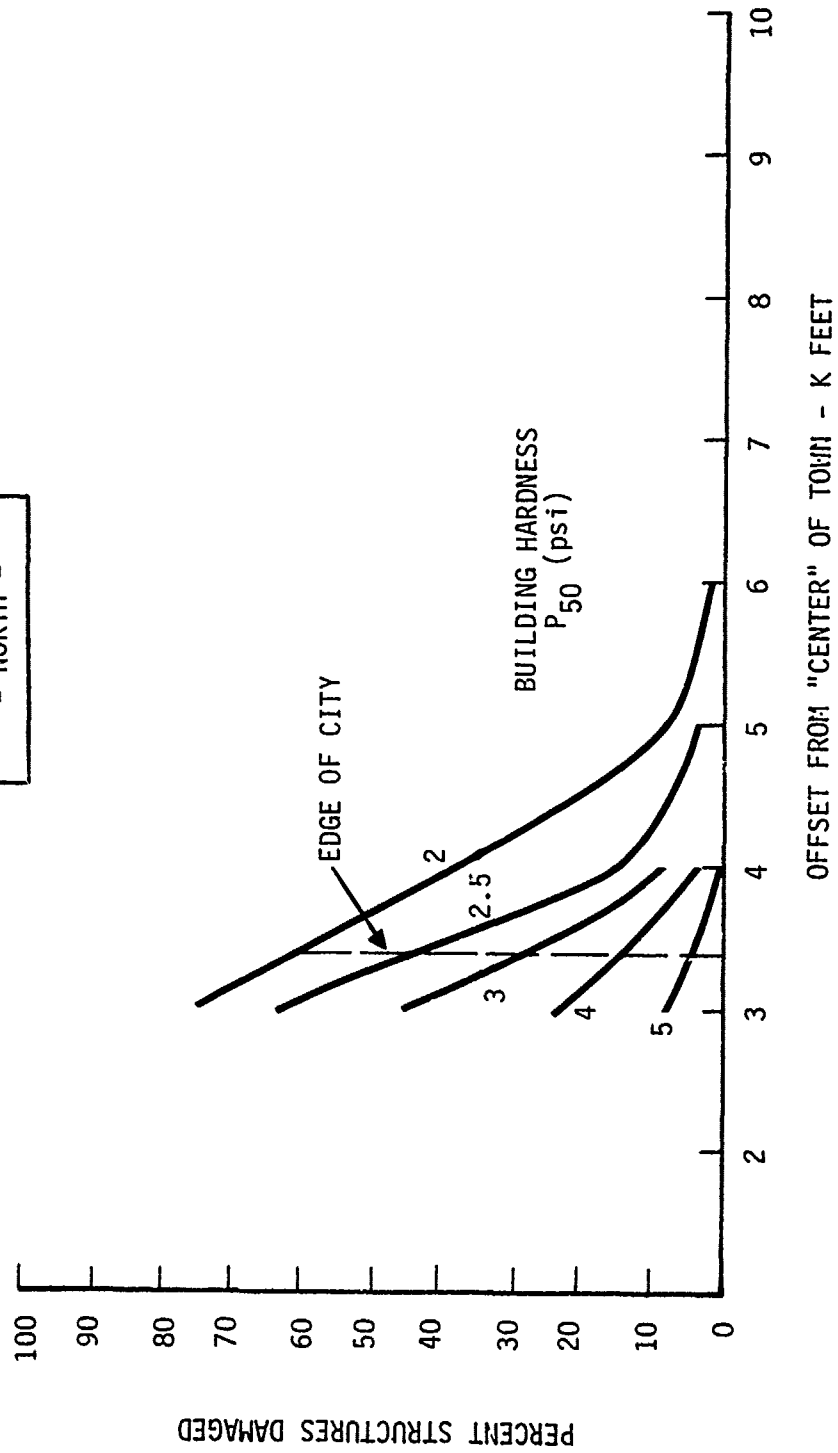


Figure A.8 Significance of Vulnerability Variation to Structures in Core of City

CITY CORE
DAMAGE FUNCTIONS
10 KT SYSTEM
- NORTH -

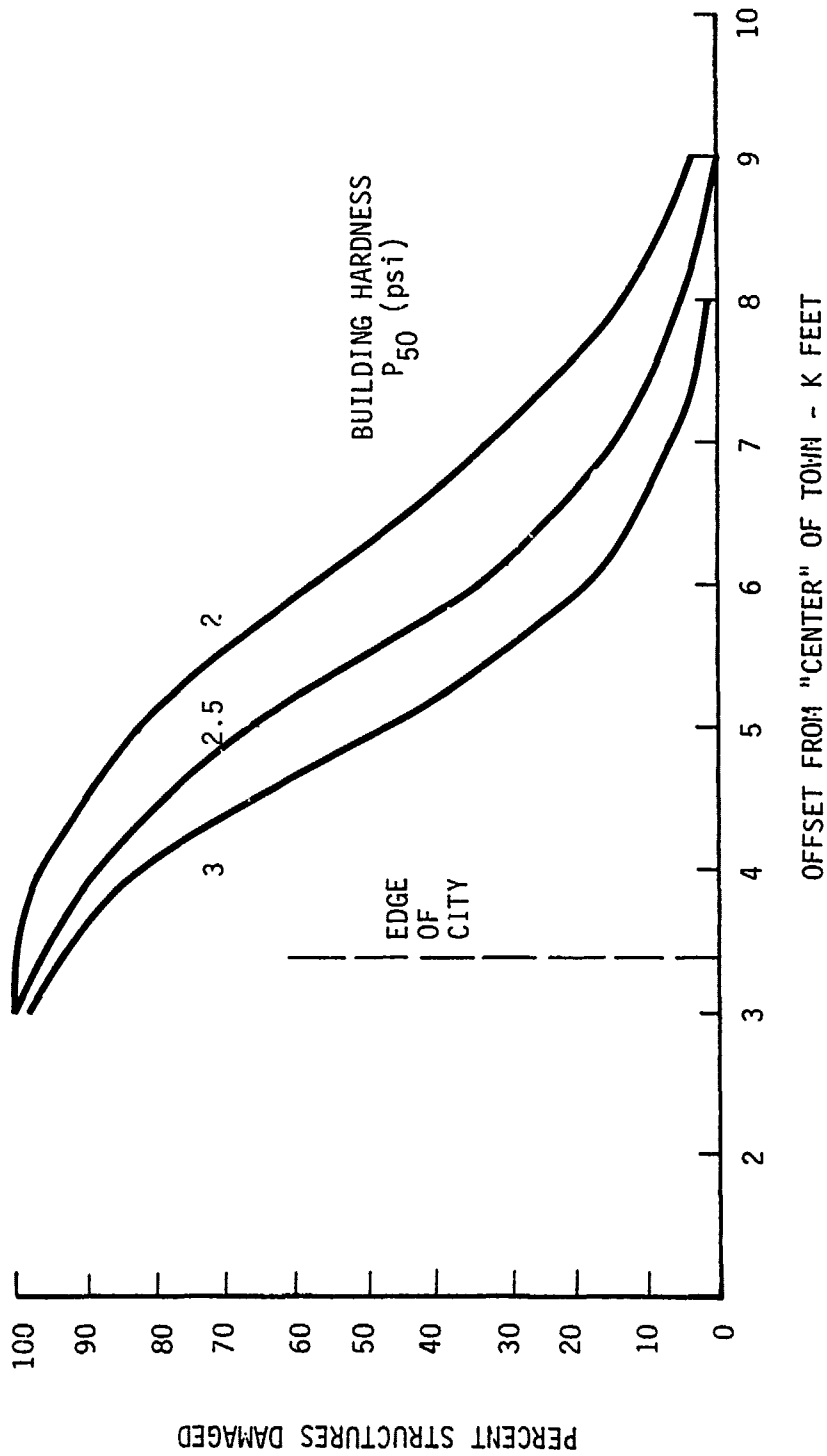


Figure A.9 Significance of Vulnerability Variation to Structures in Core of City

CITY CORE
DAMAGE FUNCTIONS
10 KT SYSTEM
- NORTH -

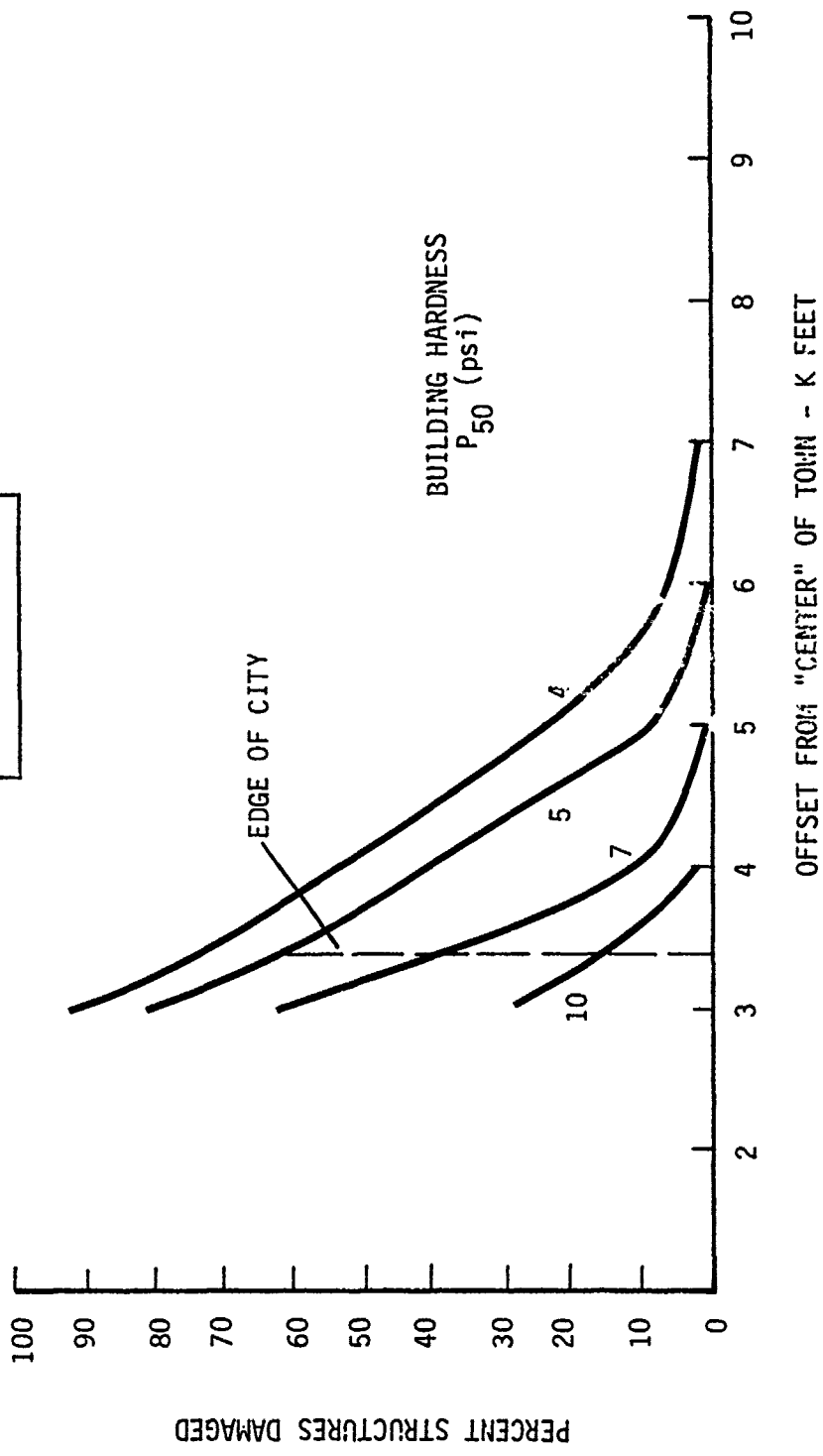


Figure A.10 Significance of Vulnerability Variation to Structures in Core of City

CITY DAMAGE FUNCTIONS
 1 KT SYSTEM
 - NORTH -

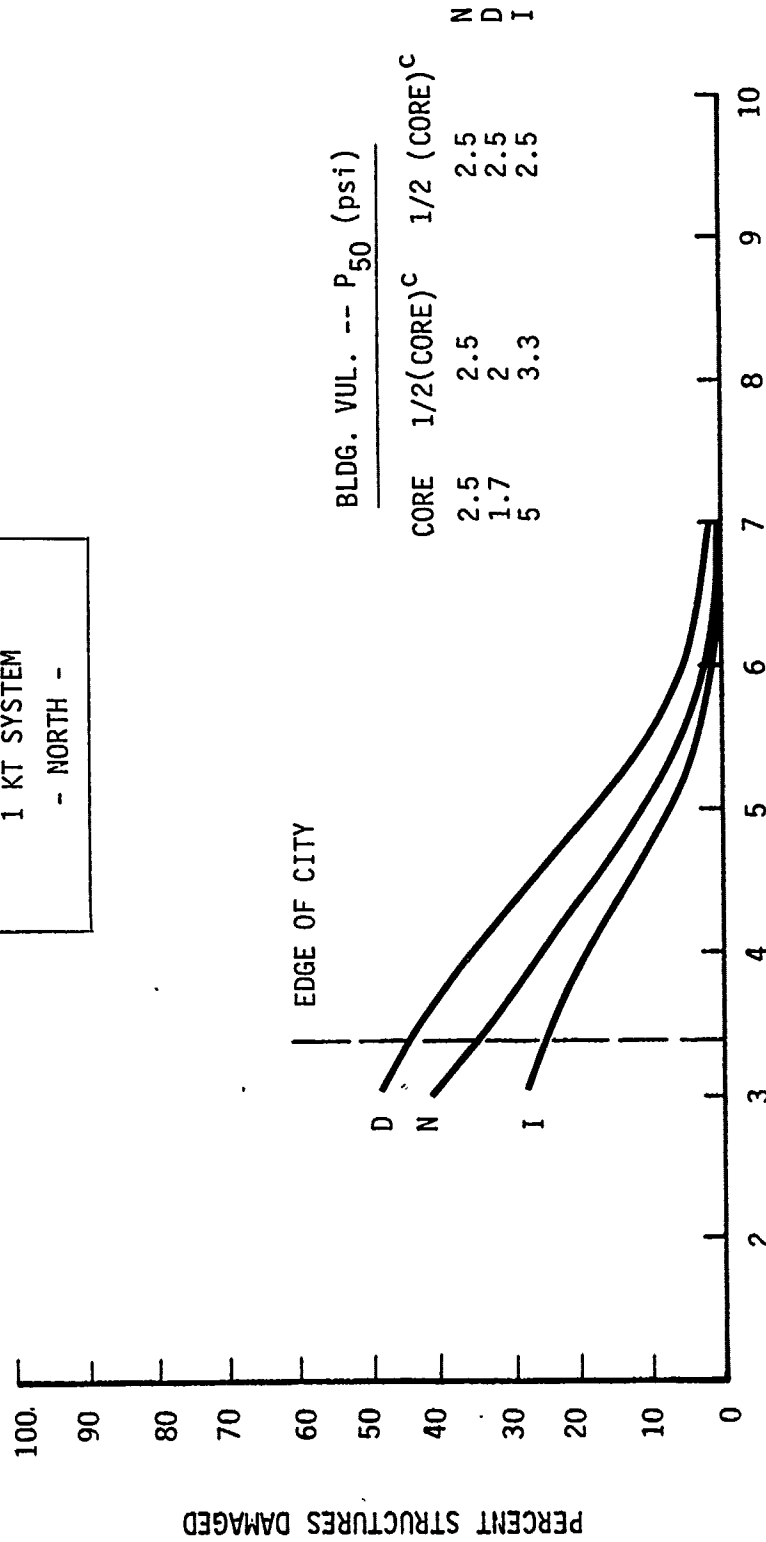


Figure A.11 Impact of Shielding on City Damage Predictions

CITY DAMAGE FUNCTIONS
 1 KT SYSTEM
 - NORTH -

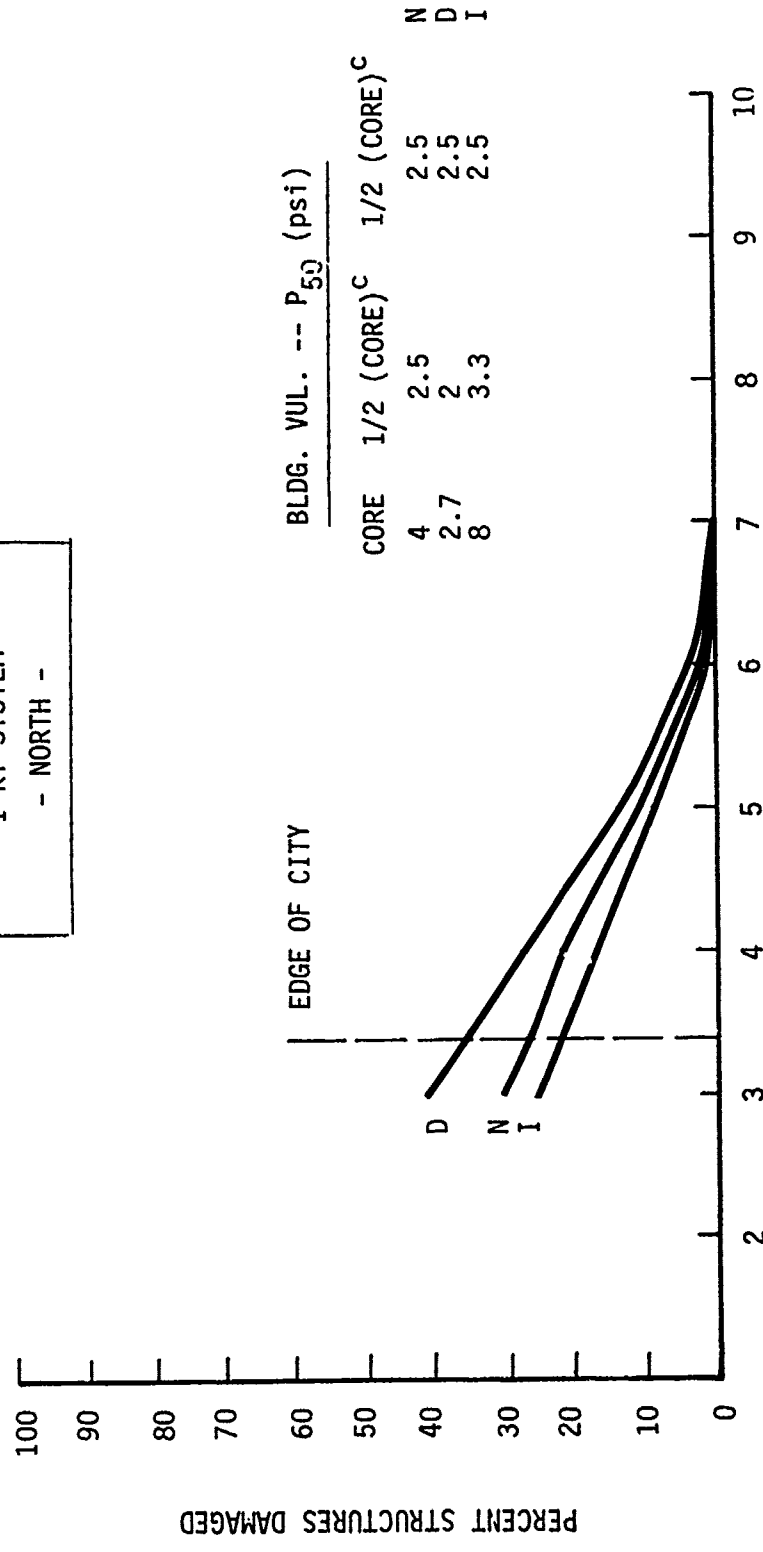


Figure A.12 Impact of Shielding on City Damage Predictions

CITY DAMAGE FUNCTIONS
 1 KT SYSTEM
 - NORTH -

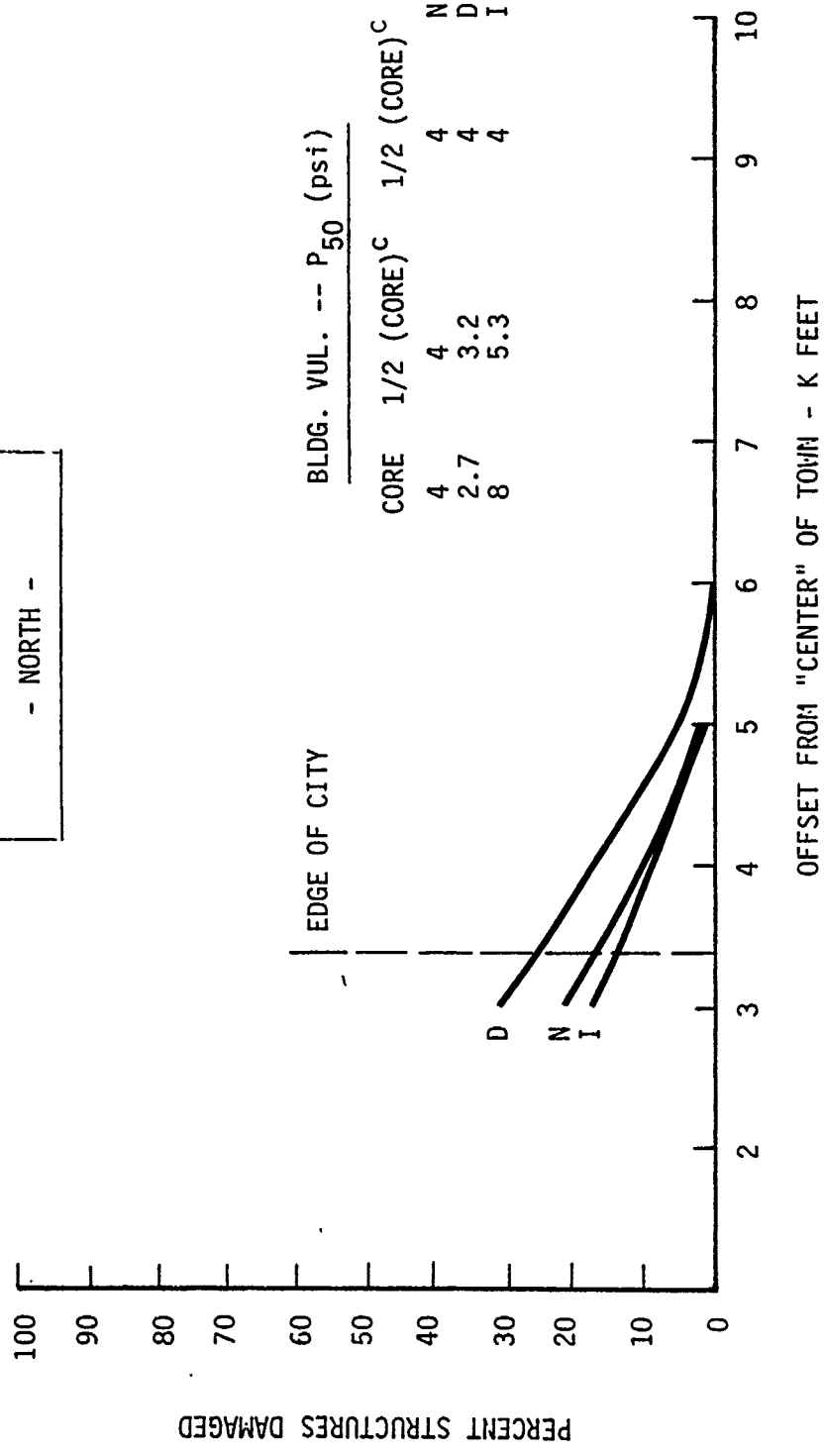


Figure A.13 Impact of Shielding on City Damage Predictions

CITY DAMAGE FUNCTIONS
 10 KT SYSTEM
 -- NORTH --

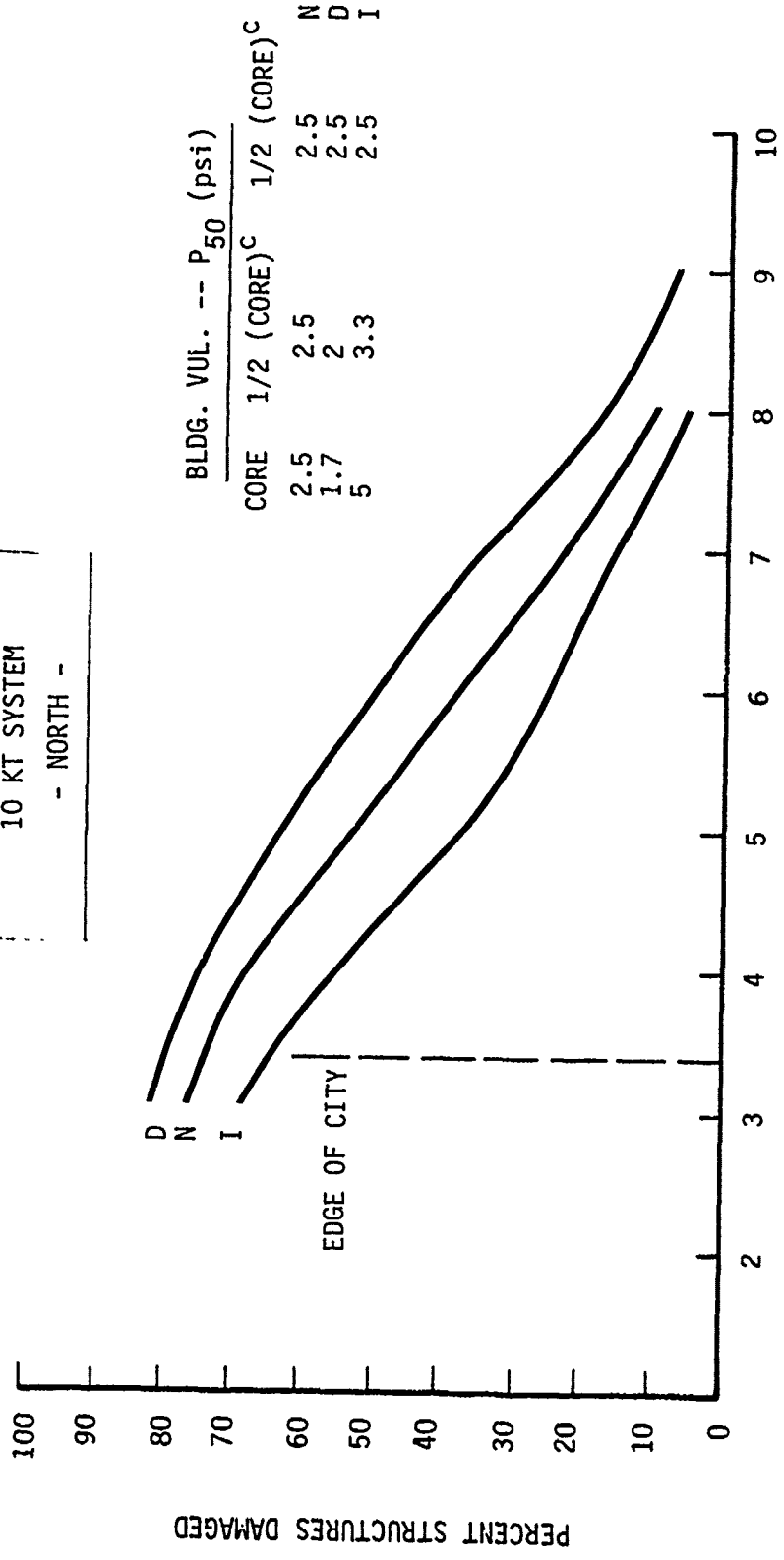


Figure A.14 Impact of Shielding on City Damage Predictions

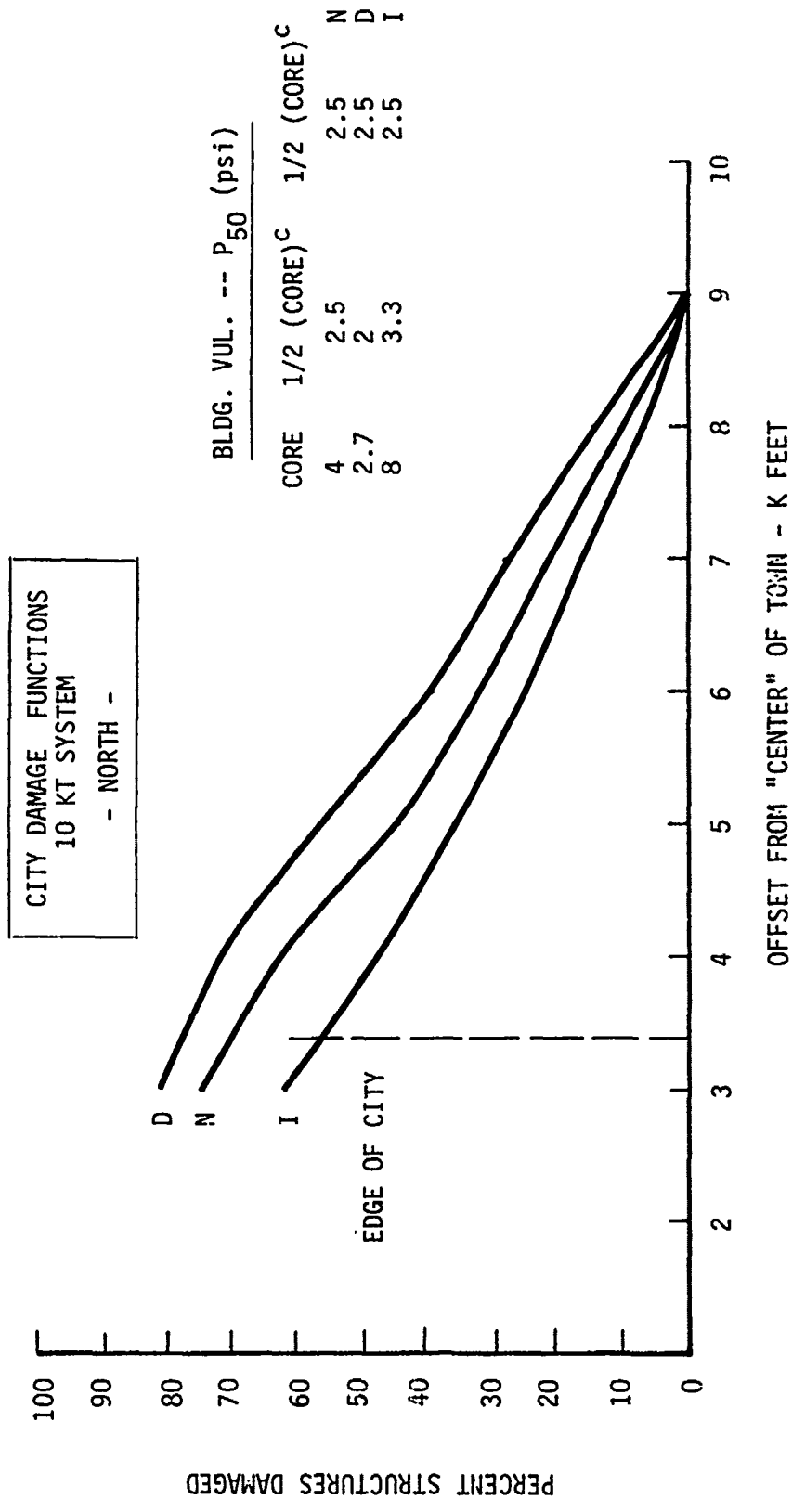


Figure A. 15 Impact of Shielding on City Damage Predictions

CITY DAMAGE FUNCTIONS
 10 KT SYSTEM
 - NORTH -

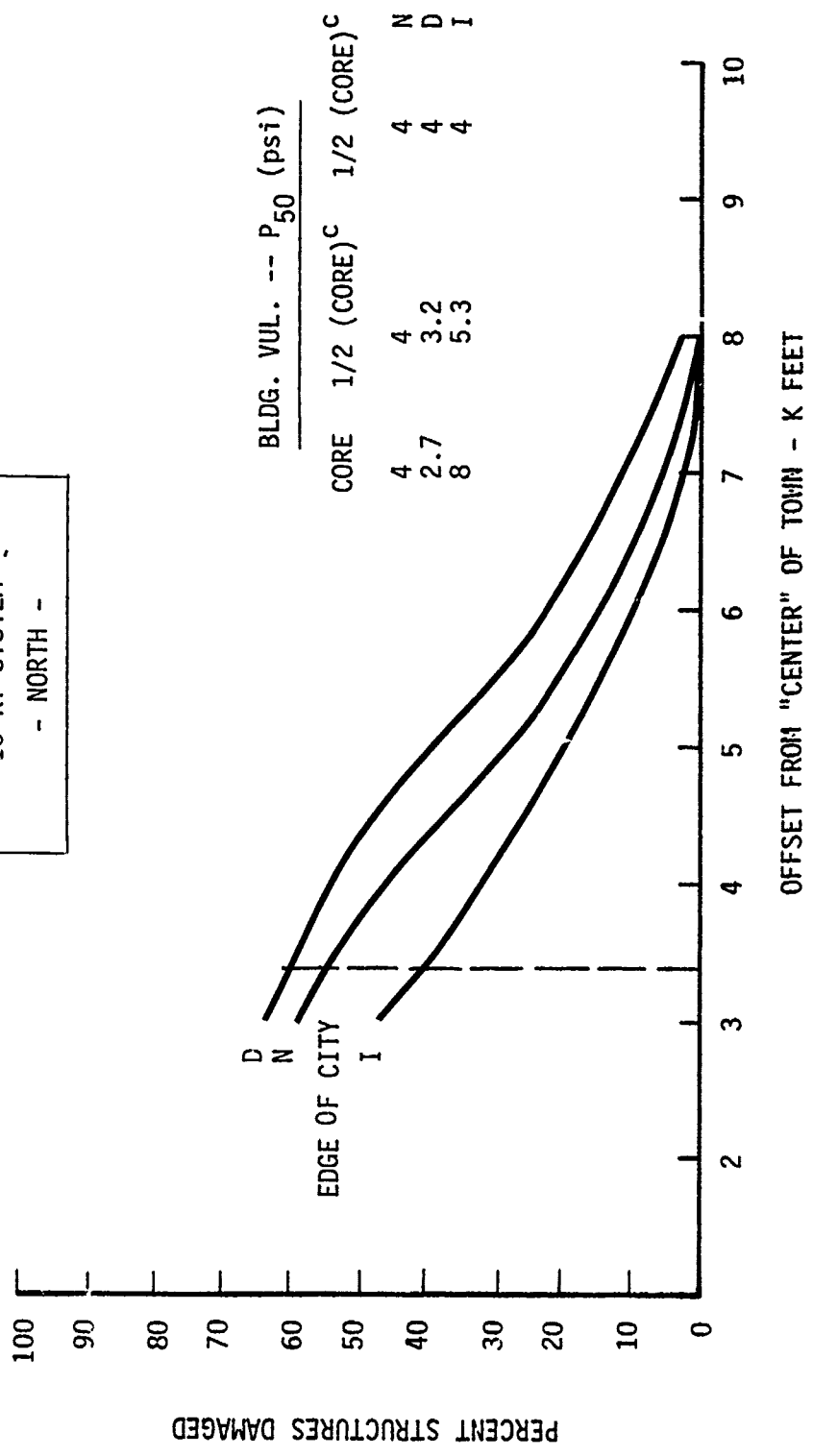


Figure A.16 Impact of Shielding on City Damage Predictions

APPENDIX B

B.1 INTRODUCTION

The methodology presented in Section 4 which permits a potential user of tactical nuclear weapons to estimate or minimize the collateral damage to a target area, easily lends itself to being programmed on a hand-held, programmable calculator. The purpose of this appendix is to describe such a program that has been written for use on a TI programmable 58/59 calculator.

B.2 EQUATIONS AND FLOW CHART

The mathematical expression that yields the expected fractional area of damage, given the weapon radius and CEP, the two radial distances from DGZ bounding the target area of interest, and the assumed damage sigma for targets within this area, is given by:

$$A_D = 1 - \left(\frac{2I}{d_2^2 - d_1^2} \right) \quad (B.1)$$

where $I = I(R, r) \Big|_{X, d_1}^{Y, d_2} = (F(R) \Big|_X^Y \left(\frac{r^2 - \mu^2 - \sigma^2}{2} \Big|_{d_1}^{d_2} \right)$

$$+ \left[f(R) \left(\sigma\mu + \frac{\sigma^2 R}{2} \right) \Big|_X^Y \right] \quad (B.2)$$

In this expression, $Y = \frac{d_2 - \mu}{\sigma}$ and $X = \frac{d_1 - \mu}{\sigma}$. Further,

$$\begin{cases} F(R) = 1 - f(R)P(R), & \text{for } X \text{ or } Y \geq 0 \\ F(R) = f(R)P(R), & \text{for } X \text{ or } Y < 0 \end{cases}$$

As in Section 4,

$$f(R) = \exp(-R^2/2) / \sqrt{2\pi}$$

$$P(R) = b_1 t(R) + b_2 t(R)^2 + b_3 t(R)^3 + b_4 t(R)^4 + b_5 t(R)^5,$$

where $t(R) = 1/(1+b_0|R|)$.

The quantities $b_0, b_1, b_2, b_3, b_4,$ and b_5 are all constants.*

Figure B.1 is the flow chart for the algorithm used in solving Equation B.1.

B.3 PROGRAM USER INSTRUCTIONS

B.3.1 Program Input and Output

The program is written on two TI magnetic cards. Card 1 (Bank 1 and Bank 2) contains the program memory locations (000-434) while Card 2 (Bank 3) supplies the data memory registers (40-56) with constants used in computing values of $\sigma, \mu, f(R)$ and $P(R)$. All three Banks must be read by the calculator prior to actual problem data input.

Problem data input consists of entering five problem variables; weapon radius (WR) and CEP, ground distances from DGZ bounding the target area of interest (d_1 and d_2), and the assumed target damage sigma for representative targets within this area. Table B.1 shows the steps required for problem solution.

*Abramowitz and Stegun, Handbook of Mathematical Functions, National Bureau of Standards, 1970.

Table B.1 Problem Input Procedures

STEP	PROCEDURE	ENTER	PRESS
1	Read program	TI Magnetic Cards Banks 1, 2, and 3	
2	Enter data	WR	<input type="checkbox"/> A
3		CEP	<input type="checkbox"/> B
4		d_1	<input type="checkbox"/> C
5		d_2	<input type="checkbox"/> D
6		Target Damage Sigma	<input type="checkbox"/> E

Upon pressing E, the program will commence running and will stop only when all calculations are completed (~25 seconds). The value displayed will be the fraction of the targets within the target area that would be expected to be damaged (assuming a uniform distribution of targets within the target area). Because of the order in which calculations are performed, values of d_2 and damage sigma must be input when running a subsequent problem - even if they do not change in the problem. If the weapon radius (WR), CEP, and nearest ground distance to target (d_1) do not change, they do not have to be reentered when running a subsequent problem.

If a PC-100A Print/Security Cradle is being used, the fractional expected damage will automatically be printed out. Intermediate steps in the calculations are stored in data memory registers (04-20) and can be obtained by pressing INV 2nd Fix, 04 INV 2nd List, and pressing R/S when all locations are listed. If a printer is not available, simply recalling the appropriate storage location, i.e., RCL XX, will display the value stored in that data memory register.

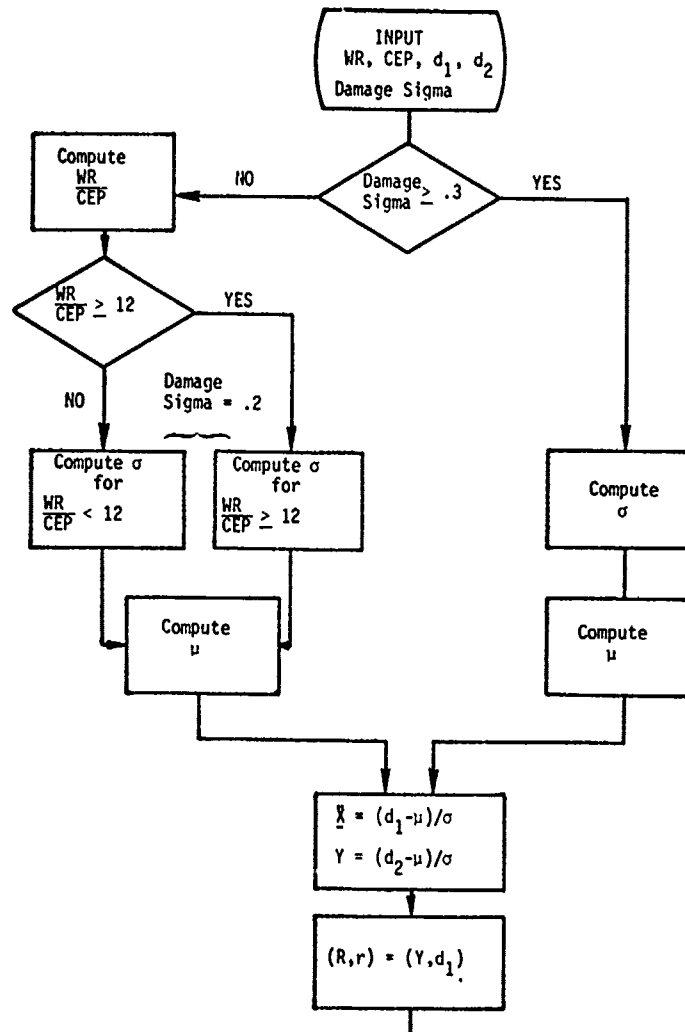


Figure B.1 Flow Chart for Targeting Algorithm
(CONTINUED ON FOLLOWING PAGE)

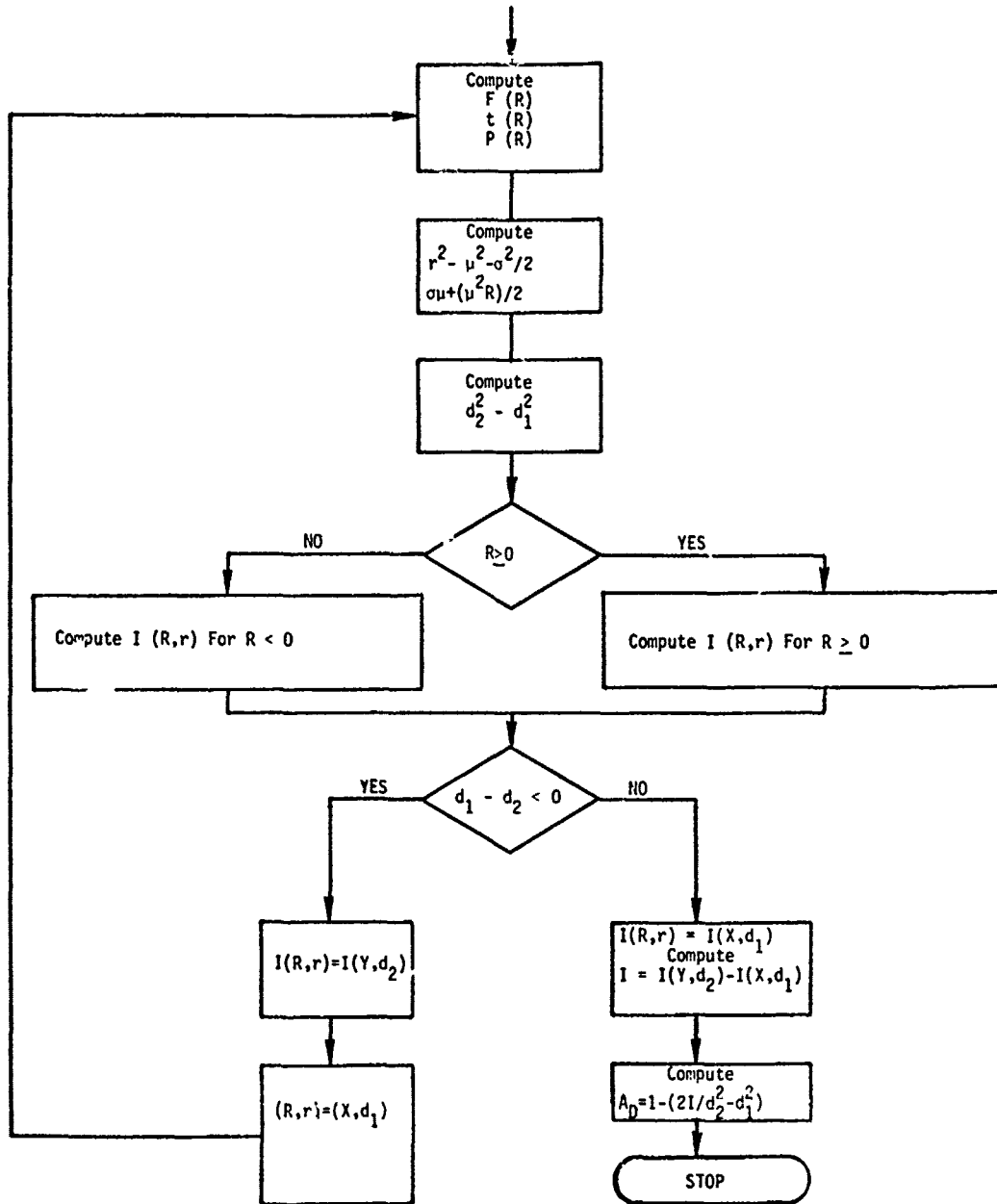


Figure B.1 Flow Chart for Targeting Algorithm
(Continued)

Table B.2 contains a listing of the TI program memory locations (000-434) and data memory registers (40-56) that must be read into the calculator prior to running any problems. Also in Table B.2, is the output of data memory registers 00-20 and a description of their contents for a sample problem where: $WR = 4000$, $CEP = 1000$, $d_1 = 2000$, $d_2 = 4000$, and damage sigma = 0.2.

B.3.2 Restrictions on Data Input

Because of several approximations made in the derivation of Equation B.1, the program is only valid for $\frac{WR}{CEP} \geq 3$. For values of $\frac{WR}{CEP} < 3$, significant errors will be incurred. The only other restriction on data input is that $d_2 \neq d_1$. If $d_1 = d_2$, the denominator in Equation B.1 will equal zero and $A_D = -\infty$; the calculator will display -9.999 99? meaning that division by zero has occurred in the calculations. It is suggested that the user select values of d_1 and d_2 such that $d_2 - d_1 \geq 10^{-3}$ which should not be over restrictive. If values of d_1 and d_2 are input such that $A_D \approx$ zero, the calculator will display 0.000?.

Table B.2 Program Listing

000	76	LBL	046	95	=	092	43	RCL
001	11	A	047	85	+	093	03	03
002	42	STO	048	43	RCL	094	75	-
003	00	00	049	48	48	095	43	RCL
004	91	R/S	050	95	=	096	06	06
005	76	LBL	051	65	X	097	95	=
006	12	B	052	43	RCL	098	55	÷
007	42	STO	053	01	01	099	43	RCL
008	01	01	054	95	=	100	05	05
009	91	R/S	055	42	STO	101	95	=
010	76	LBL	056	05	05	102	42	STO
011	13	C	057	61	GTO	103	07	07
012	42	STO	058	00	00	104	43	RCL
013	02	02	059	76	76	105	02	02
014	91	R/S	060	43	RCL	106	75	-
015	76	LBL	061	04	04	107	43	RCL
016	14	D	062	65	X	108	06	06
017	42	STO	063	43	RCL	109	95	=
018	03	03	064	49	49	110	55	÷
019	91	R/S	065	95	=	111	43	RCL
020	76	LBL	066	75	-	112	05	05
021	15	E	067	43	RCL	113	95	=
022	42	STO	068	50	50	114	42	STO
023	04	04	069	95	=	115	08	08
024	71	SBR	070	65	X	116	53	(
025	03	03	071	43	RCL	117	53	(
026	84	84	072	01	01	118	43	RCL
027	01	1	073	95	=	119	03	03
028	02	2	074	42	STO	120	33	X ²
029	32	XIT	075	05	05	121	54)
030	43	RCL	076	43	RCL	122	75	-
031	00	00	077	04	04	123	53	(
032	55	÷	078	65	X	124	43	RCL
033	43	RCL	079	43	RCL	125	02	02
034	01	01	080	51	51	126	33	X ²
035	95	=	081	95	=	127	54)
036	42	STO	082	75	-	128	54)
037	04	04	083	43	RCL	129	95	=
038	77	GE	084	52	52	130	42	STO
039	00	00	085	95	=	131	17	17
040	60	60	086	65	X	132	43	RCL
041	43	RCL	087	43	RCL	133	03	03
042	04	04	088	01	01	134	33	X ²
043	65	X	089	95	=	135	42	STO
044	43	RCL	090	42	STO	136	09	09
045	47	47	091	06	06	137	43	RCL

Table B.2 Program Listing (Continued)

138	07	07	186	11	11	234	54)
139	33	X ²	187	45	Y ^X	235	54)
140	55	÷	188	03	3	236	54)
141	02	2	189	65	X	237	55	÷
142	95	=	190	43	RCL	238	02	2
143	94	+/-	191	43	43	239	95	=
144	22	INV	192	54)	240	42	STO
145	23	LN _X	193	85	+	241	13	13
146	65	X	194	53	(242	53	(
147	43	RCL	195	43	RCL	243	43	RCL
148	46	46	196	11	11	244	06	06
149	95	=	197	45	Y ^X	245	65	X
150	42	STO	198	04	4	246	43	RCL
151	10	10	199	65	X	247	05	05
152	43	RCL	200	43	RCL	248	54)
153	07	07	201	44	44	249	85	+
154	50	IXI	202	54)	250	53	(
155	65	X	203	85	+	251	53	(
156	43	RCL	204	53	(252	43	RCL
157	40	40	205	43	RCL	253	05	05
158	95	=	206	11	11	254	33	X ²
159	85	+	207	45	Y ^X	255	65	X
160	01	1	208	05	5	256	43	RCL
161	95	=	209	65	X	257	07	07
162	35	1/X	210	43	RCL	258	54)
163	42	STO	211	45	45	259	55	÷
164	11	11	212	54)	260	02	2
165	53	(213	54)	261	54)
166	53	(214	95	=	262	95	=
167	43	RCL	215	42	STO	263	42	STO
168	11	11	216	12	12	264	14	14
169	65	X	217	53	(265	43	RCL
170	43	RCL	218	53	(266	02	02
171	41	41	219	43	RCL	267	75	-
172	54)	220	09	09	268	43	RCL
173	85	+	221	54)	269	03	03
174	53	(222	75	-	270	95	=
175	43	RCL	223	53	(271	42	STO
176	11	11	224	53	(272	15	15
177	45	Y ^X	225	43	RCL	273	00	0
178	02	2	226	06	06	274	32	XIT
179	65	X	227	33	X ²	275	43	RCL
180	43	RCL	228	54)	276	07	07
181	42	42	229	85	+	277	77	GE
182	54)	230	53	(278	03	03
183	85	+	231	43	RCL	279	06	06
184	53	(232	05	05	280	53	(
185	43	RCL	233	33	X ²	281	53	(

Table B.2 Program Listing (Continued)

282	43	RCL	329	42	STO	376	32	32
283	10	10	330	16	16	377	43	RCL
284	65	X	331	00	0	378	20	20
285	43	RCL	332	32	XIT	379	58	FIX
286	12	12	333	43	RCL	380	03	03
287	65	X	334	15	15	381	99	PRT
288	43	RCL	335	22	INV	382	98	ADV
289	13	13	336	77	GE	383	91	R/S
290	54)	337	03	03	384	93	.
291	85	+	338	62	62	385	03	3
292	53	(339	43	RCL	386	32	XIT
293	43	RCL	340	18	18	387	43	RCL
294	10	10	341	75	-	388	04	04
295	65	X	342	43	RCL	389	77	GE
296	43	RCL	343	16	16	390	03	03
297	14	14	344	95	=	391	95	95
298	54)	345	42	STO	392	61	GTO
299	54)	346	19	19	393	00	00
300	95	=	347	65	X	394	27	27
301	42	STO	348	02	2	395	43	RCL
302	16	16	349	55	÷	396	00	00
303	61	GTO	350	43	RCL	397	55	÷
304	03	03	351	17	17	398	43	RCL
305	31	31	352	95	=	399	01	01
306	43	RCL	353	94	+/-	400	95	=
307	10	10	354	85	+	401	42	STO
308	65	X	355	01	1	402	04	04
309	43	RCL	356	95	=	403	65	X
310	12	12	357	42	STO	404	43	RCL
311	95	=	358	20	20	405	53	53
312	94	+/-	359	61	GTO	406	85	+
313	85	+	360	03	03	407	43	RCL
314	01	1	361	77	77	408	54	54
315	95	=	362	43	RCL	409	95	=
316	65	X	363	16	16	410	65	X
317	43	RCL	364	42	STO	411	43	RCL
318	13	13	365	18	18	412	01	01
319	95	=	366	43	RCL	413	95	=
320	85	+	367	02	02	414	42	STO
321	53	(368	42	STO	415	05	05
322	43	RCL	369	03	03	416	43	RCL
323	10	10	370	43	RCL	417	04	04
324	65	X	371	08	08	418	65	X
325	43	RCL	372	42	STO	419	43	RCL
326	14	14	373	07	07	420	55	55
327	54)	374	61	GTO	421	75	-
328	95	=	375	01	01	422	43	RCL

Table B.2 Program Listing (Continued)

```

423 56 56
424 95 =
425 65 X
426 43 RCL
427 01 01
428 95 =
429 42 STO
430 06 06
431 61 GTO
432 00 00
433 92 92
434 92 RTN
    
```

0.23164	b_0	40	4000.	WR	00
0.31938153	b_1	41	1000.	CEP	01
-0.35656378	b_2	42	2000.	d_1	03
1.7814779	b_3	43	2000.	d_1	03
-1.82125597	b_4	44	4.	WR/CEP	04
1.33027443	b_5	45	1236.6	σ	05
0.39894	$1/\sqrt{2\pi}$	46	3782.	μ	06
0.1737	Constant	47	-1.441048035	X	07
0.5418	for	48	-1.441048035	X	08
0.297	Computing	49	4000000.	d_1^2	09
0.922	σ & μ	50	.1412457541	$f(X)$	10
0.968	↓	51	.7497351372	$t(X)$	11
0.09		52	.5294712494	$P(X)$	12
0.3034		53	-5916351.78	$d_1^2 - \mu^2 - \sigma^2/2$	13
0.3987		54	3575010.6	$\sigma\mu - \frac{\sigma^2 X}{2}$	14
0.9159		55	0.		15
0.0126		56	62497.35222	$I(X, d_1)$	16
		12000000.	$d_2^2 - d_1^2$	17	
		1937623.476	$I(Y, d_2)$	18	
		1875126.123	I	19	
		.6874789794	A_D	20	

DISTRIBUTION LIST

DEPARTMENT OF DEFENSE

Assistant to the Secretary of Defense
Atomic Energy

ATTN: Executive Assistant

Defense Advanced Rsch Proj Agency

ATTN: TIO

Defense Intelligence Agency

ATTN: DB-4C3

ATTN: DB-4C2, T. Ross

ATTN: DB-4C2, B. Morris

ATTN: RDS-3A

ATTN: DB-4C1

Defense Nuclear Agency

ATTN: STSP

2 cy ATTN: SPAS

2 cy ATTN: SPSS

4 cy ATTN: TITL

Defense Technical Information Center

12 cy ATTN: DD

Field Command

Defense Nuclear Agency

ATTN: FCPR

ATTN: FCTMOF

ATTN: FCT

Field Command

Defense Nuclear Agency

ATTN: FCPRL

Field Command Test Directorate

Test Construction Division

Defense Nuclear Agency

ATTN: FCTC

Interservice Nuclear Weapons School

ATTN: TTV

Joint Strat Tgt Planning Staff

ATTN: NRI-STINFO Library

ATTN: DOXT

ATTN: JLTW-2

ATTN: JLA

ATTN: XPFS

NATO School

SHAPE

ATTN: U.S. Documents Officer

Undersecretary of Def for Rsch & Engrg

ATTN: Strategic & Space Systems (OS)

DEPARTMENT OF THE ARMY

BMD Advanced Technology Center

Department of the Army

ATTN: ICRDABH-X

ATTN: ATC-T

BMD Systems Command

Department of the Army

ATTN: BMDSC-H, N. Hurst

DEPARTMENT OF THE ARMY (Continued)

Chief of Engineers

Department of the Army

ATTN: DAEN-MCE-D

ATTN: DAEN-RDM

Construction Engineering Rsch Lab

Department of the Army

ATTN: CERL-SOI-L

Deputy Chief of Staff for Ops & Plans

Department of the Army

ATTN: DAMO-HC

Deputy Chief of Staff for Rsch Dev & Acq

Department of the Army

ATTN: DAMA-CSS-N

Engineer Studies Center

Department of the Army

ATTN: DAEN-FES, LTC Hatch

Harry Diamond Laboratories

Department of the Army

ATTN: DELHD-I-TL

ATTN: DELHD-N-P

U.S. Army Armament Material Readiness Cmd

ATTN: MA Library

U.S. Army Ballistic Research Labs

ATTN: DRDAR-BLE, J. Keefer

ATTN: DRDAR-BLV

ATTN: DRDAR-BLT, C. Kingery

ATTN: DRDAR-BLT, W. Taylor

ATTN: DRDAR-BLT, A. Ricchiazzi

U.S. Army Communications Command

ATTN: Technical Reference Division

U.S. Army Concepts Analysis Agency

ATTN: CSSA-ADL

U.S. Army Engineer Center

ATTN: ATZA

U.S. Army Engineer Div Huntsville

ATTN: HNDED-SR

U.S. Army Engineer Div Ohio River

ATTN: ORDAS-L

U.S. Army Engineer School

ATTN: ATZA-CDC

ATTN: ATZA-DTE-ADM

U.S. Army Engr Waterways Exper Station

ATTN: Library

ATTN: WESSD, J. Jackson

ATTN: J. Strange

ATTN: WESSE, L. Ingram

ATTN: WESSA, W. Flathau

ATTN: WESSS, J. Ballard

ATTN: F. Brown

DEPARTMENT OF THE ARMY (Continued)

U.S. Army Foreign Science & Tech Ctr
ATTN: DRXST-SD

U.S. Army Mat Cmd Proj Mgr for Nuc Munitions
ATTN: DRCPM-NUC

U.S. Army Material & Mechanics Rsch Ctr
ATTN: Technical Library
ATTN: DRXMR-TE, R. Shea
ATTN: DRXMR, J. Mescall

U.S. Army Materiel Dev & Readiness Cmd
ATTN: DRUDE-D, L. Flynn
ATTN: DRXAM-TL

U.S. Army Missile Command
ATTN: RSIC
ATTN: DRDMI-XS

U.S. Army Mobility Equip R&D Cmd
ATTN: DRDME-WC
ATTN: DRDME-HT, A. Tolbert

U.S. Army Nuclear & Chemical Agency
ATTN: Library

U.S. Army War College
ATTN: Library

U.S. Military Academy
Department of the Army
ATTN: R. La Frenz

DEPARTMENT OF THE NAVY

Marine Corps
Department of the Navy
ATTN: POM

David Taylor Naval Ship R&D Ctr
ATTN: Code 1700, W. Murray
ATTN: Code 177, E. Palmer
ATTN: Code L42-3
ATTN: Code 1740.5
ATTN: Code 1740, R. Short
ATTN: Code 2740

Marine Corp Dev & Education Command
Department of the Navy
ATTN: D091, J. Hartneady

Naval Air Systems Command
ATTN: F. Marquardt

Naval Construction Battalion Center
ATTN: Code L51, R. Odello
ATTN: Code L51, W. Shaw
ATTN: Code L51, S. Takahashi
ATTN: Code L51, J. Crawford

Naval Electronic Systems Command
ATTN: PME 117-21

Naval Electronics Systems Command
ATTN: Commander

Naval Explosive Ord Disposal Fac
ATTN: Code 504, J. Petrusky

DEPARTMENT OF THE NAVY (Continued)

Naval Facilities Engineering Command
ATTN: Code 09M22C
ATTN: Code 03T
ATTN: Code 04B

Naval Material Command
ATTN: MAT 08T-22

Naval Ocean Systems Center
ATTN: Code 013, E. Cooper
ATTN: Code 4471

Naval Postgraduate School
ATTN: Code 1424 Library
ATTN: Code 0142 Library

Naval Research Laboratory
ATTN: Code 8404, H. Pusey
ATTN: Code 2627
ATTN: Code 8440, G. O'Hara
ATTN: Code 8440, F. Rosenthal
ATTN: Code 8403, R. Belsham

Naval Sea Systems Command
ATTN: SEA-033
ATTN: SEA-06J, R. Lane
ATTN: SEA-09G53
ATTN: SEA-9931G
ATTN: SEA-0351

Naval Surface Weapons Center
ATTN: Code U401, M. Kleinerman
ATTN: Code R14
ATTN: Code R10
ATTN: Code F31

Naval Surface Weapons Center
ATTN: Tech Library & Info Ser Br
ATTN: W. Wishard

Naval War College
ATTN: Code C-11

Naval Weapons Center
ATTN: Code 3263, J. Bowen
ATTN: Code 266, C. Austin
ATTN: Code 233

Naval Weapons Evaluation Facility
ATTN: Code 10
ATTN: R. Hughes

Office of Naval Research
ATTN: Code 463, J. Heacock
ATTN: Code 715
ATTN: Code 474, N. Perrone

Office of the Chief of Naval Operations
ATTN: OP 604C3, R. Piacesi
ATTN: OP 982E, M. Lenzini
ATTN: OP 098T8
ATTN: OP 982
ATTN: OP 981
ATTN: OP 03EG

DEPARTMENT OF THE NAVY (Continued)

Strategic Systems Project Office
Department of the Navy
ATTN: NSP-43
ATTN: NSP-272
ATTN: NSP-273

DEPARTMENT OF THE AIR FORCE

Aerospace Defense Command
Department of the Air Force
ATTN: XPX

Air Force Armament Laboratory
ATTN: DLYV, J. Collins

Air Force Geophysics Laboratory
ATTN: LWV, K. Thompson

Air Force Institute of Technology
ATTN: Library
ATTN: Commander

Air Force Office of Scientific Research
ATTN: NA, B. Wolfson

Headquarters
Air Force Systems Command
ATTN: DLW
ATTN: R. Cross

Air Force Weapons Laboratory
Air Force Systems Command
ATTN: NTES-C, R. Henny
ATTN: NTE, M. Plandon
ATTN: SUL
ATTN: NTES-G, S. Melzer
ATTN: NTED

Assistant Chief of Staff
Intelligence
Department of the Air Force
ATTN: IN

Ballistic Missile Office
Air Force Systems Command
ATTN: DEB

Ballistic Missile Office
Air Force Systems Command
ATTN: MNRTE
ATTN: MMH
ATTN: MNNH

Deputy Chief of Staff
Research, Development, & Acq
Department of the Air Force
ATTN: R. Steere
ATTN: AFRDQSM

Deputy Chief of Staff
Logistics & Engineering
Department of the Air Force
ATTN: LEEE

Foreign Technology Division
Air Force Systems Command
ATTN: TQTD
ATTN: NIIS Library
ATTN: SDBG
ATTN: SDBF, S. Spring

DEPARTMENT OF THE AIR FORCE (Continued)

Rome Air Development Center
Air Force Systems Command
ATTN: Commander
ATTN: TSLD
ATTN: RBES, R. Mair

Strategic Air Command
Department of the Air Force
ATTN: NRI-STINFO Library
ATTN: XPFS

United States Air Force Academy
ATTN: DFCEM, W. Fluhr

DEPARTMENT OF ENERGY

Department of Energy
Albuquerque Operations Office
ATTN: CTID

Department of Energy
ATTN: OMA/RD&T

Department of Energy
Nevada Operations Office
ATTN: Mail & Records for Tech Library

DEPARTMENT OF ENERGY CONTRACTORS

Lawrence Livermore National Laboratory
ATTN: M. Fernandez
ATTN: Tech Information Dept Library
ATTN: J. Goudreau
ATTN: T. Gold
ATTN: J. Thomsen
ATTN: L-7, J. Kahn
ATTN: L-200, J. Cortez
ATTN: L-205, J. Hearst
ATTN: L-200, T. Butkovich
ATTN: L-90, D. Norris
ATTN: L-96, L. Woodruff
ATTN: L-437, R. Schock
ATTN: L-90, R. Dong

Los Alamos National Scientific Laboratory
ATTN: G. Spillman
ATTN: M/S632, T. Dowler
ATTN: MS 670, J. Hopkins
ATTN: RMS 364
ATTN: A. Davis

Oak Ridge National Laboratory
ATTN: Civil Def Res Proj
ATTN: Central Research Library

Sandia National Laboratories
ATTN: Library & Security Class Div

Sandia National Laboratories
ATTN: 3141
ATTN: W. Herrman
ATTN: W. Roherty
ATTN: L. Vortman
ATTN: L. Hill
ATTN: A. Chaban

OTHER GOVERNMENT

Central Intelligence Agency
ATTN: OSI/NED

Department of the Interior
Bureau of Mines
ATTN: Tech Lib

Department of the Interior
U.S. Geological Survey
ATTN: D. Roddy

Federal Emergency Management Agency
ATTN: Hazard Eval & Vul Red Div

NASA
Ames Research Center
ATTN: R. Jackson

U.S. Nuclear Regulatory Commission
ATTN: Div of Security for L. Shao

DEPARTMENT OF DEFENSE CONTRACTORS

Acurex Corp
ATTN: J. Stockton

Aerospace Corp
ATTN: P. Mathur
ATTN: L. Seizer
2 cy ATTN: Technical Information Services

Agbabian Associates
ATTN: C. Bagge
ATTN: M. Agbabian

Analytic Services, Inc
ATTN: G. Hesselbacher

Applied Theory, Inc
2 cy ATTN: J. Trulio

Artec Associates, Inc
ATTN: S. Gill

AVCO Research & Systems Group
ATTN: Library A830
ATTN: W. Broding
ATTN: J. Atanasoff
ATTN: D. Henderson

BDM Corp
ATTN: Corporate Library
ATTN: A. Lavagnino
ATTN: T. Neighbors

BDM Corp
ATTN: R. Hensley

Bell Telephone Labs
ATTN: J. White

Boeing Co
ATTN: R. Hager
ATTN: Aerospace Library
ATTN: M/S 42/37, R. Carlson
ATTN: R. Dyrdaahl
ATTN: J. Wooster
ATTN: R. Holmes

DEPARTMENT OF DEFENSE CONTRACTORS (Continued)

Boeing Co
ATTN: M/S 42/37, K. Friddell

California Institute of Technology
ATTN: T. Ahrens

California Research & Technology, Inc
ATTN: S. Schuster
ATTN: K. Kreyenhagen
ATTN: Library

California Research & Technology, Inc
ATTN: D. Orphal

Calspan Corp
ATTN: Library

Center for Planning & Rsch, Inc
ATTN: R. Shnider

Civil Systems Inc
ATTN: J. Bratton

University of Denver
Colorado Seminary
Denver Research Institute
ATTN: Sec Officer for J. Wisotski

EG&G Washington Analytical Services Ctr, Inc
ATTN: Library
ATTN: Director

Electric Power Research Institute
ATTN: G. Sliter

Electromechanical Sys of New Mexico, Inc
ATTN: R. Shunk

Eric H. Wang
Civil Engineering Rsch Fac
University of New Mexico
ATTN: D. Calhoun
ATTN: N. Baum

Franklin Institute
ATTN: Z. Zudans

Gard, Inc
ATTN: G. Neidhardt

General Dynamics Corp
ATTN: K. Anderson

General Electric Co
ATTN: M. Bortner

General Electric Co
ATTN: A. Ross

General Electric Company—TEMPO
ATTN: DASIAC

General Research Corp
ATTN: B. Alexander

Geocenters, Inc
ATTN: E. Marram

DEPARTMENT OF DEFENSE CONTRACTORS (Continued)

H-Tech Labs, Inc
ATTN: B. Hartenbaum

Honeywell, Inc
ATTN: T. Helvig

IIT Research Institute
ATTN: Documents Library
ATTN: A. Longinow

Institute for Defense Analyses
ATTN: Director
ATTN: Library

J. H. Wiggins Co, Inc
ATTN: J. Collins

Kaman Avidyne
ATTN: N. Hobbs
ATTN: G. Zartarian
ATTN: Library

Kaman Sciences Corp
ATTN: Library
ATTN: D. Sachs
ATTN: F. Shelton

Karagozian and Case
ATTN: J. Karagozian

Lockheed Missiles & Space Co, Inc
ATTN: B. Almroth
ATTN: T. Geers

Lockheed Missiles & Space Co, Inc
ATTN: TIC-Library

Management Science Associates
ATTN: K. Kaplan

Martin Marietta Corp
ATTN: A. Cowan
ATTN: G. Fotieo

Martin Marietta Corp
ATTN: J. Donathan

University of Massachusetts
Astronomy Research Facility
ATTN: W. Nash

McDonnell Douglas Corp
ATTN: R. Halprin

Merritt CASES, Inc
ATTN: J. Merritt
ATTN: Library

Meteorology Research, Inc
ATTN: W. Green

Mitre Corp
ATTN: Director

Nathan M. Newmark Consult Eng Svcs
ATTN: J. Haltiwanger
ATTN: N. Newmark
ATTN: W. Hall

DEPARTMENT OF DEFENSE CONTRACTORS (Continued)

University of New Mexico
Dept of Police & Parking Security
ATTN: G. Triandafalidis

University of Oklahoma
ATTN: J. Thompson

Pacific-Sierra Research Corp
ATTN: H. Brode

Pacifica Technology
ATTN: R. Bjork
ATTN: R. Allen
ATTN: G. Kent

Physics International Co
ATTN: F. Sauer
ATTN: E. Moore
ATTN: C. Vincent
ATTN: R. Swift
ATTN: L. Behrmann
ATTN: Technical Library

University of Pittsburgh
School of Engineering
ATTN: M. Williams, Jr

R & D Associates
ATTN: W. Wright, Jr
ATTN: A. Latter
ATTN: A. Field
ATTN: C. MacDonald
ATTN: J. Lewis
ATTN: P. Rausch
ATTN: Technical Information Center
ATTN: R. Port
ATTN: P. Haas

Rand Corp
ATTN: C. Mow
ATTN: A. Laupa
ATTN: Library

Science Applications, Inc
ATTN: Technical Library

Science Applications, Inc
ATTN: S. Oston

Science Applications, Inc
ATTN: R. Hoffmann
ATTN: D. Maxwell
ATTN: D. Bernstein

Science Applications, Inc
ATTN: W. Layson
ATTN: B. Chambers III
ATTN: G. Binninger

Southwest Research Institute
ATTN: W. Baker
ATTN: A. Wenzel

SRI International
ATTN: W. Wilkinson
ATTN: G. Abrahamson

DEPARTMENT OF DEFENSE CONTRACTORS (Continued)

Systems, Science & Software, Inc

ATTN: T. Riney
ATTN: R. Sedgewick
ATTN: Library
ATTN: T. McKinley
ATTN: D. Gaine
ATTN: T. Cherry

Teledyne Brown Engineering

ATTN: J. Ravenscraft

Terra Tek, Inc

ATTN: Library
ATTN: S. Green
ATTN: A. Jones

Tetra Tech, Inc

ATTN: L. Hwang
ATTN: Library

Texas A & M University System

ATTN: H. Coyle

Westinghouse Electric Corp

ATTN: W. Voiz

DEPARTMENT OF DEFENSE CONTRACTORS (Continued)

TRW Defense & Space Sys Group

ATTN: D. Jortner
ATTN: P. Bhutta
ATTN: B. Sussholtz
ATTN: A. Narevsky
ATTN: Technical Information Center
ATTN: A. Feldman
2 cy ATTN: N. Lipner

TRW Defense & Space Sys Group

ATTN: P. Dai
ATTN: E. Wong
ATTN: F. Pieper
ATTN: G. Hulcher

Weidlinger Assoc, Consulting Engineers

ATTN: J. McCormick
ATTN: M. Baron

Weidlinger Assoc, Consulting Engineers

ATTN: J. Isenberg